Modification of LIN-12 NOTCH signalling during vulval development in *C. elegans*

Dissertation

zur

Erlangung der naturwissenschaftlichen Doktorwürde

(Dr. sc. nat.)

vorgelegt der

Mathematisch-naturwissenschaftlichen Fakultät

der Universität Zürich

von

Stefanie Nusser-Stein

aus

Deutschland

Promotionskomitee

Prof. Dr. Alex Hajnal (Vorsitz)

Prof. Dr. Yves Barral

Prof. Dr. Konrad Basler

PD Dr. Adrian Streit

Zürich, 2013

For Soki

and

for the best reason to study developmental biology,

our unborn child in my belly.

TABLE OF CONTENTS

1 ZUSAMMENFASSUNG

Zellkommunikation ist eine der wichtigsten Eigenschaften, die im Laufe der Evolution entwickelt worden ist, um vom Einzellstadium zu Organismen, die aus vielen verschiedenen Zellarten bestehen, zu wechseln. Deshalb wurden bereits sehr früh in der Geschichte der Vielzeller Signale erfunden, die von einer Zelle an die andere weitergeleitet werden, und deshalb sind diese Signalwege in Vielzellern stark konserviert. Das NOTCH Signal wird zum Beispiel von Zellen verwendet, die ihre benachbarten Zellen davon abbringen müssen, dasselbe Standard-Zellschicksal wie sie selbst anzunehmen. Beispiele für diese NOTCH-vermittelte laterale Hemmung findet man in der Entwicklung des Eiablage- und Kopulationsorgans von Fadenwürmern und während der Bildung von Nervenzellen in *Drosophila*. Das NOTCH Signal ist auch bei der Neubildung von Blutgefässen, der Entwicklung von Nervenzellen und der Spezifizierung von T-Zellen im Menschen wichtig.

Der NOTCH-Signaltransduktionsweg kann als eine Art Schalter betrachtet werden, um schnell bestimmte Zellschicksale an- oder auszuschalten. Die spezifische Antwort der Zelle, die ein NOTCH Signal zugesendet bekommt, hängt von ihrer molekularen Zusammensetzung und den vorhandenen Zielfaktoren ab. Obwohl die Kernelemente des NOTCH Signals weitgehend bekannt sind, bleiben viele Zielfaktoren und Modifikatoren des NOTCH-Signaltransduktionsweges ungeklärt.

Im ersten Teil dieser Doktorarbeit beschreibe ich einen neuen Zusammenhang zwischen dem Voranschreiten des Zellzykluses und dem NOTCH Signal in *Caenorhabditis elegans*: Ein bestimmter CDK/Cyclin Komplex (CDK-1/CYB-3), der während der G2 Phase des Zellzykluses aktiv ist, vermittelt nicht nur den Eintritt in die Mitose, sondern ist auch während des dritten Larvenstadiums für die korrekte Herabregulation des NOTCH Signals in der primären Vulvazelle wichtig. Zellzykluskomponenten, die während der G1 Phase aktiv sind, wie zum Beispiel die Cycline CYD-1 und

CYE-1, haben dagegen einen positiven Einfluss auf das NOTCH Signal. Auf diese Weise ist die Spezifizierung von Zellschicksalen mittels des NOTCH-Signaltransduktionsweges eng verknüpft mit dem Voranschreiten des Zellzykluses. Ich schlage deshalb vor, dass das Durchlaufen des Zellzykluses zeitlich gesehen verschiedene intrazelluläre Zusammensetzungen schafft und somit einen Zeitgeber für Signaltransduktionsabläufe während bestimmter Entwicklungsphasen darstellt.

Im zweiten Teil dieser Doktorarbeit zeige ich, dass das Gen *ttr-11* ein Zielgen des NOTCH-Signaltransduktionsweges während der Entwicklung der Vulva von *Caenorhabditis elegans* ist. Das Gen *ttr-11* wurde in einem Screen nach Kandidaten für NOTCH-Zielgene identifiziert und gehört zu einer großen Fadenwurm-spezifischen Genfamilie. Erst vor Kurzem haben Forscher begonnen die Funktion von manchen *ttr* Genen aufzudecken. Da Einzelmutationen in angehörigen Genen dieser Genfamilie nur geringe oder keine phänotypischen Effekte zeigen, und da das Genexpressionslevel von einzelnen *ttr* Genen oft niedrig ist, ist es schwierig die Aufgaben von *ttr* Genen in Fadenwürmern aufzuklären. Verschiedene Allele von *ttr-11* haben milde aber gegenläufige Auswirkungen in verschiedenen mutanten Hintergründen zur Folge: Das NOTCH Signal von einer NOTCH Gain-of-Function-Mutante wird von wildtypischem *ttr-11* gehemmt, wohingegen *ttr-11* in einem mutanten Hintergrund mit erhöhter EGFR/RAS/MAPK-Signaltransduktion einen positiven Einfluss auf das laterale Signal zeigt. Die milden Auswirkungen durch mutiertes *ttr-11* könnten durch teilweise redundante Funktionen anderer Mitglieder der *ttr* Familie erklärt werden. Zum Beispiel zeigt *ttr-57* hohe Sequenzähnlichkeit zu *ttr-11*. Jedoch halfen weder *ttr-11 ttr-57* Doppelmutanten noch Überexpression von *ttr-11* weiter die Aufgabe von *ttr-11* während der Entwicklung der Vulva zu klären. Deshalb müssen weitere Experimente, wie zum Beispiel die Untersuchung der Funktionen von anderen nah verwandten *ttr* Genen in *ttr-11* Mutanten, durchgeführt werden, um Licht ins Dunkel um die Funktion von *ttr-11* zu bringen.

2 SUMMARY

Communication between cells is one of the most important features established during evolution to switch from a single cell organism to an organism made out of many different cell types. Therefore, signals that are sent from one cell to another have been invented quite early during the history of multicellular organisms and the signalling pathways transducing the signals are highly conserved in metazoans. For example, the NOTCH signal is used by cells to inhibit neighbouring cells from adopting the same, default cell fate. Examples for NOTCH-mediated lateral inhibition are nematode vulval development and *Drosophila* neurogenesis. NOTCH signalling is also important during human angiogenesis, neuronal development and T cell specification.

The NOTCH signalling pathway can be regarded as a switch used to rapidly turn a specific fate on or off. The specific response of the cell receiving a NOTCH signal depends on the molecular environment and the downstream targets present in the cell. Although the roles of the core components of NOTCH signalling are well known, many downstream targets and modifiers of the NOTCH pathway remain to be elucidated.

In the first part of this thesis, I describe a new connection between cell cycle progression and NOTCH signalling in the nematode *Caenorhabditis elegans*: One particular CDK/Cyclin complex (CDK-1/CYB-3) that is active during the G2 phase of the cell cycle not only mediates entry into mitosis, but it is also important for proper downregulation of the NOTCH signal in the primary vulval cell of the L3 larva. In contrast, cell cycle components active during the G1 phase, such as the cyclins CYD-1 and CYE-1, positively regulate NOTCH signalling in the vulval cells. Thus, cell fate specification via NOTCH signalling is tightly linked to cell cycle progression. I suggest that progression through cell cycle creates temporally different intracellular

environments and therefore provides a timer for signalling events to occur during specific developmental phases.

In a second part of this thesis, I show that the gene *ttr-11* is a downstream target of NOTCH signalling during *Caenorhabditis elegans* vulval development. The gene *ttr-11* was found in a screen for candidate NOTCH targets and belongs to a large nematode-specific gene family. Only recently, researchers have begun to uncover the function of some *ttr* genes. Since single mutants in members of this gene family show only a mild or no phenotype at all and because expression levels of individual *ttr* genes are often low, it is difficult to elucidate the role of *ttr* genes in nematodes. Different alleles of *ttr-11* result in mild but contradictory effects in different mutant backgrounds: In a NOTCH gain-of-function background, wild-type *ttr-11* inhibits the NOTCH signal, whereas *ttr-11* shows a positive influence on lateral signalling in a background with elevated EGFR/RAS/MAPK signalling. The mild effects of mutated *ttr-11* might be explained by partially redundant functions of other *ttr*-family members. For example, *ttr-57* shows high sequence similarity to *ttr-11*. However, neither *ttr-11 ttr-57* double mutants nor *ttr-11* overexpression helped to clarify the role of *ttr-11* during vulval development. Thus, further experiments, for example by examining the functions of other closely related *ttr* genes in *ttr-11* mutants, need to be performed to shed light on the function of *ttr-11*.

3 ABBREVIATIONS

1°	primary
2°	secondary
3°	tertiary
Abeta protein	amyloid beta protein
AC	anchor cell
ADAM	a disintegrin and metalloproteinase
AICD	APP intracellular domain
ANK repeats	ankyrin repeats
APF	adjacent primary fate
APP	amyloid precursor protein
apx	anterior pharynx in excess
C. elegans	*Caenorhabditis elegans*
cdk	cyclin dependent kinase
cDNA	complementary DNA
ced	cell death abnormality
ChIP	Chromatin immunoprecipitation
cki	cyclin dependent kinase inhibitor
CSL	CBF1/Su(H)/LAG-1
cul	cullin
cyc or *cy*(*a*,*b*,…*e*)	cyclin (A, B,…E)
D. melanogaster	*Drosophila melanogaster*
dep	density enhanced phosphatase
DNA	deoxyribonucleic acid
DSL	Delta/Serrate/LAG-2
E. coli	*Escherichia coli*
EGF	epidermal growth factor
egl	egg-laying defective
ESTs	expressed sequence tags
G1 and G2 phases	gap 1 and gap 2 phases
gf	gain-of-function

GFP	green fluorescent protein
glp	germline proliferation
hox gene	homeobox gene
hrt	hairy-related transcription factor
kip	kinase interacting protein
L1-4	larval stage 1-4
lag	*lin-12* and *glp-1* phenotype
let	lethal
lf	loss-of-function
lin	lineage defective
Lin repeats	also called LNR (LIN-12 NOTCH) repeats
lip	lateral signal induced phosphatase
lst	lateral signal target
M phase	mitotic phase
MAPK	mitogen-activated protein kinase
mRNA	messenger RNA
Muv	multivulva
NICD	NOTCH intracellular domain
PEST	peptide sequence which is rich in proline (P), glutamic acid (E), serine (S), and threonine (T)
Pvl	protruding vulva
RAM	Regulation of Amino Acid Metabolism
RAS	rat sarcoma
rf	reduction of function
RING (finger protein)	really interesting new gene
RNA	ribonucleic acid
RNAi	RNA interference
S phase	DNA synthesis phase
S. cerevisiae	*Saccharomyces cerevisiae*
sel	suppressor/enhancer of *lin-12*
SIRT	sirtuin / silent mating type information regulation 2, homologue
skp	mammalian Ski (Sloan-Kettering Institute) interacting protein homologue
Su(H)	suppressor of hairless

SynMuv	synthetic multivulva
trp	transthyretin related protein
ttl	transthyretin-like
ttr (*C. elegans* gene class)	transthyretin related family domain
TTR (in context with mammals)	transthyretin
unc	uncoordinated
utse	uterine seam cell
uv1	uterine-vulval cells 1
VPC	vulva precursor cell
VU	ventral uterine
Vul	vulvaless
wnt	portmanteau of *int* (integration) and *wg* (wingless)

4 INTRODUCTION

4.1 NOTCH Signalling

Molecular Signalling events

NOTCH Signalling is evolutionary highly conserved and used in many multicellular organisms for intercellular communication and cell fate specification (Fleming, 1998). First, Thomas Hunt Morgan identified alleles of Notch in *Drosophila melanogaster* in 1917 (Morgan, 1917). The Notch signalling pathway is very often used to select one cell for a specific fate out of a group of equipotent cells during development of an organism. For example, the sensory organ precursor cell during sensory bristle development in *D. melanogaster* is selected in this way (Heitzler and Simpson, 1991). However, NOTCH is also involved in development of various kinds of cancer during adulthood. For example, activated mutations of NOTCH are associated with T cell acute lymphoblastic leukaemia (Weng *et al*, 2004). NOTCH signalling is also activated in breast cancer cells (Weijzen *et al*, 2002) and in human colon adenocarcinomas (Zagouras *et al*, 1995).

The molecular core mechanism of NOTCH signalling is quite well understood (Figure 1). NOTCH is a single-pass transmembrane receptor and presented at the plasma membrane as a heterodimeric protein that consists out of an extracellular segment and a transmembrane segment that are linked non-covalently. In mammals, the NOTCH precursor protein is cleaved in the trans-Golgi by a furin-like convertase creating the two segments of the receptor (Logeat *et al*, 1998). This event is also called the S1 cleavage. However, this cleavage is not required for NOTCH function in *D. melanogaster* (Kidd and Lieber, 2002). In *Caenorhabditis elegans* the S1 cleavage had not been analysed so far. The NOTCH extracellular segment contains 26 - 36 EGF-like repeats, two of which are responsible for ligand

binding. Ca^{2+} can also bind to some EGF-like repeats to stiffen the receptor (Hambleton *et al*, 2004). Additionally, the extracellular segment contains three cystein rich repeats. This so-called Lin repeats harbour the site for the S2 cleavage. After binding to the N-terminal DSL (Delta/Serrate/LAG-2) motif of a ligand, the NOTCH receptor is activated by two cleavages: An ADAM family-metalloprotease removes the extracellular Lin repeats (S2) and a γ-secretase complex releases the NOTCH intracellular domain (NICD) by cleavage in the transmembrane domain (S3) (Mumm *et al*, 2000; Schroeter *et al*, 1998). As consequence, NICD migrates to the nucleus where it binds to the transcription factor CSL (CBF1/Su(H)/LAG-1) by its RAM domain and ankyrin repeats of the intracellular segment. This complex recruits co-activators that convert CSL from a transcriptional repressor into an activator (Fryer *et al*, 2002; Kurooka and Honjo, 2000; Zhou *et al*, 2000).

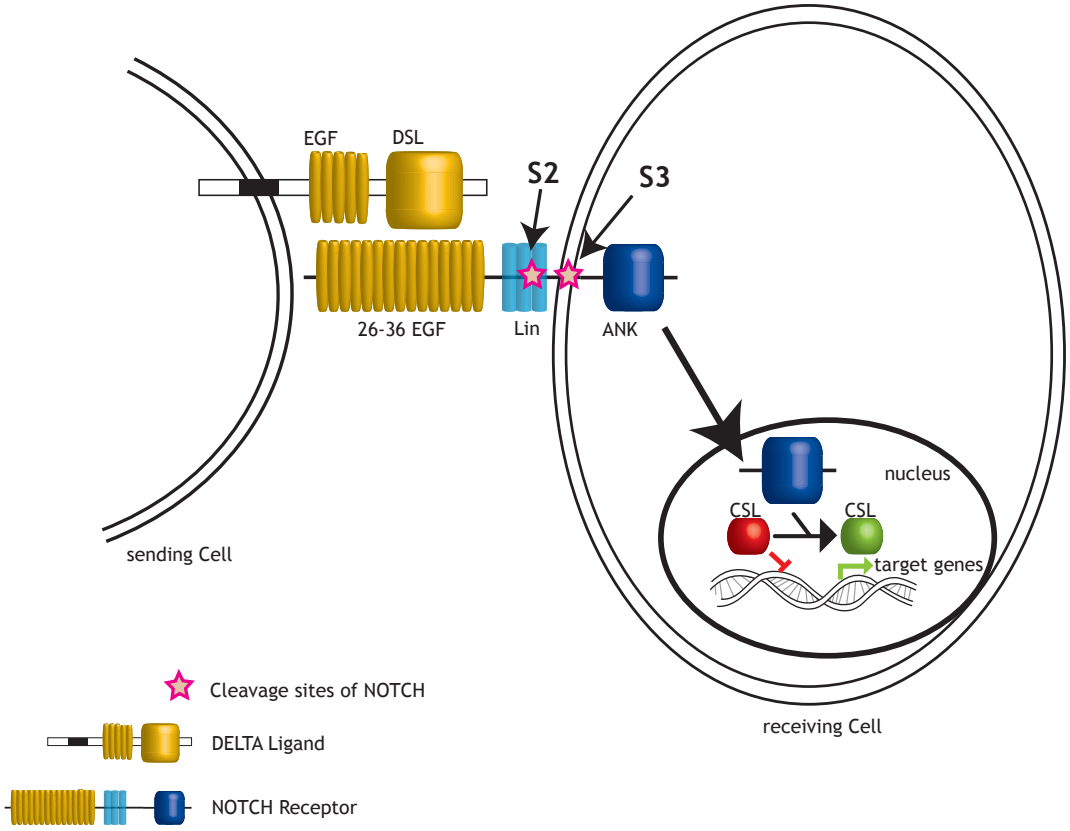

Figure 1: Molecular events of the NOTCH signalling pathway.
Upon activation through binding to the ligand, the NOTCH receptor is cleaved twice, once by a metalloprotease (S2) and a second time by a γ-secretase complex (S3). The freed activated NOTCH intracellular domain (NICD) migrates to the nucleus. There it binds to CSL proteins located at specific sites of promoters of target genes, and leads to transcription of these target genes.

Since NOTCH signalling provides a switch to turn on gene transcription in a very fast manner, the organism also has to be able to turn off this switch very fast. In other words, there has to be a potential NICD degradation mechanism: In mice, Mastermind, one of the co-activating factors, recruits in parallel to the transcriptional activation the protein kinase complex CycC/CDK8 that leads to NICD hyperphosphorylation in the PEST domain and subsequent recognition by the E3-ubiquitin ligase complex containing the F-box protein Sel-10, the cullin Cul-1, Skp-1 and the RING finger protein Hrt-1 (Fryer *et al*, 2004; Lai, 2002). The polyubiquitylated NICD is sent to the proteasome for degradation (Schweisguth, 1999). However, this knowledge is so far a patchwork comprising single facts that had been uncovered in different model organisms. For example, the identity of the kinase, whose modification of NICD allows recognition by the F-box protein Sel-10, was just identified in specific mouse cells (Fryer *et al*, 2004). If this mechanism is also true for other tissues and organisms remains to be examined. It seems to be obvious that the activity of NICD has to be tightly controlled once the NOTCH signalling pathway is activated since even in cells with active NOTCH signalling the NICD levels are kept very low. Repeated attempts to locate endogenous NICD in the nucleus in cells with active NOTCH signalling failed so far. This leads to the assumption that there might be various ways to target NICD for degradation. For example, another kind of NICD modification has been published by Guarani *et al.*, who postulated that the deacetylase SIRT1 opposes acetylation-induced NICD stabilisation (Guarani *et al*). Further ways of NICD regulation have to be elucidated.

NOTCH signalling in *C. elegans*

C. elegans uses NOTCH signalling for various cell fate decisions during its development from an embryo through four larval stages each followed by a moulting step to become an adult worm after the last moulting step (Greenwald, 2005). *C. elegans* has, in contrast to *D. melanogaster*, two instead of one NOTCH homologue: LIN-12 and GLP-1.

NOTCH signalling during embryogenesis

The first known event of NOTCH signalling happens already during the embryonic four-cell stage and is implicated in pharyngeal cell fate decision (Priess, 2005). The embryo consists out of the cells ABa, ABp, P_2 and EMS. ABa and ABp initially are equipotent cells. ABp receives a NOTCH signal from the P_2 cell, which prevents ABp from producing pharyngeal cells. Interestingly, also the second NOTCH signalling event during embryonic twelve-cell stage influences pharynx development (Priess, 2005). However, while the first event inhibits the target cell from adopting a pharyngeal fate, the second event promotes pharyngeal tissue specification. Although during both events the homologue GLP-1 is used the outcome is different. Therefore, NOTCH signalling can result in totally different fate decisions and the outcome depends mostly on the molecular background of the cell that receives the signal. NOTCH signalling provides a switch to turn specific developmental programs on or off, but which programs are concerned that is decided by the origin of the signal-receiving cell.

In addition, the NOTCH homologue LIN-12 plays a role in embryonic development (Priess, 2005). LIN-12 NOTCH signalling for example contributes to the bilaterally symmetry of the head by specifying the left head precursor cell and it is involved in the specification of the excretory cell (Hutter and Schnabel, 1995; Lambie and Kimble, 1991; Moskowitz and Rothman, 1996).

NOTCH signalling during post-embryogenesis

Additionally, NOTCH signalling is important during post-embryonic development. While GLP-1 plays a role in promoting germline cell proliferation (Seydoux and Schedl, 2001) LIN-12 is involved in specifying the vulva, which connects the hermaphrodite's uterus with the outside and functions as copulation and egg-laying organ of *C. elegans*. This organ is a very useful tool for developmental biology, due to its dispensability for a living worm. Thus, mutants in vulval development still can produce a sufficient amount of progeny: The young worms hatch inside of the

hermaphrodite's body, which forms a "bag of worms" until the progeny escapes from the dead body. Thus, vulval mutant lines can be kept over generations. Additionally, the cells and structure of this organ can be easily examined by microscopy and several phenotypes like Vul (vulvaless), Muv (multivulva) or Pvl (protruding vulva) can be scored even under low magnifications (Sternberg, 2005). Another advantage of the nematode's vulva as model organ is the fact that highly conserved signalling pathways contribute to its specification and morphogenesis. Besides LIN-12 NOTCH signalling also the EGFR/RAS/MAPK pathway and WNT signalling are involved (Sternberg, 2005).

The first decision that is important for vulval development and is influenced by LIN-12 NOTCH is made during the end of the second larval stage L2 (Greenwald, 2005). Two equipotent gonad cells Z1.ppp and Z4.aaa express both the NOTCH receptor LIN-12 and the NOTCH ligand LAG-2 (Figure 2). Due to a small difference in LIN-12 activity at the beginning one of the cells results in producing more receptor protein, the other one produces more ligand protein. This effect is enhanced by an internal feedback loop. Activated LIN-12 results in increased LIN-12 expression and LAG-2 inhibition (Seydoux and Greenwald, 1989; Wilkinson *et al*, 1994). In this manner the signal-receiving cell becomes a uterine precursor cell and the signal-sending cell adopts the anchor cell (AC) fate that induces later on vulval induction and connects vulval with uterine tissue.

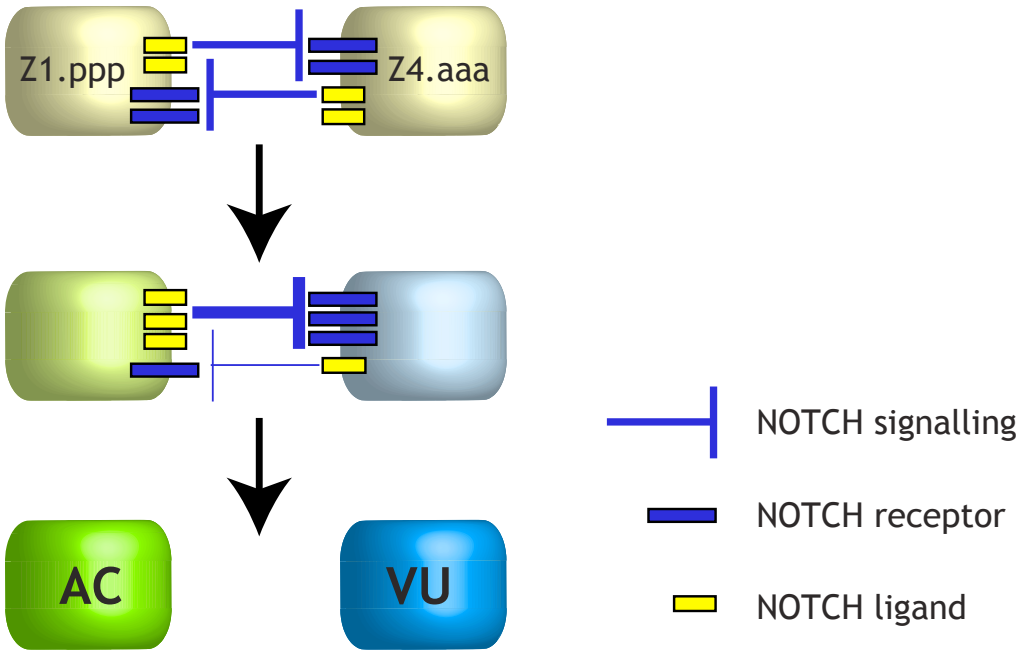

Figure 2: AC/VU decision.
Two equipotent gonadal cells (Z1.ppp and Z4.aaa) express both, NOTCH ligand and receptor. A slight disequilibrium leads to one cell expressing a higher amount of ligand. Thus the other cell accumulates a higher amount of receptor due to a positive feedback loop. In the end, the signal-receiving cell adopts a ventral uterine fate (VU), the signal-sending cell adopts the anchor cell fate (AC).

The second LIN-12 NOTCH mediated decision during vulval development occurs in the vulval epidermal tissue. However, before lateral induction can happen other signalling events take place: WNT signalling induces expression of the hox gene *lin-39* selecting six cells (P3.p - P8.p) out of eleven Pn.p cells for the vulval competence group (Clark *et al*, 1993; Eisenmann *et al*, 1998) (Figure 3 A). Every cell of this equivalence group has the potential to adopt a vulval fate (Sternberg, 2005). The primary (1°) vulval fate leads to a specific division pattern resulting in eight descendants that will form the inner part of the egg-laying organ. Each of the two secondary (2°) vulval cells divides into seven descendants that form the outer vulval rings of the tube-shaped organ. The uninduced fate is called tertiary (3°) fate and does not count as vulval fate. 3° cells divide once and fuse to the hypodermis. The decision, which cell adopts which fate is mediated by the AC that sends an EGF (LIN-3) signal in a graded manner

(Sternberg, 2005). P6.p is the closest vulval precursor cell (VPC) and therefore receives most of this inductive signal and adopts the 1° fate. The activated EGFR/RAS/MAPK pathway in P6.p leads through the execution of the 1° fate via the phosphorylation of the complex consisting out of the transcription factors LIN-1 and LIN-31 (Tan *et al*, 1998) to the expression of several LIN-12 NOTCH ligands, like LAG-2, APX-1 and DSL-1 (Chen and Greenwald, 2004) (Figure 3 B). Thus, P6.p inhibits its neighbouring cells from also adopting a 1° fate and induces the 2° fate via lateral LIN-12 NOTCH signalling. Consequently, P5.p and P7.p inhibit EGFR/RAS/MAPK signalling via NOTCH targets like the MAPK phosphatase *lip-1* or the EGFR phosphatase *dep-1* (Berset *et al*, 2001; Berset *et al*, 2005). However, NOTCH targets that actively promote the 2° fate, have to be elucidated.

The AC induces not only the VPC fates but also the π cell fates in the ventral uterus (Cinar *et al*, 2001; Newman *et al*, 1995). And this induction is again mediated via LIN-12 NOTCH signalling. The six π cells divide once. Amongst their progeny there are four uv1 cells that form the connection to specific primary VPC descendants to create the opening of the vulva (Newman *et al*, 1995).

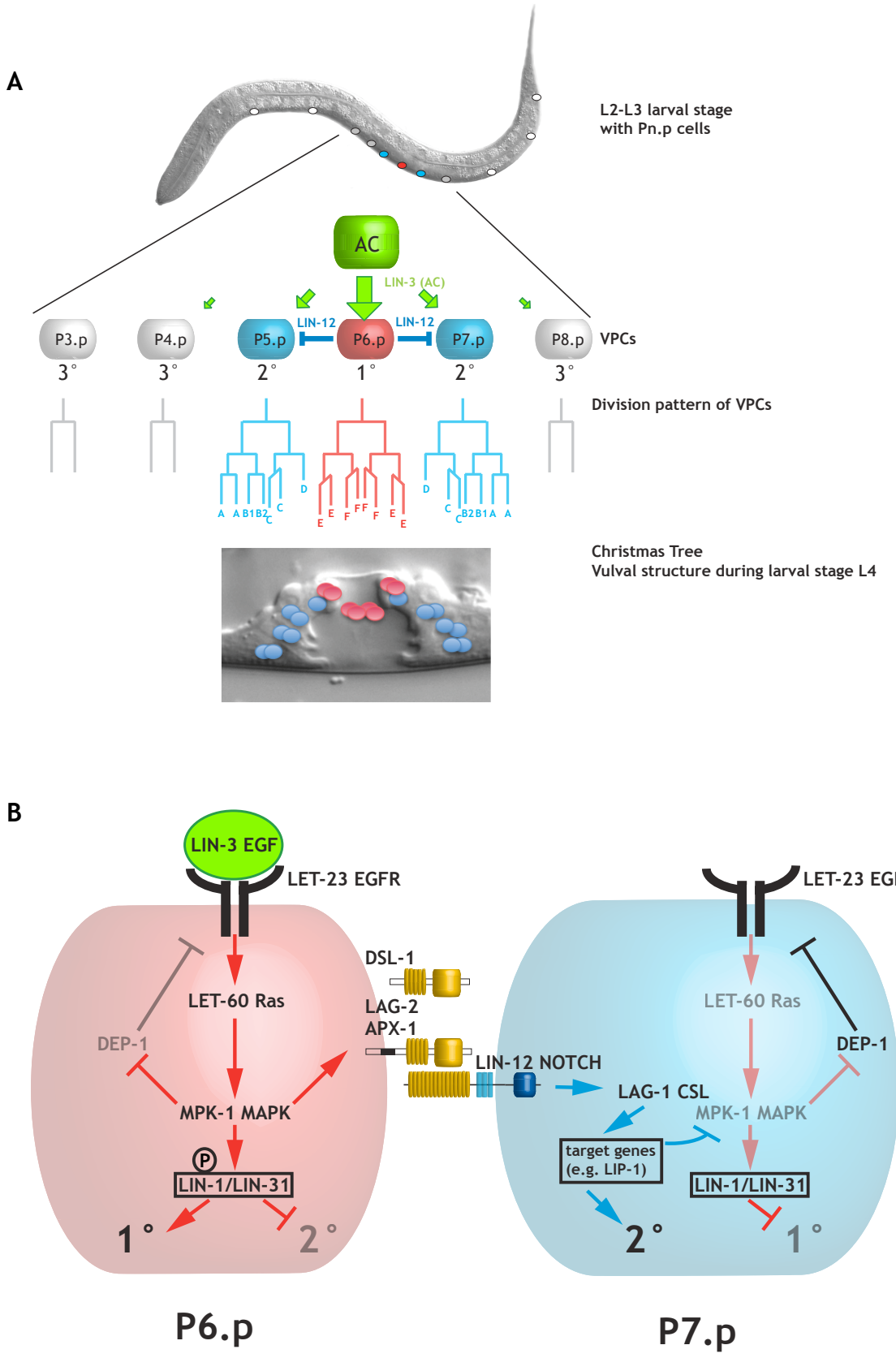

Figure 3: Signalling events during vulval cell fate specification.
(A) Six of eleven Pn.p cells form the vulval equivalence group (P3.p-P6.p). These six vulval precursor cells (VPCs) have the potential to adopt a vulval fate. A specific gonadal cell, the anchor cell (AC) initiates vulval development, leading to the primary (1°) fate in P6.p and

secondary fates (2°) in P5.p and P7.p. The tertiary (3°) fate is a non-vulval fate. Due to their fates VPCs undergo a specific division pattern and form special parts of the vulva. (B) In C. elegans the epidermal growth factor receptor (EGFR) LET-23 is activated by LIN-3 EGF and activates via LET-60 Ras the MPK-1 MAPK that phosphorylates the transcription factor complex LIN-1/LIN-31. Thus, 1° fate is established in P6.p. Activated MPK-1 MAPK additionally results in inhibition of the LET-23 EGFR phosphatase DEP-1 and in presentation of LIN-12 NOTCH ligands (DSL-1, LAG-2, APX-1) at the cell surface of P6.p. These LIN-12 NOTCH ligands activate the LIN-12 NOTCH receptor presented on the surface of P5.p and P7.p (Only P7.p is shown in this figure). Activation of LIN-12 NOTCH leads via LAG-1 CSL to the expression of target genes that inhibit 1° fate and promote 2° fate.

4.2 Cell cycle and developmental timing

Cell cycle regulation in *C. elegans*

The cell cycle is a key component of life. It is the main mechanism that allows an organism to grow and develop various kinds of tissues because the cell cycle produces "new" cells, the raw material needed for differentiation. Additionally, the cell cycle allows life to exist over time; cells and whole organisms just can generate descendants thanks to duplication of the genome (S phase) and segregation of chromosomes, organelles and cytoplasm to daughter cells (M phase).

In *C. elegans*, different cell cycle variations are used during development (van den Heuvel, 2005a, b) (Figure 4). There is the meiotic cell cycle that plays a role in the germline. The germ cells in the distal end of the gonadal tube are just partly enclosed by a plasma membrane and share a common cytoplasm. These cells undergo a prolonged meiotic prophase, to allow homologous chromosomes to condensate, pair and form crossovers. Only after fertilisation meiosis is completed and embryogenesis with a different cell cycle variation starts. The main features of the embryonic cell cycle are that it is mainly regulated by maternal products and it is very fast, because it abstains from the gap phases G1 and G2 (Edgar and McGhee, 1988). Only seven hours after fertilisation most of the embryonic cell divisions are completed. After several additional hours of differentiation and morphogenesis a L1 larva hatches consisting of 558 cells. During post-embryonic development 10 % of these cells proliferate and form a hermaphroditic organism out of 959 cells or a male nematode out of 1031 cells. Components of this cell cycle variation will be described in detail.

The endoreduplication cycle is the fourth variation. It lacks M phase and so it duplicates the DNA ploidy with each cycle. For example, this fourth variation plays a role in intestine development or formation of the hypodermis. Some of the intestinal cells undergo an endoreduplication at

the end of each larval stage, resulting in intestinal nuclei with a 32n DNA content in adults. Seam cells produce new hypodermal cells, which undergo an additional round of DNA replication before they fuse with the major hypodermal syncytium hyp7 (Hedgecock and White, 1985). Due to the increase in the number of gene copies more protein can be translated in a shorter time span, so the endoreduplication cycle may support cell growth.

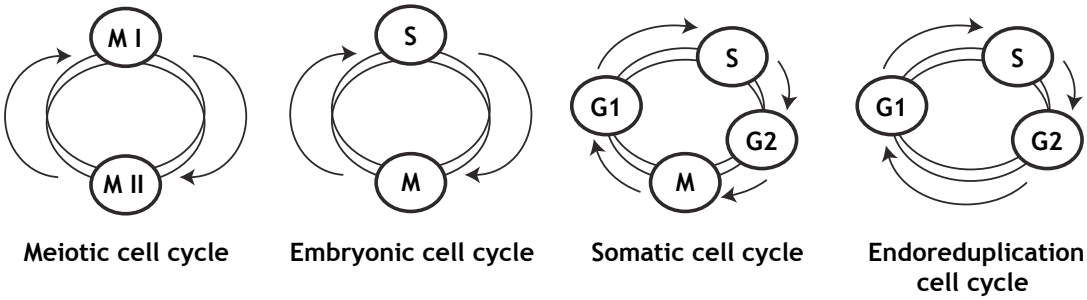

Figure 4: Cell cycle variations in *C. elegans*.
In *C. elegans* four different cell cycle variations are used during different developmental stages. (adapted from wormbook.org (van den Heuvel, 2005a))

Molecular components of the cell cycle

An important mechanism like the cell cycle has to be tightly regulated (van den Heuvel, 2005a). The more complex an organism is, the more complex is the regulation. For example, the single cell organism *Saccharomyces cerevisiae* uses only one cyclin dependent kinase (CDK) to modify target proteins and so promote cell cycle progression. However, *S. cerevisiae* uses different cyclins to distinguish and support the different cell cycle phases. *C. elegans* and other multicellular organisms use for each phase a different CDK. CDKs are small protein kinases that phosphorylate substrates at serine/threonine residues to influence their functionality. These CDKs themselves can be regulated by activating or inhibitory phosphorylation or dephosphorylation events. Additionally, CDKs need different cyclin subunits for their functionality and specificity. These cyclins provide another working point for regulation: During cell cycle progression they “cycle”, meaning they are expressed and degraded during specific cell cycle phases. A third possibility to regulate cell cycle progression is

provided by CDK inhibitory proteins that associate with CDKs and prevent their action.

In *C. elegans* one of the essential CDKs is CDK-4, a mammalian Cdk4/6 homologue. CDK-4 acts together with cyclin CYD-1 to promote progression through G1 phase (Park and Krause, 1999) (Figure 5). The CDK-4/CYD-1 complex is mainly needed for larval development, since mutant analysis revealed defects in only few and very late embryonic divisions (Boxem and van den Heuvel, 2001; Yanowitz and Fire, 2005).

Escape from G1 followed by transition into S phase is mediated by a complex out of CDK-2 and CYE-1 (Figure 5). RNAi against both components results next to sterility of adults also in embryonic lethality, leading to the assumption that CDK-2/CYE-1 plays additionally a role in embryogenesis (Boxem *et al*, 1999; Fay and Han, 2000).

The G2 phase cyclin dependent kinase CDK-1 shows highest similarity to the mammalian Cdk1 that is responsible for progression from G2 to M phase (Boxem *et al*, 1999) (Figure 5). Mutant analysis revealed that CDK-1 acts also in *C. elegans* during G2 phase since proper S phase marker expression could be detected in arrested post-embryonic precursor cells of loss-of-function (*lf*) mutants for *cdk-1* and endoreduplication cycles are not affected by mutations in *cdk-1* (van den Heuvel, 2005a). CDK-1 acts in complex with different cyclins of the subfamilies A and B. These cyclins can partly replace each other, suggesting overlapping functions (van der Voet *et al*, 2009).

In the *C. elegans* genome also homologous genes for Cdk7 and Cdk5 have been found. Wallenfang *et al*. suggest for CDK-7 a similar function like for mammalian Cdk7 as CDK-activating kinase and part of the RNA polymerase II phosphorylation complex (Wallenfang and Seydoux, 2002). CDK-5 is quite similar to human Cdk5 that plays a role in neuronal survival, differentiation and migration (Zhu *et al*, 2011).

For CDK-8 and CDK-9 so far no cell cycle related function could be discovered. In *C. elegans* they seem to be involved in transcriptional regulation (Liu and Kipreos, 2000; Shim *et al*, 2002). However, for

mammalian Cdk8 an additional function in post-translational protein regulation has been identified. Thus, next to the control of RNA polymerase II, Cdk8 together with Cyclin C coordinates turnover of the activated NOTCH intracellular domain (NICD) (Fryer *et al*, 2004; Leclerc and Leopold, 1996).

As already mentioned above, various mechanisms exist to regulate CDK activity, amongst them CDK inhibitory proteins. The *C. elegans* genome encodes one cyclin dependent kinase inhibitor (CKI), which is CKI-1, a close homologous gene to mammalian $p27^{Kip1}$. Like $p27^{Kip1}$, CKI-1 seems to promote cell cycle arrest throughout development (Hong *et al*, 1998). Fujita *et al*. proposed that CKI-1 inhibits specifically the CDK-2/CYE-1 complex and thus regulates G1 to S phase progression (Fujita *et al*, 2007). Furthermore, studies of mouse embryonic fibroblasts, lacking the mammalian homologues of CKI-1, revealed that the Cdk4/Cyclin D complex failed to assemble in the absence of CKI-1 activity (Cheng *et al*, 1999). Additionally, LaBaer *et al*. showed that mammalian homologues of CKI-1 promote the *in vitro* association of the Cdk4/Cyclin D complex and the direction of the Cdk4/Cyclin D complex to the nucleus (LaBaer *et al*, 1997). These facts support speculations about a positive effect of CKI-1 on CDK-4/CYD-1 assembly and activity also in *C. elegans*. Thus, CKI-1 might promote cell cycle arrest during G1 phase not only through inhibition of the transition to S phase but also through the stimulation of the activity of the G1 phase complex CDK-4/CYD-1 (Figure 5).

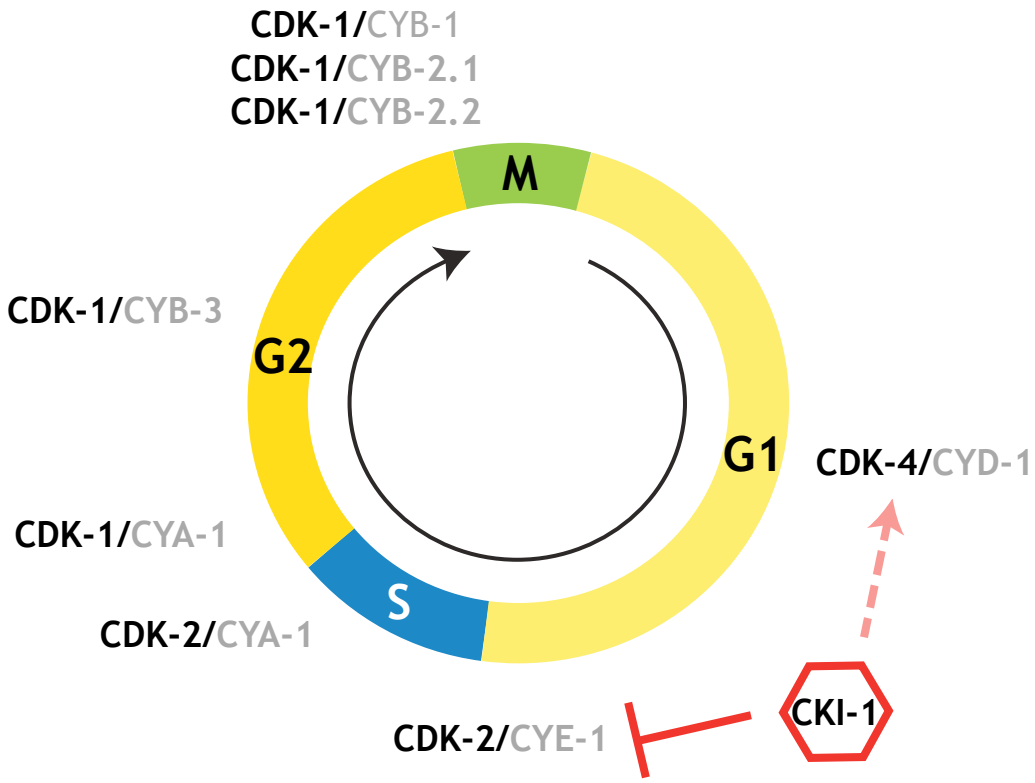

Figure 5: Relative timing of components during the *C. elegans* cell cycle.
Cyclin dependent kinases (CDKs) function in complex with their specific cyclins (grey) and drive the cell cycle through its phases M, G1, S and G2. The CDK inhibitor CKI-1 impairs CYE-2 (red inhibitory bar) in *C. elegans* and might activate CDK-4/CYD-1 (light red dashed arrow), what is suggested for its mammalian homologues. (Adapted from wormbook.org; Fujita *et al.*, Cheng *et al.* and LaBaer *et al.* (Cheng *et al*, 1999; Fujita *et al*, 2007; LaBaer *et al*, 1997))

Heterochronic genes

The cell cycle itself is not the essential mechanism for timing of development; it just provides a tool for the regulation by timing. The scheduler of developmental timing is probably provided by a different molecular mechanism: the pathway of heterochronic genes (Euling and Ambros, 1996). Defects in heterochronic genes show two different phenotypes. Either developmental events are skipped, so the specific heterochronic genes are called “precocious” or the developmental programs are reiterated, so the specific heterochronic genes show a “retarded” effect (Moss, 2007). Both phenotypes hint at a disruption of a global temporal mechanism controlling cell fates. For example, loss-of-function mutants for *lin-4*, which encodes for a microRNA, repeat lineage patterns specific for

the first larval stage also during the second larval stage: VPCs that are quiescent during L1 stage stay quiescent permanently and don't divide during L3 stage like VPCs in wild-type animals. On the other hand, nuclei of the intestinal syncytium that divide only during L1 stage continue to divide also during L2 stage (Chalfie *et al*, 1981; Sulston and Horvitz, 1981). An example for a precocious heterochronic gene is displayed by *lin-14*, which encodes a transcription factor. Animals with *lin-14(lf)* mutations suppress the retarded *lin-4* mutant phenotype (Ambros, 1989). On their own, *lin-14(lf)* mutants show premature appearance of stage specific developmental programs. For example, VPCs already divide during L2 stage rather than during L3 stage (Euling *et al*, 1996). Translation of *lin-14* messenger RNA seems to be negatively regulated by the *lin-4* microRNA (Lee *et al*, 1993; Wightman *et al*, 1993). Thus, both genes act in one pathway. *lin-14* induces L1 specific events, then *lin-4* accumulates and its expression peaks at the end of L1 leading to the repression of *lin-14* translation to prevent repetition of L1 specific programs and to allow rather L2 events to proceed. Additional heterochronic genes are involved in this process since one microRNA usually is insufficient to repress a specific messenger RNA. Other microRNAs cooperate to regulate target repression and additionally a positive feedback loop between *lin-14* and the cytoplasmic protein LIN-28 seems to exist, as reviewed by Eric Moss (Moss, 2007).

As a downstream effector of the heterochronic pathway in the VPCs the CDK inhibitor CKI-1 could be identified. In *lin-14*(*lf*) and *lin-28*(*lf*) animals the G1 phase of VPCs is five hours shorter and a precocious entry into S phase can be detected in these mutant strains (Euling *et al*, 1996). Additionally, expression of CKI-1 is reduced in *lin-14*(*lf*) animals. Thus, Hong *et al*. propose that the heterochronic gene *lin-14* and its negative regulator *lin-4* temporally regulate CKI-1 expression to control the timing of G1 to S transition in the VPCs (Hong *et al*, 1998).

Thus, generally speaking, the heterochronic pathway provides temporal switches for different developmental programs during specific larval stages. And the cell cycle provides the downstream target, setting the boundaries, in which specification and differentiation is allowed to happen.

4.3 Computational modelling

Computational models describing biological systems gain more and more importance due to the growing biological information that has to be stored, visualized and disclosed to researchers of other fields like chemistry, physics and others (Fisher and Piterman, 2010; Kitano, 2002). Before computational models became realisable thanks to computers that are able to calculate fast enough and thanks to their increasing possibility of capacity, mathematical models represented many situations in natural sciences. The core of mathematical models is the “transfer function” that is usually represented by a differential equation and that describes how quantities of substances change over time. The higher the number of transfer functions of a mathematical model, the more complex the model is. In contrast to mathematical models, computational models are hierarchical: They are composed out of objects that can adopt different states (Figure 6). Computer programs provide the recipe or rules according to that states may change. States of smaller objects define the state of the larger object that are composed of the smaller objects, like the state of a cell is defined by the states of its organelles, molecules, et cetera. Computational models can have a high number of states. The states are discrete: Either the object adopts a specific state or another one, but nothing in between. Thus, computational models are usually discrete. They are highly non-deterministic and non-linear, since they can be executed several times and always result in a different outcome, which is also often observed in biological systems.

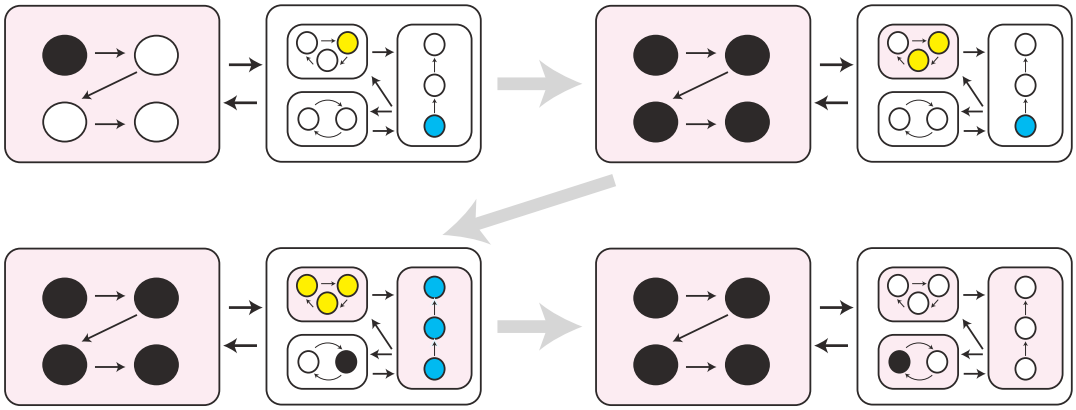

Figure 6: Two state machines communicate.
As example for computational modelling using state machines: Two boxes represent two state machines that consist out of different objects (small boxes and circles). Colour changes (black, yellow, blue) represent state changes of a single object. When an object with higher hierarchical level or a state machine itself turns into an activated state, this is indicated with a reddish background. Black arrows represent communication pathways, grey arrows indicate time passing.

There exist several efforts in research to describe biological systems via computational modelling (Fisher and Henzinger, 2007a). One of them uses state machines to resemble the behaviour of biological objects. A state machine yields the reactive system of the model, which consists of parallel processes and each process may change a state in reaction to another process changing a state (Figure 6). Thus, state machines may resemble cells communicating with each other and acting or reacting under different circumstances simultaneously. The advantage of this kind of model is that it does not require quantitative data relating to reaction rates but the biological system modelled has to be well understood in qualitative terms. For example Fisher *et al*. modelled vulval development of *C. elegans* based on collected experimental data (Fisher *et al*, 2007b; Fisher *et al*, 2005; Sternberg and Horvitz, 1989). Albeit an execution of the model could be used to check if the model or rather the distribution of the outcomes of several executions satisfy the data, it would be very time consuming and nearly impossible due to the possibility of repeated execution outcomes. Therefore, a technique called model checking is very helpful, because it analyses all of the various possible outcomes by exploring all the states and possible state changes of the model (Clarke *et al*, 1999). Thus, no execution at all is required and usually there are more possible executions than states.

If the model checking reveals that the model satisfies the data, then the model is quite accurate and new experimental data could be collected and compared to execution outcomes of the model. However, more interesting are cases where the computational model produces additional outcomes that are not present in nature. Then the model has to be extended by additional factors or mechanisms to restrict the outcomes to the experimental data. If the model cannot reproduce some experimental data, it has to be refined or completely revised (Figure 7). The challenge for biologists consists in finding the missing correcting component in real life or in designing new experiments to elucidate the additional outcomes if experimental data are incomplete. Hence, computational modelling helps in phrasing new questions and identifies loose points in our knowledge of well studied biological systems that easily might be overlooked in a different way of representation.

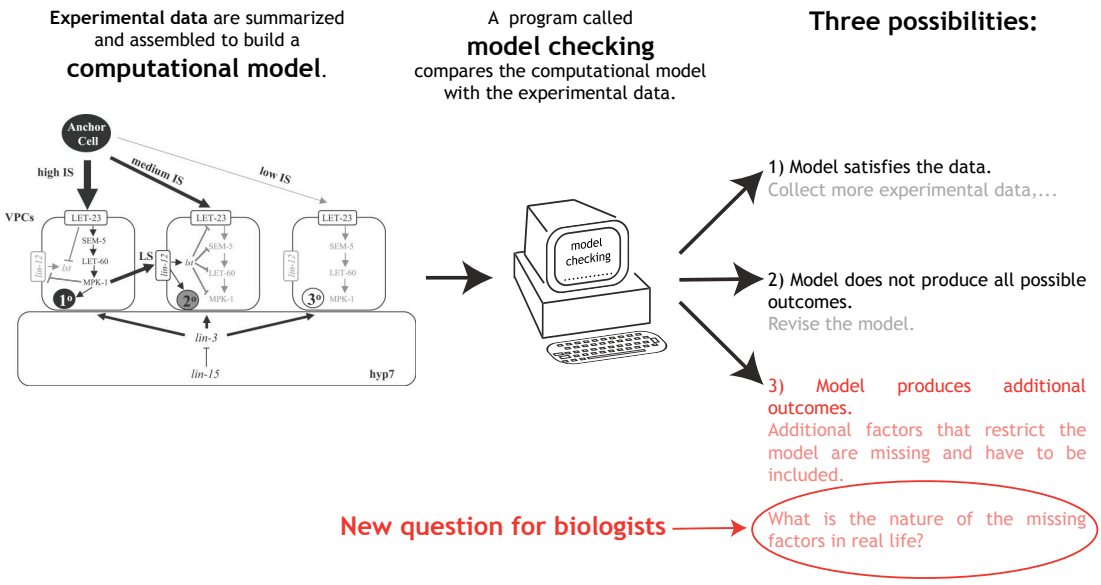

Figure 7: Computational modelling as a tool to phrase new biological questions.
Working principle of computational modelling and model checking (in discussion with Jasmin Fisher).

4.4 Nematode-specific transthyretin-like genes

The *C. elegans* genome codes for about 20,000 genes. Although the high divergence in size, shape, life cycle and behaviour of *C. elegans* compared to mammals is obvious, the small worm possesses more than 7,500 genes having human orthologues (Shaye and Greenwald, 2011). These genes are usually the main targets of research efforts, since they seem to be most relevant for humans and the knowledge about human diseases. Nevertheless, also genes that are nematode-specific can be quite interesting subjects for research.

The phylum of nematodes is the most abundant group of organisms with estimates adding up to 80 % of all animals on earth (Platt, 1994). The individual clades contain highly diverged strains that live in a variety of different niches including marine or terrestrial habitats (Figure 8). However, in each clade also plant and animal parasites can be found (Parkinson *et al*, 2004). Although the mortality caused by nematode infections is low compared to lung cancer or diabetes, in tropical regions the high number of 2.9 billion people are infected and impaired and annually 100,000 people die of these infections (Chan, 1997). Additionally, parasitic nematodes cause a considerable damage in farm animals and economic plant cultures (Barker *et al*, 1994). These facts highlight the need to investigate nematode-specific drugs and vaccines. At this point, the interest focuses on nematode-specific gene families as drug or vaccine targets. Ideally these genes also should be conserved between nematodes and essential for the worm's life cycle.

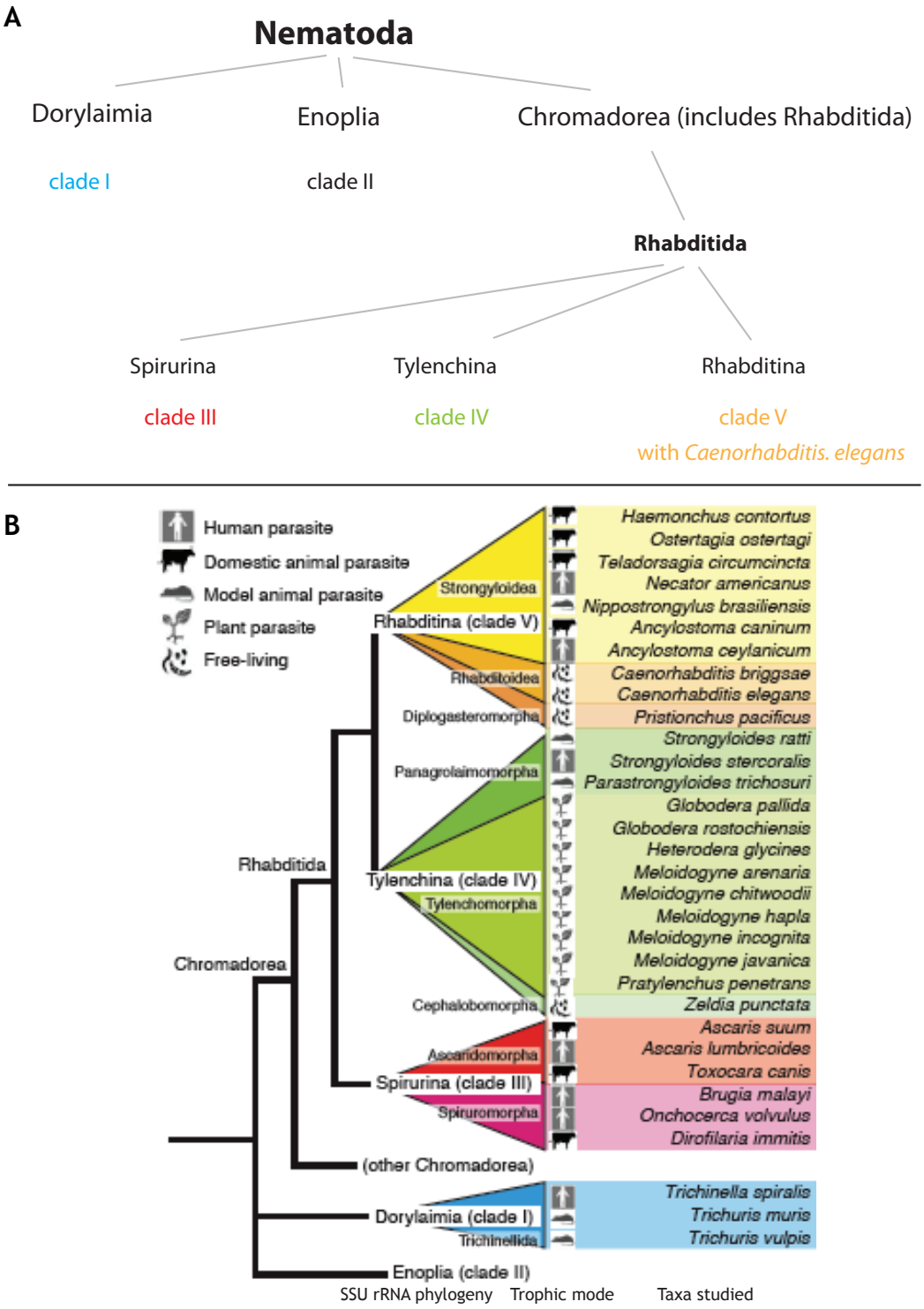

Figure 8: The phylum nematoda.
(A) The five major clades of nematodes are shown. *C. elegans* belongs to clade V. (B) In different clades several individual strains occupy different niches. For example, Rhabditina (clade V) can be found as parasites of animals or plants, but also free-living species like *C. elegans* belong to this clade. Adapted from Parkinson *et al.* (Parkinson *et al*, 2004)

One of the largest nematode-specific gene families is the *ttl* (transthyretin-like) family. TTLs have similarities in sequences to transthyretins (TTRs). However, TTRs are specific to vertebrates and responsible for the transport of thyroid hormones and associate with vitamin A_1. They could be found in the serum and other extracellular fluids and are produced in the liver and in a special structure of the ventricles in the brain called choroid plexus (Foss *et al*, 2005). Several human diseases are known, caused by mutations of TTR. The most common one is amyloidosis (Connors *et al*, 2003). Hennebry *et al*. hypothesise that TTRs and TTLs have evolved from transthyretin related proteins (TRPs) that are found in a much broader range of species longing from bacteria to vertebrates and even plants (Hennebry *et al*, 2006). (She refers to them as TLPs, transthyretin-like proteins, however, since this term in this work is also used for transthyretin-like protein family (TTL) they are here called TRPs.) TRPs function in different metabolic pathways, as the oxidation of uric acid in *Salmonella dublin* (Lee *et al*, 2005) or in brassinosteroid signalling in *Arabidopsis thaliana* (Li, 2005).

However, the role of the nematode-specific TTLs remains largely unknown till this day. Only the function of one of the 59 members, *ttr-52*, could be enlightened so far. It plays a role in recognition of apoptotic cells by CED-1, which leads to engulfment of the cell corpses in the nematode's germline (Wang *et al*).

In the Hajnal lab one member of the TTLs was identified in a reverse genetic screen for LIN-12 NOTCH targets: RNAi against *ttr-11* resulted in diminished secondary cell fate marker expression suggesting a role in NOTCH signalling (Rimann, 2008). Interestingly, TTR in mammals might influence the cleavage process of the amyloid precursor protein (APP) that is involved in Alzheimer's disease (Costa *et al*, 2008). Both proteins, APP and NOTCH are cleaved in a similar manner (Kopan and Goate, 2000). These facts make *ttr-11* to an interesting candidate to be involved in the cleavage process of the NOTCH receptor in *C. elegans*.

5 AIM OF THE PRESENT STUDY

NOTCH signalling is investigated by many research groups due to its importance during proper development of the human organs such as specification of cell fates in the developing nervous system (Gaiano and Fishell, 2002) or during arteriogenesis and angiogenesis (Liu *et al*, 2003). Moreover, the NOTCH signalling pathway is deregulated in several cancer cell lines (Weijzen *et al*, 2002; Weng *et al*, 2004; Zagouras *et al*, 1995). Nowadays the core components of the NOTCH signalling pathway are known quite well. This is also true for LIN-12 NOTCH signalling during *C. elegans* vulval development. However, there is still a gap in our knowledge about downstream targets and modifiers of the NOTCH pathway. For example, in *C. elegans* no NOTCH target gene that promotes the 2° vulval fate is known so far, only the LIN-12 NOTCH targets *lip-1*, *dpy-23*, *lst-1*, *lst-2* and *lst-3* are known to inhibit the 1° cell fate in 2° cells (Berset *et al*, 2001,Yoo, 2004 #64). The nematode *C. elegans* provides a suitable model system and relative simple tools exist to address these questions of NOTCH targets and modifiers and several screens to identify LIN-12 NOTCH downstream targets had been done in the Hajnal lab (Farooqui, 2012; Rimann, 2008).

The gene *ttr-11* was identified in one of these screens and seemed to be a promising NOTCH downstream target and/or possible modifier of NOTCH signalling due to its predicted peptidase activity (Rimann, 2008). Therefore, one aim of my PhD was to characterise the gene *ttr-11*, analyse its transcriptional regulation and investigate its function during vulval development and its possible effect on lateral LIN-12 NOTCH signalling (Chapter 6.3).

While the study of *ttr-11* was ongoing, Jasmin Fisher, Nir Piterman and Antje Beyer at Microsoft Research Cambridge modelled *in silico* vulval development. They came across the question if some boundaries that might be represented by the progression through cell cycle could be necessary for

a proper fate specification. With this question in mind a tight collaboration started with Jasmin Fisher's group. The first experiments we did in the Hajnal lab indeed showed a connection between cell cycle progression and VPC signalling and in particular LIN-12 NOTCH signalling. Therefore, cell cycle checkpoints can be designated as modifiers of LIN-12 NOTCH signalling. Further investigations were aimed to identify the components of the NOTCH signalling pathway on the one hand and the cell cycle components on the other, which mediate this connection. Additionally, attempts were made to illuminate the detailed molecular mechanism lying behind this connection. Finally, expression patterns of single cell cycle components were investigated to test if NOTCH signalling itself has an impact on its own modifier, the cell cycle. (Chapter 6.1 and 6.2)

This second project that was started as a side project, became more and more interesting and promising during the time of my PhD. Finally, it replaced the project addressing the gene *ttr-11* in interest and importance. Therefore, the research focus during my PhD changed over time and the investigation of *ttr-11* moved to the second place. For this reason, this thesis first describes how NOTCH signalling is influenced by cell cycle progression and then it addresses *ttr-11* as putative NOTCH signalling target.

6 RESULTS

6.1 Manuscript: Cell-cycle regulation of NOTCH signaling during *C. elegans* vulval development. Nusser-Stein *et al*. (Molecular Systems Biology, in press)

Molecular Systems Biology 8; Article number 618; doi:10.1038/msb.2012.51
Citation: ***Molecular Systems Biology*** **8:618**

www.molecularsystemsbiology.com

molecular systems biology

Cell-cycle regulation of NOTCH signaling during *C. elegans* vulval development

Stefanie Nusser-Stein[1,2], Antje Beyer[3], Ivo Rimann[1], Magdalene Adamczyk[1,2], Nir Piterman[4], Alex Hajnal[1,*] and Jasmin Fisher[5,*]

[1] Institute of Molecular Life Sciences, University of Zürich, Zürich, Switzerland, [2] Molecular Life Sciences PhD program, Uni ETH Zürich, Switzerland, [3] Department of Genetics, University of Cambridge, Cambridge, UK, [4] Department of Computer Science, University of Leicester, Leicester, UK and [5] Microsoft Research Cambridge, Cambridge, UK
* Corresponding authors. A Hajnal, Institute of Molecular Life Sciences, University of Zürich, Winterthurerstrasse 190, Zürich 8057, Switzerland. Tel.: +41 44 635 4854; Fax: +41 44 635 6898; E-mail: alex.hajnal@imls.uzh.ch or J Fisher, Microsoft Research Cambridge, 7 JJ Thomson Avenue, Cambridge CB3 0FB, UK. Tel.: +44 1223 479 947; Fax: +44 1223 479 999; E-mail: jasmin.fisher@microsoft.com

Received 5.3.12; accepted 4.9.12

C. elegans **vulval development is one of the best-characterized systems to study cell fate specification during organogenesis. The detailed knowledge of the signaling pathways determining vulval precursor cell (VPC) fates permitted us to create a computational model based on the antagonistic interactions between the epidermal growth factor receptor (EGFR)/RAS/MAPK and the NOTCH pathways that specify the primary and secondary fates, respectively. A key notion of our model is called *bounded asynchrony*, which predicts that a limited degree of asynchrony in the progression of the VPCs is necessary to break their equivalence. While searching for a molecular mechanism underlying *bounded asynchrony*, we discovered that the termination of NOTCH signaling is tightly linked to cell-cycle progression. When single VPCs were arrested in the G1 phase, intracellular NOTCH failed to be degraded, resulting in a mixed primary/secondary cell fate. Moreover, the G1 cyclins CYD-1 and CYE-1 stabilize NOTCH, while the G2 cyclin CYB-3 promotes NOTCH degradation. Our findings reveal a synchronization mechanism that coordinates NOTCH signaling with cell-cycle progression and thus permits the formation of a stable cell fate pattern.**
Molecular Systems Biology **8:** 618; published online 9 October 2012; doi:10.1038/msb.2012.51
Subject Categories: development; cell cycle
Keywords: Caenorhabditis elegans; cell cycle; modeling; NOTCH; signal transduction

Introduction

During metazoan development, NOTCH signaling is involved in a multitude of cell fate decisions, especially when single cells are selected from a group of equivalent precursor cells (Fanto and Mlodzik, 1999; Baron *et al*, 2002). Well-studied examples include *Drosophila* wing formation, mammalian angiogenesis (Liu *et al*, 2003), or neuronal fate decisions (Hitoshi *et al*, 2002; Aguirre *et al*, 2010). Moreover, the NOTCH pathway is deregulated in different types of human cancer (Stylianou *et al*, 2006; Sharma *et al*, 2007). The binding of a DSL (Delta/Serrate/LAG-2) family NOTCH ligand activates two specific proteolytic cleavage events that result in the release of the NOTCH intracellular domain (NICD) from the plasma membrane (Baron, 2003). NICD then enters the nucleus, where it interacts with CSL (CBF1, Suppressor of Hairless, LAG-1) family transcription factors to induce the expression of target genes. Therefore, NOTCH signaling is often used as a cell fate switch that can be rapidly turned on. However, since NOTCH signaling also needs to be turned off at specific time points, the turnover of NICD in the nucleus is a critical aspect of NOTCH signaling. Experiments with mammalian cells have shown that NICD phosphorylation and/or deacetylation targets it for degradation (Fryer *et al*, 2004; Guarani *et al*, 2011). Furthermore, the F-box and WD repeat containing protein SEL-10/Fbw7 inhibits NOTCH signaling by inducing ubiquitination leading to proteasomal degradation of NICD (Hubbard *et al*, 1997; Gupta-Rossi *et al*, 2001). However, the specific mechanisms regulating NICD stability are largely unknown.

The development of the *Caenorhabditis elegans* hermaphrodite vulva is one of the best-studied systems to investigate the molecular mechanisms governing cell fate determination during organogenesis (Sternberg, 2005). NOTCH signaling has a prominent role in this process (Greenwald, 2005; Sundaram, 2005). During vulval induction, an organizer cell in the somatic gonad, called anchor cell (AC), induces the adjacent VPC P6.p the primary (1°) vulval cell fate by activating the epidermal growth factor receptor (EGFR) signaling pathway (Figure 1A). As a consequence of adopting the 1° fate, P6.p expresses the DSL ligands that activate lateral LIN-12 NOTCH signaling in the neighboring VPCs P5.p and P7.p. NOTCH signaling in P5.p and P7.p prevents these cells from adopting the 1° fate and induces the alternate secondary (2°) fate (blue arrows in Figure 1A). On the other hand, EGFR/RAS/MAPK signaling in P6.p inhibits NOTCH signaling by promoting the endocytosis and subsequent lysosomal degradation of LIN-12 NOTCH, thus allowing P6.p to irreversibly adopt the 1° cell fate (Shaye and Greenwald, 2002). The precise timing of the activation and inactivation of the EGFR/RAS/MAPK and

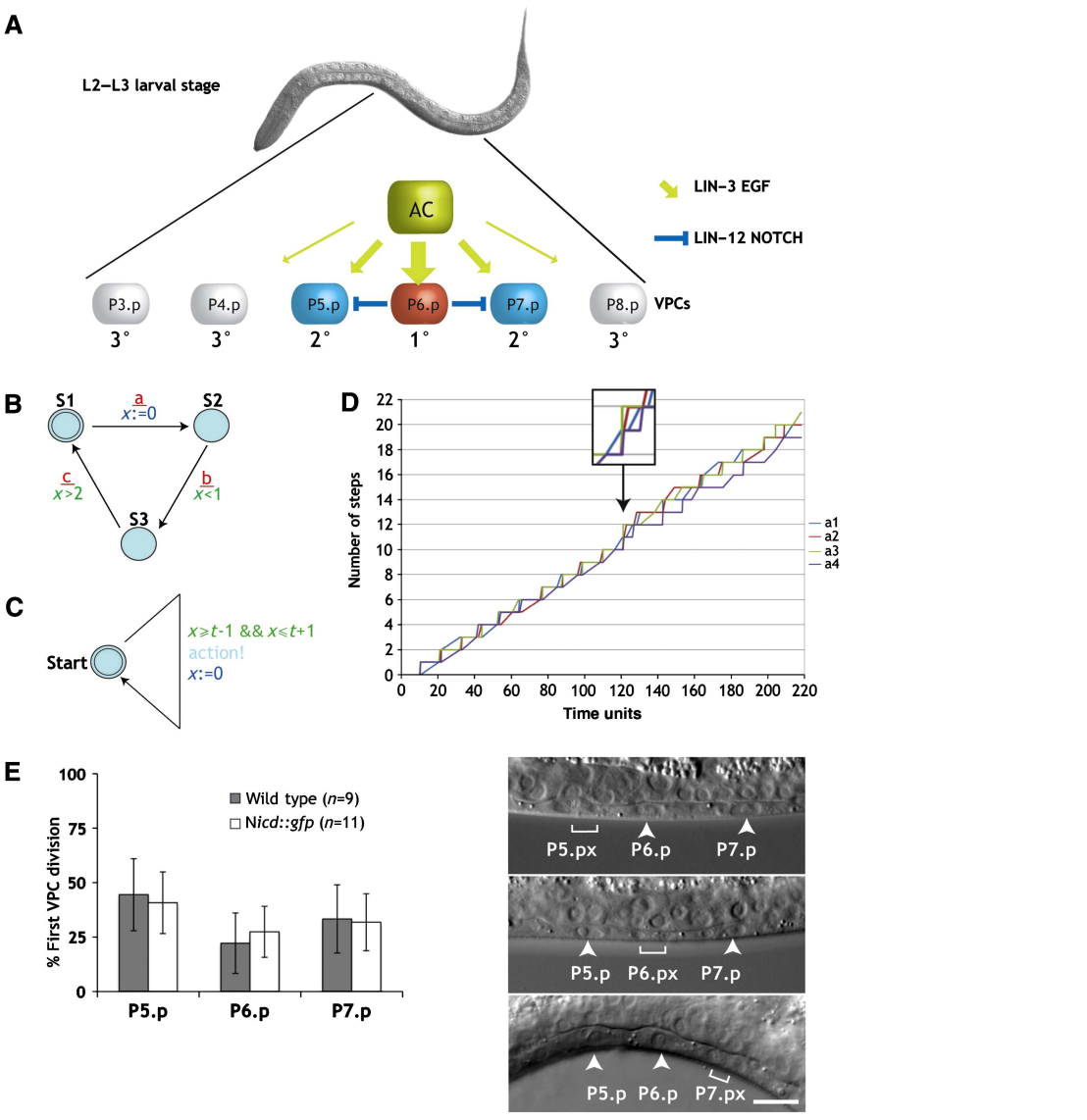

Figure 1 A model for *bounded asynchrony* during VPC differentiation. (**A**) Intercellular signals determining the VPC fates. The AC signal induces the 1° fate in P6.p. P6.p then inhibits its neighbors P5.p and P7.p via lateral LIN-12 NOTCH signaling from adopting the 1° fate and induces the 2° fate. (**B**) An example illustrating the concept of timed automata. This automaton outputs possible sequences of a, b, and c events. The automaton starts in state S1 from where it can transit to state S2, signaling this with event a. After this transition, the automaton starts measuring time by setting clock *x* to 0. Then, the transition from S2 to S3 (with output event b) has to occur <1 time unit after a, and the transition from S3 back to S1 (with output event c) has to occur at least 2 time units after a. Overall, the observable communication events are rounds of a, b, and c events, where b is <1 time unit after a and c is at least 2 time units after a. There is no restriction on the time of the next a. (**C**) A timed automaton modeling an independent scheduler. A run starts in the state start and sets the clock *x* to 0. The automaton can perform an action between time $t-1$ and time $t+1$, and once it performs the action starts counting time again to the next action. Possible behaviors include sequences of actions where the time between every two actions is between $t-1$ and $t+1$. Running an independent copy of this automaton in each VPC gives rise to bounded asynchrony. (**D**) Random simulation of four copies of the timed automaton shown in (C) running in parallel. Every automaton moves between 9 and 11 time units. The first point where one process makes two actions more than another process is after 120 time units where a3 action was performed 12 times and a4 actions only 10 times (arrow and magnification). The earliest time point where such a difference is theoretically possible is after 99 time units, when a process moving very fast could perform 11 actions and a process moving very slowly could perform 9 actions. (**E**) The 1° and 2° VPCs divide asynchronously without a significant bias for one VPC entering M phase before the others. VPC divisions were observed in wild-type (gray bars) and *nicd::gfp* (white bars, see below) animals. The panels to the right show three examples of asynchronous VPC divisions where the brackets indicate the dividing VPC and the arrowheads the undivided VPCs. Error bars indicate the standard error as described in Materials and methods. The scale bar represents 10 μm. Source data is available for this figure in the Supplementary Information.

NOTCH signaling pathways is essential to achieve a robust cell fate pattern during vulval development (Euling and Ambros, 1996; Ambros, 1999; Shaye and Greenwald, 2002; Fisher *et al*, 2007). One important question is therefore to identify the molecular mechanisms that link these signaling pathways to the temporal regulation of vulval development.

Computational models are excellent tools to describe and systematically analyze the dynamic behavior of a biological system and generate new hypotheses that can be tested experimentally (Kitano, 2002; Fisher and Henzinger, 2007). To this aim, we have previously developed a state-based computational model incorporating the current mechanistic

understanding of gene interactions during *C. elegans* vulval development (Fisher *et al*, 2005). State-based models are particularly suitable for building mechanistic models of such well-studied biological systems, as they do not require quantitative data relating to the number of molecules or reaction rates. One characteristic feature of our model was the inclusion of multiple modes of crosstalk between the EGFR/RAS/MAPK and LIN-12 NOTCH signaling pathways (Berset *et al*, 2001; Fisher *et al*, 2007). Our computational model defines the behavior of biological objects (i.e., the VPCs) over time, based on the various states that an object can enter over its lifetime. *Interacting* state machines specify causal relationships between state changes in different objects to describe how objects communicate and collaborate. Usually, the state of an object is determined by the states of its parts such as the genes or proteins regulating the process of interest. Each part has its own reaction to the states of other parts. Changes in the state of an object are thus determined by the interdependent state changes of all parts. A hierarchical structure allows one to view a system at different levels of detail. State-based models have previously been used to model a variety of processes such as T-cell activation and differentiation in the thymus (Kam *et al*, 2001; Efroni *et al*, 2003, 2005), or pancreatic development (Setty *et al*, 2008).

In this study, we tested through an iterative process of computational modeling, prediction, and experimentation whether cell-cycle progression could provide a mechanism that coordinates the temporal activities of the different signaling pathways involved in VPC fate specification. Although the VPCs progress through the cell cycle in a largely cell-autonomous manner, global synchronization mechanisms imposed by the heterochronic genes that regulate cell-cycle checkpoints may prevent the VPCs from progressing in an uncoordinated manner (Euling and Ambros, 1996; van den Heuvel, 2005). To test this idea, we arrested cell-cycle progression in individual VPCs to 'de-synchronize' them. As predicted by our computational model based on *bounded asynchrony* (Fisher *et al*, 2008), this perturbation prevented VPCs from adopting a stable cell fate. Moreover, we found a synchronization mechanism acting on the NOTCH signaling pathway. In particular, the termination of the NOTCH signal is tightly coupled to cell-cycle progression, as the degradation of NICD occurs only after entry into the G2 phase. Thus, the formation of a stable cell fate pattern during vulval development involves a strict temporal control of NOTCH signaling during cell-cycle progression.

Results

A state-based model for VPC differentiation based on bounded asynchrony

Our previous models of *C. elegans* vulval development used high-level abstractions and described the biological process with an interacting state machine (Fisher *et al*, 2005, 2007). These models were constructed by defining the behavior of sub-components and then letting them work in parallel. In our initial model, there were six identical sub-components, each representing one VPC. There are two standard notions of such parallel composition: synchronous composition and asynchronous composition. Using synchronous composition, all sub-components perform actions together exactly at the same time. When we tried to model the VPC interactions, we found that a synchronous composition was too rigid, making it impossible to break the symmetry within the VPC equivalence group without introducing additional mechanisms for breaking symmetry. Indeed, as the VPCs are equipotent, they all proceeded in exactly the same way and it was only possible to differentiate them if they experienced differences in their environment. For example, in the case of mutants displaying an alternating 1° and 2° fate pattern, a model with a perfectly synchronous progression resulted in all VPCs adopting the 1° cell fate. On the other hand, using an asynchronous composition, where every sub-component performs actions independently, it was possible to differentiate the VPCs. However, some VPCs adopted a 1° instead of a 2° fate because they did not sense the progress of their neighbors and proceeded much faster than others. A completely asynchronous model of VPC differentiation therefore resulted in a variable and unpredictable pattern of cell fates due to excess 'noise' in the temporal progression of the VPCs. To limit the degree of asynchrony between the VPCs, we introduced the concept of *bounded asynchrony*, a notion of concurrency tailored to the modeling of biological cell–cell interactions (Fisher *et al*, 2008). *Bounded asynchrony* is achieved via a scheduler that limits the number of steps that one VPC is allowed to get ahead of the others. This allows the components of a system to move independently, while keeping them coupled to a certain degree. The constrained non-deterministic nature of a model incorporating *bounded asynchrony* captures the variability observed in cells that, although equipotent, assume distinct fates. Although a scheduler may be an artificial mechanism, it does highlight the need to precisely coordinate the timing of different events between the VPCs. Hence, we searched for a distributed computational mechanism that can keep the VPCs together for a long time and requires infrequent global synchronizations. Such a mechanism seems plausible since global synchronization mechanisms do exist in many biological systems including VPC differentiation (Euling and Ambros, 1996). Here, we used timed automata to build such a mechanism (Alur and Dill, 1994). The general principle of timed automata is illustrated in Figure 1B. Abstractly, each timed automaton represents a VPC that takes approximately t time units to perform an action (Figure 1C). We therefore allowed the timed automaton to perform the action between times $t-1$ and $t+1$. Depending on the value of t, the system can perform approximately t rounds (i.e., every cell t actions), allowing each cell to perform at the maximum one more action than the other cells. A simulation composed of four such timed automata, where each automaton moves after $\sim$10 time units, is shown in Figure 1D. In this exemplary simulation, up to time point 120 the difference in number of steps between cells (Δx) does not exceed 1. At time point 120, 'cell' a3 (green line) has taken 12 steps, while 'cell' a4 (violet line) has only taken 10 steps ($\Delta x = 2$). The mechanism ensures that $\Delta x = 1$ up to time point 99, after which the potential difference increases gradually. If an additional mechanism synchronizes these automata every 100 time units, then the difference Δx will continue to be restricted to 1 indefinitely. Thus, a model that

combines approximate time keeping together with global synchronization might be an appropriate way to represent the variability that is inherent to all cellular systems.

VPCs enter M phase in a random order

One feature of *bounded asynchrony* is the fact that the sub-components may enter the next state in an arbitrary order. If VPC differentiation was to be governed by a mechanism resembling *bounded asynchrony*, then the VPCs should indeed progress through the cell cycle in a slightly asynchronous manner. To address this question, we examined the order in which the VPCs enter the M phase of the cell cycle. For this purpose, we observed the divisions of the proximal VPCs P5.p, P6.p, and P7.p in wild-type larvae using Nomarski optics and scored the time of entry into prometaphase based on nuclear envelope breakdown (Figure 1E). Among the three proximal VPCs, we observed no bias in the order at which they entered M phase, as each of the three VPCs was equally likely to divide first. Using time-lapse imaging, we measured the temporal differences in VPC divisions. The average time span between the first and last proximal VPC divisions was 33.4 min with a maximum divergence of 71 min ($n = 6$). These results indicate that the VPCs adopting 1° and 2° cell fates do indeed enter the M phase in a random order, suggesting that the cell cycle of the VPCs progresses in a slightly asynchronous and unbiased manner.

Cell-cycle arrest interferes with VPC fate specification

We next tested the biological significance of the computational concept of *bounded asynchrony* by manipulating the cell cycle in single VPCs. We hypothesized that, although the VPCs progress with slightly variable speed through the cell cycle, external mechanisms may keep them 'more or less' synchronized and thereby align the relative timing of the signal transduction events between the VPCs. Under this assumption, the repeated use of cell-cycle checkpoints may represent such a synchronization mechanism. The VPCs are born during the first larval stage and remain in the G1 phase until the transition from the second to the third larval stage (Euling and Ambros, 1996). During the second larval stage, 1° cell fate markers can be detected in P6.p, but the other five VPCs remain uncommitted (Ambros, 1999). After the G1/S-phase arrest has been relieved, P5.p and P7.p adopt the 2° fate during the G2 phase, while the 3°, uninduced fate of the distal VPCs (P3.p, P4.p, and P8.p) is only sealed after these cells have divided and fused with the surrounding hypodermis (hyp7).

We therefore performed an experiment to specifically arrest the cell cycle in P6.p without affecting the progression of the other VPCs. For this purpose, we expressed the cyclin-dependent kinase (CDK) inhibitor *cki-1* under control of the 1° fate-specific *egl-17* promoter (*egl-17p::cki-1*) to arrest P6.p in the G1 phase without affecting cell-cycle progression in the other VPCs (Hong *et al*, 1998). We then observed the effect of this intervention on the VPC fate specification using 1° and 2° cell fate markers. As a readout for the 1° cell fate, we used a transcriptional *gfp* reporter of the RAS/MAP kinase target *egl-17* (Burdine *et al*, 1998), and for the 2° fate, we observed a reporter of the LIN-12 NOTCH target *lip-1* (Berset *et al*, 2001).

In *egl-17p::cki-1* animals, in which P6.p was arrested and P5.p and P7.p had progressed to the Pn.px or Pn.pxx stage, expression of the 2° fate marker *lip-1p::gfp* persisted in the undivided P6.p cells at levels that were significantly higher than those detected in control animals (Figure 2A). To rule out the possibility that the differences in *lip-1p::gfp* levels between arrested and non-arrested cells are due to a dilution of the GFP signal during the cell divisions, we corrected the signal intensities for the total nuclear areas. Even with this correction, we detected a significant difference in total *lip-1p::gfp* signal intensity between arrested P6.p and non-arrested P6.p descendants (Supplementary Figure S1). Furthermore, expression of the 1° fate marker *egl-17p::gfp* in arrested P6.p cells was not affected (Supplementary Figure S2), confirming the previous observation that 1° fate specification begins already during the G1 phase (Ambros, 1999). However, our results also indicate that G1-arrested P6.p cells could not establish a fate-specific gene expression pattern, as they simultaneously expressed 1° and 2° cell fate markers. We conclude that a coordinated cell-cycle progression of the VPCs is necessary for the specification of a stable cell fate as judged by the expression of cell-fate markers.

Termination of NOTCH signaling is linked to cell-cycle progression

The finding that G1-arrested P6.p cells continued to express the 2° cell fate marker suggested that G1 cell-cycle arrest in P6.p might block the proper termination of LIN-12 NOTCH signaling. To investigate this possibility, we examined the expression of a functional, translational LIN-12::GFP reporter that reflects the expression pattern and sub-cellular localization of the endogenous LIN-12 protein (Levitan and Greenwald, 1998; Shaye and Greenwald, 2002). Before vulval induction, LIN-12::GFP is expressed at low levels in all VPCs. Most of the LIN-12 protein is localized to the apical plasma membrane of the VPCs. After vulval induction, LIN-12 is upregulated in the 2° P5.p and P7.p lineages and downregulated in the 1° P6.p lineage.

In control animals lacking the *egl-17p::cki-1* transgene, LIN-12::GFP was absent from the 1° P6.p descendants at the Pn.px stage, because LIN-12 NOTCH undergoes rapid endocytosis and degradation in the 1° lineage (Shaye and Greenwald, 2002). In contrast, in *egl-17p::cki-1* transgenic animals at the Pn.px stage, in which P6.p had remained undivided, we detected elevated levels of LIN-12::GFP in the cytoplasm and nucleus of P6.p (Figure 2B). However, the LIN-12::GFP signal was lost from the apical plasma membrane, indicating that the endocytosis of the full-length LIN-12 protein in P6.p is not affected by G1 arrest. Since the GFP tag in LIN-12::GFP is inserted in the intracellular domain (NICD) that is cleaved off the transmembrane domain during LIN-12 NOTCH activation, the persisting cytoplasmic and nuclear GFP signal in G1-arrested P6.p cells suggested that the downregulation of the cleaved, intracellular LIN-12 NICD occurs only after exit from the G1 phase. In this way, the termination of the LIN-12 NOTCH signal in the 1° lineage might be coupled to cell-cycle progression.

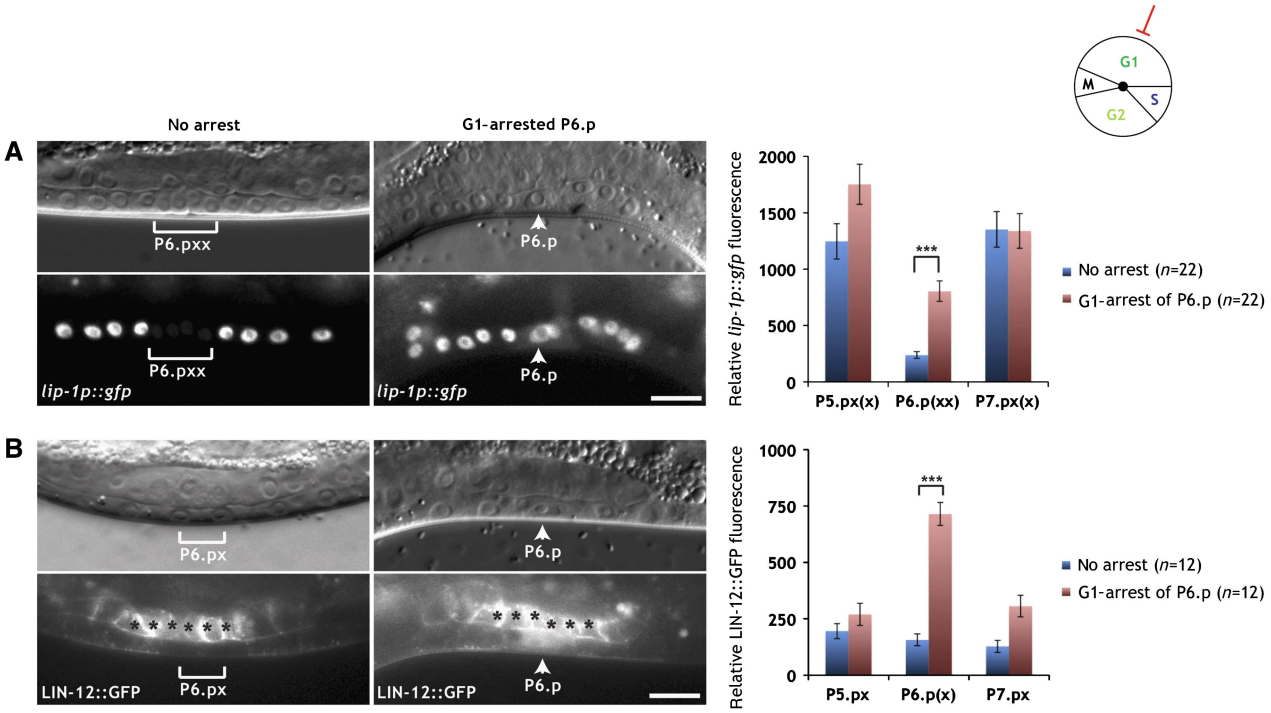

Figure 2 Degradation of LIN-12 NOTCH is blocked in G1-arrested P6.p. (**A**) Expression of the 2° fate marker *lip-1p::gfp* persists in the G1-arrested P6.p cell of an *egl-17p::cki-1* transgenic animal (arrowheads in the right panels), while *lip-1p::gfp* expression is downregulated in the P6.p descendants of a sibling that had lost the *egl-17p::cki-1* array (brackets in the left panels). (**B**) LIN-12::GFP persists in the G1-arrested P6.p cell of an *egl-17p::cki-1* transgenic animal (arrowheads in the right panels), while LIN-12::GFP is efficiently degraded in the P6.p descendants of a sibling that had lost the *egl-17p::cki-1* array (brackets in the left panels). Note the accumulation of the GFP signal in the nucleus and cytoplasm of the arrested P6.p cell. Black asterisks denote uterine LIN-12::GFP expression. In all panels, the corresponding Nomarski images are shown on top. The scale bars represent 10 μm. Quantifications of *lip-1p::gfp* and intracellular LIN-12::GFP expression are shown to the right. Error bars indicate the standard error and asterisks indicate the significance as described in Materials and methods. Source data is available for this figure in the Supplementary Information.

Degradation of NICD is blocked in G1-arrested VPCs

To directly test the connection between lateral signaling, NICD degradation, and the cell cycle, we integrated via the MosSCI technique (Frokjaer-Jensen *et al*, 2008) a single copy of an *nicd::gfp* transgene expressed under control of a *bar-1* promoter fragment into the genome at a specific site on chromosome II (*zhIs39[nicd::gfp]*). Importantly, the *bar-1* promoter fragment used drives uniform expression in the six VPCs and their descendants until the Pn.pxx stage (Natarajan *et al*, 2004; Figure 6A). Thanks to the single copy integration, we achieved a stable and reproducible NICD::GFP expression in the VPCs. The increased dosage of NOTCH signaling caused by *nicd::gfp* resulted in the ectopic induction of the 2° fate in P3.p, P4.p and P8.p and a Multivulva phenotype in all of the animals examined (Table I, row 1; Supplementary Figure S3). However, P6.p in *nicd::gfp* animals still adopted the 1° fate as determined by its cell lineage (see insets in Supplementary Figure S3). Moreover, the proximal VPCs in *nicd::gfp* animals entered M phase in a random order similar to the wild type (Figure 1E).

We next performed a time-course analysis to follow NICD::GFP degradation in the induced VPCs and their descendants (Figure 3A and B). NICD::GFP was uniformly expressed in the VPCs of early L2 larvae (+24 h relative to hatching, see Materials and methods). Interestingly, NICD::GFP expression first increased until the mid L2 stage (+27 h) and then started to decline in all VPCs. A significant difference between the 1° and 2° VPCs could first be detected at +32 h, shortly before the first VPCs started dividing (Figure 3A). After this time point, NICD::GFP expression rapidly faded in P6.p. At the Pn.px stage, NICD::GFP was barely detectable in the 1° P6.p descendants, while expression persisted in the 2° P5.p and P7.p descendants, though at lower levels when compared with Pn.p stage animals (right panel in Figure 3B). By the Pn.pxx stage, NICD::GFP was undetectable in P6.p descendants and further reduced in P5.p and P.7.p descendants. Similarly to full-length LIN-12::GFP, NICD::GFP in *egl-17p::cki-1* animals persisted in the nuclei of the arrested P6.p cells (Figure 3C). Thus, NICD::GFP is progressively degraded in the induced VPCs and their descendants. Though, the rate of NICD degradation is significantly higher in the 1° than in the 2° lineage and depends on cell-cycle progression.

A computational model of VPC fate specification based on the cell cycle

Based on the experimental evidence, which indicated a linkage of VPC fate specification to cell-cycle progression, we incorporated the cell cycle as a key timing factor in our revised computational model. To implement *bounded asynchrony* in our refined computational model, we used an independent

Table I Positive regulation of NOTCH signaling by G1 cyclins

Row	Genotype	Induction ± s.e.		*n*
1	*zhIs039[nicd::gfp]*	5.85 ± 0.04		36
2	*zhEx500[nicd::gfp]*	5.27 ± 0.12	***	34
3	*cyd-1(q626); zhEx500[nicd::gfp]*	4.63 ± 0.14		36
4	*cye-1(ku256)/+; zhIs39[nicd::gfp]*	5.96 ± 0.03	***	56
5	*cye-1(ku256); zhIs39[nicd::gfp]*	5.52 ± 0.09		30

Induction indicates the average number of induced VPCs (1° or 2° fate) per animal and s.e. the standard error determined by bootstrapping (see Materials and methods). ***Indicates a significance of $P<0.001$ and *n* the number of animals scored for each genotype. For *cye-1(ku256)*, the homozygous mutants were compared with their heterozygous siblings on the same plates. Source data is available for this table in the Supplementary Information.

scheduler that recreates the same interactions between cells by limiting the number of steps one process gets ahead of the other as exhibited by the timed automata model described earlier. In our previous VPC models, an artificial delay in LIN-12 NOTCH downregulation was necessary to reproduce the proper behavior of *lin-12* and predict the correct fate patterns in lateral signaling mutants (Fisher *et al*, 2007). With the introduction of the cell cycle, we removed this artificial delay and coupled the inhibition of LIN-12 to the state of the cell-cycle phases G1, S, or G2 (see Supplementary information for a detailed description of the computational model). In a first *in silico* experiment, we allowed for the inhibition of lateral LIN-12 signaling to happen

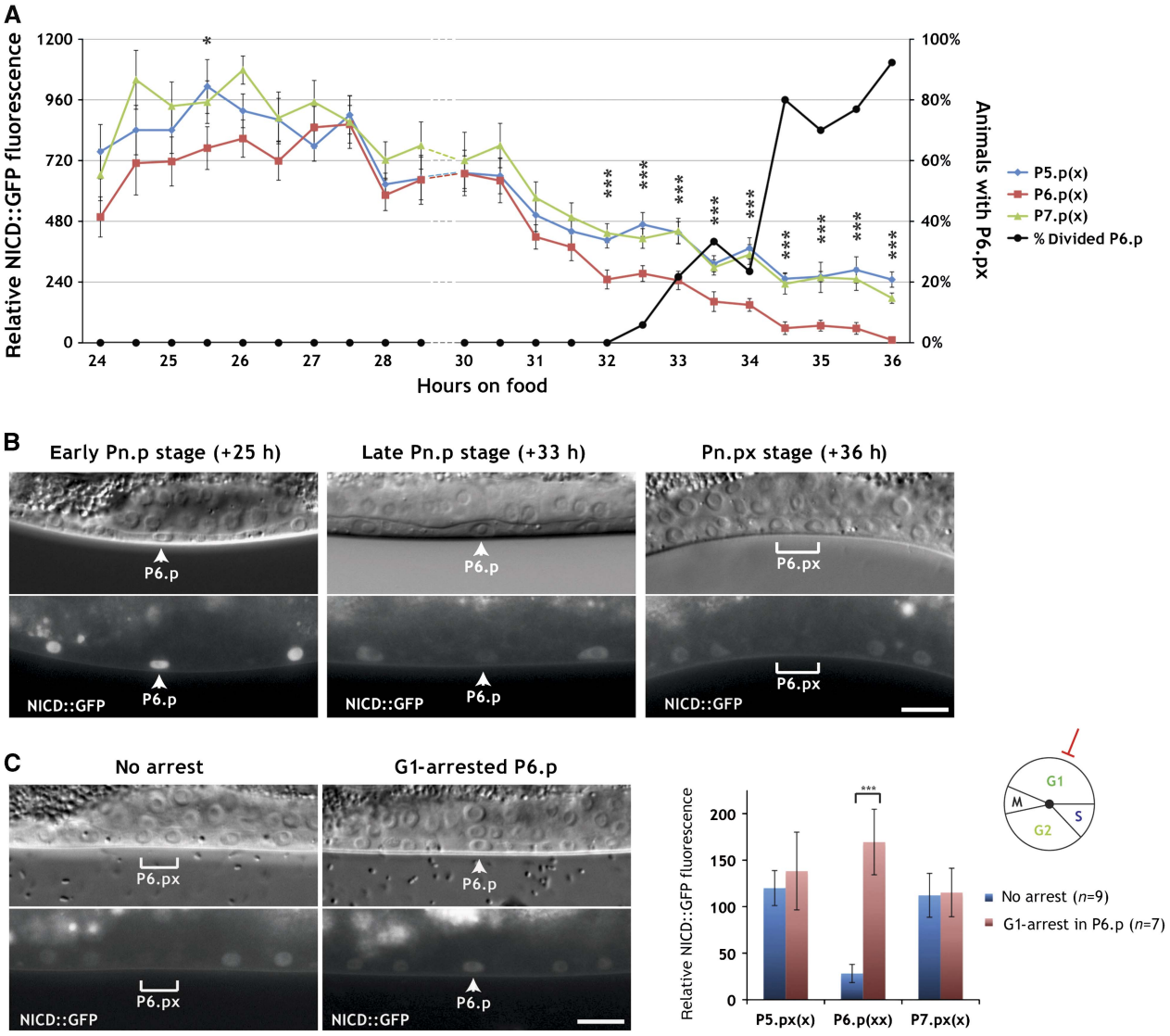

Figure 3 Time-course analysis of NICD degradation. (**A**) NICD::GFP levels in P5.p, P6.p, and P7.p were measured every half an hour in around 20 synchronized animals at each time point (left scale). The time is indicated in hours after hatching (see Materials and methods). Error bars indicate the standard errors and asterisks significant differences between 1° and 2° lineages as described in Materials and methods. The percentage of animals with at least one proximal VPC division is indicated by the black line (right scale). (**B**) Representative pictures of NICD::GFP expression in an early L2 (+25 h, Pn.p stage), a late L2 (+33 h, Pn.p stage), and an early L3 (+36 h, Pn.px stage) larva. Note the uniform NICD::GFP expression in the VPCs at +25 h and the downregulation in P6.p at +33 h (arrowheads) and in P6.px at +36 h (bracket). (**C**) NICD::GFP persists in the G1-arrested P6.p cell of an *egl-17p::cki-1* transgenic animal (arrowheads in the right panels), whereas NICD::GFP is downregulated in the P6.p descendants of a sibling that had lost the *egl-17p::cki-1* array (brackets in the left panels). In all panels, the corresponding Nomarski images are shown on top. The scale bars represent 10 μm. A quantification of NICD::GFP expression is shown to the right. Error bars indicate the standard error and asterisks indicate the significance as described in Materials and methods. Source data is available for this figure in the Supplementary Information.

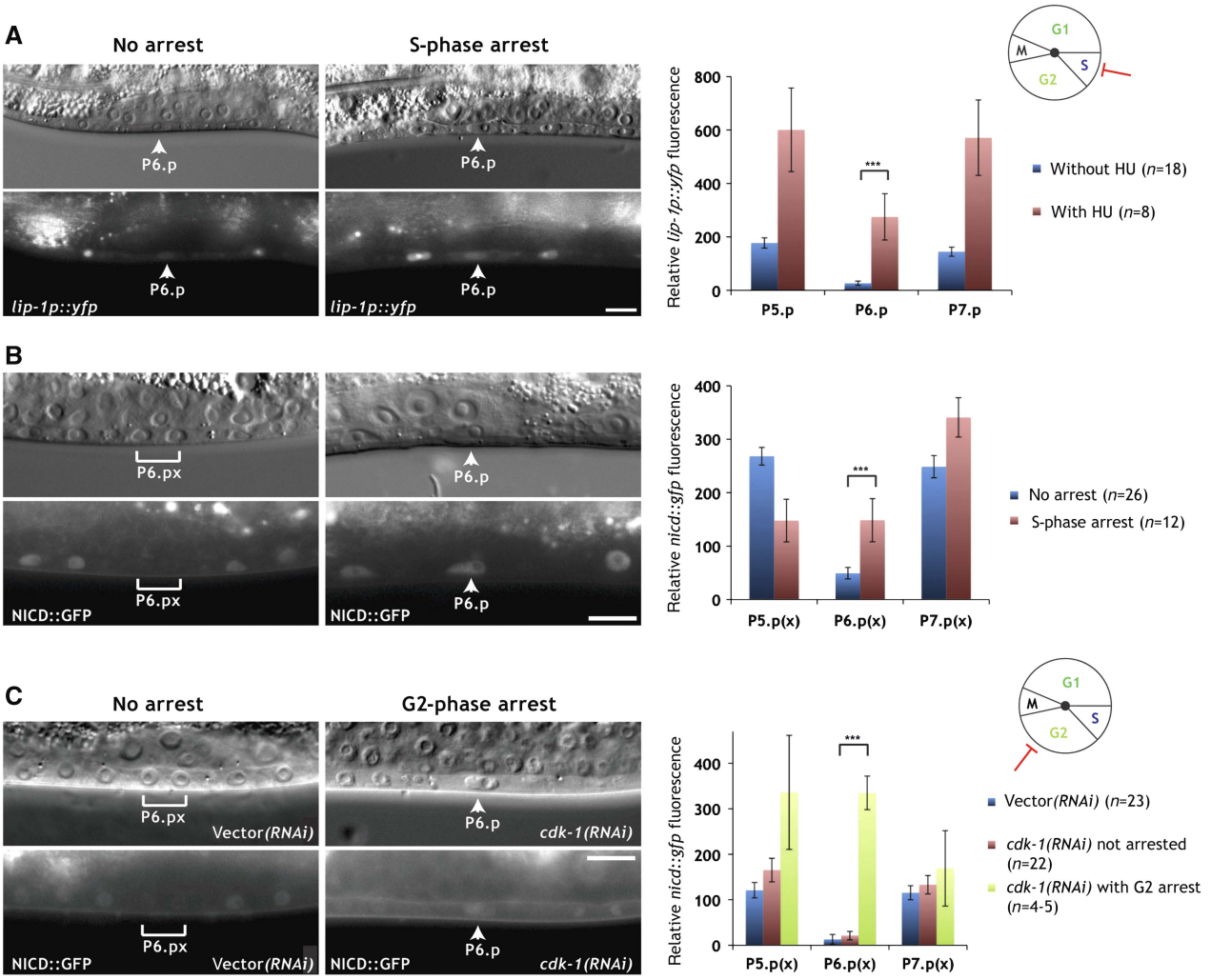

Figure 4 NICD is degraded during the G2 phase. (**A**) Expression of the 2° fate marker *lip-1p::yfp* persists in P6.p of a hydroxyurea (HU)-treated larva (arrowheads in the right panels), while expression is downregulated in an untreated control animal at the Pn.p stage (arrowheads in the left panels). (**B**) NICD::GFP persists in the undivided P6.p cell of a hydroxyurea-treated larva (arrowheads in the right panels), but NICD::GFP is downregulated in the P6.p descendants of an untreated control larva at the Pn.px stage (brackets in the left panels). (**C**) NICD::GFP persists in the G2-arrested P6.p cell of a *cdk-1* RNAi-treated animal at the Pn.px stage (arrowheads in the right panels), while NICD::GFP is downregulated in the P6.p descendants of an empty vector RNAi-treated control animal (brackets in the left panels). Note that due to the incomplete penetrance of the *cdk-1* RNAi effect, only P6.p had arrested in the example shown in the right panels. In all panels, the corresponding Nomarski images are shown on top. The scale bars represent 10 μm. Quantifications of *lip-1p::yfp* and NICD::GFP expression are shown to the right. Error bars indicate the standard error and asterisks indicate the significance as described in Materials and methods. Source data is available for this figure in the Supplementary Information.

during the G1 phase. However, this configuration of the model failed to reproduce published experimental data. We further tested a model where inhibition of LIN-12 Notch was forbidden in the G1 phase but allowed during the S or G2 phase. This model was consistent with published experimental results (checked using model checking, see Supplementary Table 2). Furthermore, the coupling between cell-cycle progression and LIN-12 NOTCH degradation was implemented in all VPCs in an identical manner (see Supplementary Figure S17). However, when executing the model we found that LIN-12 levels in VPCs progressing toward a 1° fate stabilized at lower levels than in VPCs adopting a 2° fate. Taken together, the notion of *bounded asynchrony* introduced into our computational model through the cell cycle predicted that a temporal delay in the termination of the LIN-12 NOTCH signal after G1 is critical for the formation of a stable cell fate pattern.

NICD degradation occurs during the G2 phase

To further narrow down the time window, during which NICD is degraded, we arrested the VPCs in the S phase by hydroxyurea treatment (Ambros, 1999). Expression of the 2° cell fate reporter *lip-1p::yfp* persisted in the arrested P6.p cells and increased in the adjacent P5.p and P7.p cells (Figure 4A). Overall, *lip-1p::yfp* reached significantly higher levels in S phase-arrested VPCs compared with the VPCs of untreated control animals. Accordingly, the degradation of NICD::GFP in P6.p was blocked in hydroxyurea-treated animals (Figure 4B).

We then arrested the VPCs in the late G2 phase by RNAi-mediated knockdown of *cdk-1*, which is essential for the G2-to-M phase progression (Mori *et al*, 1994; Boxem *et al*, 1999). Since the *cdk-1* RNAi phenotype is incompletely penetrant, this procedure resulted in the random arrest of single or multiple VPCs per affected animal. Similarly to hydroxyurea-treated animals, the undivided VPCs in *cdk-1* RNAi animals expressed elevated levels of NICD::GFP, and the bias in P6.p versus P5.p and P7.p-specific expression was lost in the G2-arrested VPCs (Figure 4C). Taken together, the cell-cycle arrest and time-course experiments indicate that NICD is degraded in the VPCs either during the late G2 phase or at the time of entry into the M phase. The persisting expression of NICD::GFP in VPCs arrested by *cdk-1* RNAi may also indicate a direct involvement of a CDK-1/Cyclin complex in NICD degradation (see below).

The G1 cyclins CYE-1 and CYD-1 promote while the G2 cyclin CYB-3 inhibits NOTCH activity

To investigate which CDK/Cyclin complexes are responsible for the changes in NOTCH stability and signaling activity during cell-cycle progression, we examined the expression of the full-length LIN-12::GFP and the NICD::GFP reporters as well as the expression of the target gene *lip-1* in different cyclin mutants.

We first examined the influence of the G1-specific D-type cyclin gene *cyd-1* on NOTCH signaling using the reduction-of-function allele *cyd-1(q626)* (Tilmann and Kimble, 2005). Although no VPC cell-cycle arrest was observed, *cyd-1(q626)* mutants displayed reduced levels of LIN-12::GFP in P5.p and P7.p (Figure 5A). Moreover, the expression of the LIN-12 target gene *lip-1* was strongly decreased in the P5.p and P7.p descendants of *cyd-1(q626)* mutants (Figure 5B). Due to the proximity of the *nicd::gfp* integration site to the *cyd-1* locus on LGII, it was not possible to examine NICD::GFP expression in *cyd-1(q626)* animals. However, *cyd-1* RNAi did not cause an obvious reduction in NICD::GFP expression in the VPCs. Rather, in the six cases, in which P6.p was arrested, P6.p continued to express NICD::GFP at high levels similar to the expression pattern observed in *egl-17p::cki-1* animals (Supplementary Figure S4; Figure 3C).

Furthermore, we tested if the *cyd-1(q626)* mutation modifies the vulval phenotype caused by NICD::GFP expression. For this purpose, we used an extrachromosomal *nicd::gfp* array (*zhEx500*) to score vulval induction in the *cyd-1(q626)* background. The *cyd-1(q626)* mutation significantly decreased vulval induction in animals carrying the *zhEx500[nicd::gfp]* array when compared with *cyd-1(+); zhEx500[nicd::gfp]* controls (Table I, rows 2, 3). Taken together, we conclude that *cyd-1* controls NOTCH signaling at the level of the full-length LIN-12 receptor and possibly also downstream of NICD at the level of target gene expression. Since NOTCH signaling prevents the degradation of full-length LIN-12 (Levitan and Greenwald, 1998; Shaye and Greenwald, 2002), it is possible that the reduced expression of the LIN-12::GFP reporter in *cyd-1(q626)* mutants is caused by a disruption of this positive feedback loop.

We next analyzed the effect of the G1-specific E-type cyclin *cye-1* using the strong reduction-of-function or null allele *ku256* (Fay and Han, 2000). Expression of the NICD::GFP reporter in homozygous *cye-1(ku256)* mutants was strongly reduced, in both the 1° and the 2° VPCs and their descendants (Figure 5C). Moreover, vulval induction was slightly but significantly suppressed in homozygous *cye-1(ku256); nicd::gfp* mutants when compared with heterozygous *cye-1(ku256)/+; nicd::gfp* controls (Table I, rows 4, 5).

Finally, we investigated the influence of the G2-specific B-type cyclins *cyb-1*, *cyb-2*, and *cyb-3* on NICD stability. Since the available deletion mutations in the *cyb* genes cause embryonic or larval lethality, we reduced *cyb* gene activities by RNAi-mediated knockdown. *cyb-2* represents two highly similar and functionally redundant genes, *cyb-2.1* and *cyb-2.2*, that were simultaneously affected by the same RNAi treatment. Only *cyb-3* RNAi caused an increase in NICD::GFP expression (Figure 5D). Even though RNAi against *cyb-3* did not cause a cell-cycle arrest in the VPCs, *cyb-3* RNAi animals exhibited significantly higher NICD::GFP levels in the P6.p descendants at the Pn.px stage compared with control RNAi animals (Figure 5D). We thus conclude that both the G1 cyclins CYD-1 and CYE-1 positively regulate LIN-12 NOTCH signaling. CYD-1 appears to act primarily by regulating full-length LIN-12, while CYE-1 seems to exert a stabilizing effect on the intracellular pool of NICD. On the other hand, CYB-3 may act together with CDK-1 during the late G2 phase to directly or indirectly target NICD for degradation before M-phase entry.

The N-terminal ankyrin and the C-terminal PEST domain regulate NICD stability

To identify the domains necessary for NICD degradation, we performed a structure function analysis. The LIN-12 NICD is composed of a nuclear localization signal (NLS) at the N-terminus followed by the RBP-Jkappa-associated module (RAM) containing the downregulation targeting signal (DTS) motif, which promotes NOTCH endocytosis (Shaye and Greenwald, 2002, 2005; Kopan and Ilagan, 2009). The central part contains seven ankyrin repeats (ANK) that are essential for the interaction with CSL and other transcription factors and for NICD dimerization. Near its C-terminus, NICD contains a proline/glutamic acid/serine/threonine (PEST) motif that binds to the F-Box protein SEL-10 and regulates protein degradation (Gupta-Rossi *et al*, 2001). We integrated different NICD::GFP deletion constructs as single copy transgenes into the genome via MosSCI, allowing us to compare expression levels between different transgenes (Frokjaer-Jensen *et al*, 2008). A construct lacking the C-terminus with the PEST domain (NICD::GFPΔCT) showed persistent expression in the P6.p descendants and elevated levels in the P5.p and P7.p descendants (Figure 6C). However, the reciprocal construct harboring just the C-terminal PEST domain (NICD::GFPΔNT) was only partially downregulated in the 1° lineage (Figure 6D). Since the NICD::GFPΔNT signal was detected mainly in the cytoplasm, we examined if nuclear localization was necessary for proper NICD degradation by deleting the seven ANK repeats but leaving the N-terminal 67 amino acids containing the NLS, RAM, and DTS domains in place (NICD::GFPΔANK). Even though the NICD::GFPΔANK protein localized to the nuclei of the VPCs and their descendants, it was not efficiently

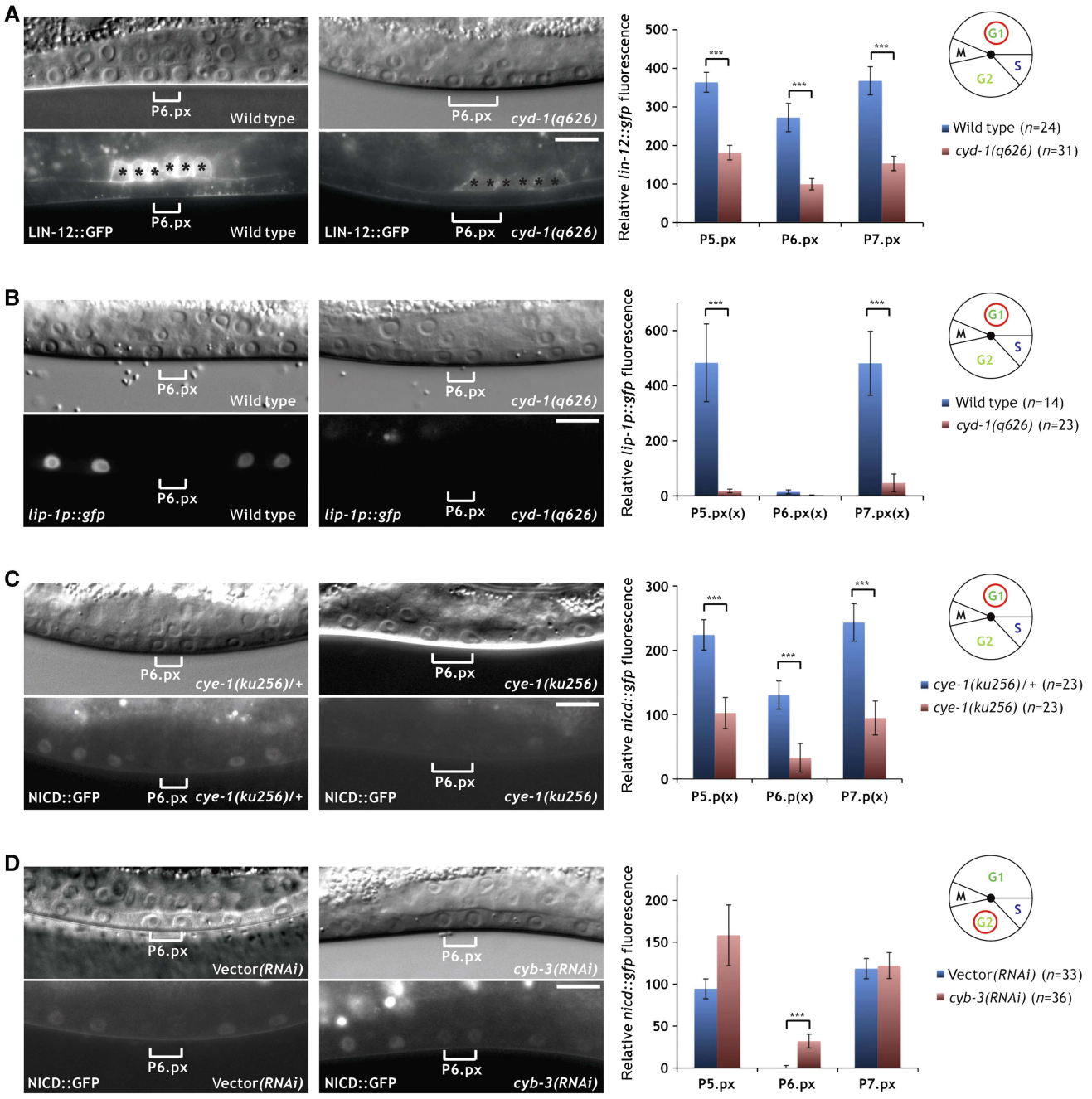

Figure 5 Differential regulation of NOTCH signaling by G1 and G2 cyclins. (**A**) Localization of LIN-12::GFP to the apical plasma membrane is diminished in the VPC descendants in *cyd-1(q626)* mutants (right panels) when compared with wild-type controls (left panels). Black asterisks denote uterine LIN-12::GFP expression. (**B**) Expression of the 2° fate marker *lip-1p::gfp* is reduced in the P5.p and P7.p descendants in *cyd-1(q626)* mutants (right panels) compared with wild-type controls (left panels). (**C**) NICD::GFP expression is reduced in the VPC descendants in homozygous *cye-1(ku256)* mutants (right panels) when compared with heterozygous *cye-1(ku256)/+* controls (left panels). (**D**) NICD::GFP expression persists in the P6.p descendants of a *cyb-3* RNAi-treated animal at the Pn.px stage (brackets in the right panels). Note that in contrast to *cdk-1* (Figure 4C), *cyb-3* RNAi did not induce a cell-cycle arrest. An empty vector RNAi-treated control animal is shown in the left panels. In all panels, the corresponding Nomarski images are shown on top. The scale bars represent 10 μm. Quantifications of LIN-12::GFP, *lip-1p::gfp* and NICD::GFP expression are shown to the right. Error bars indicate the standard error and asterisks indicate the significance as described in Materials and methods. Source data is available for this figure in the Supplementary Information

downregulated in the 1° lineage. Since the deletion of the N-terminal RAM and DTS resulted in the formation of a very unstable protein that was only weakly expressed at the early or mid L2 stage, before NICD is normally degraded, the combination of ANK and PEST domains alone could not be analyzed. Taken together, our structure function analysis indicates that the PEST domain and the ANK repeats together regulate the NICD degradation.

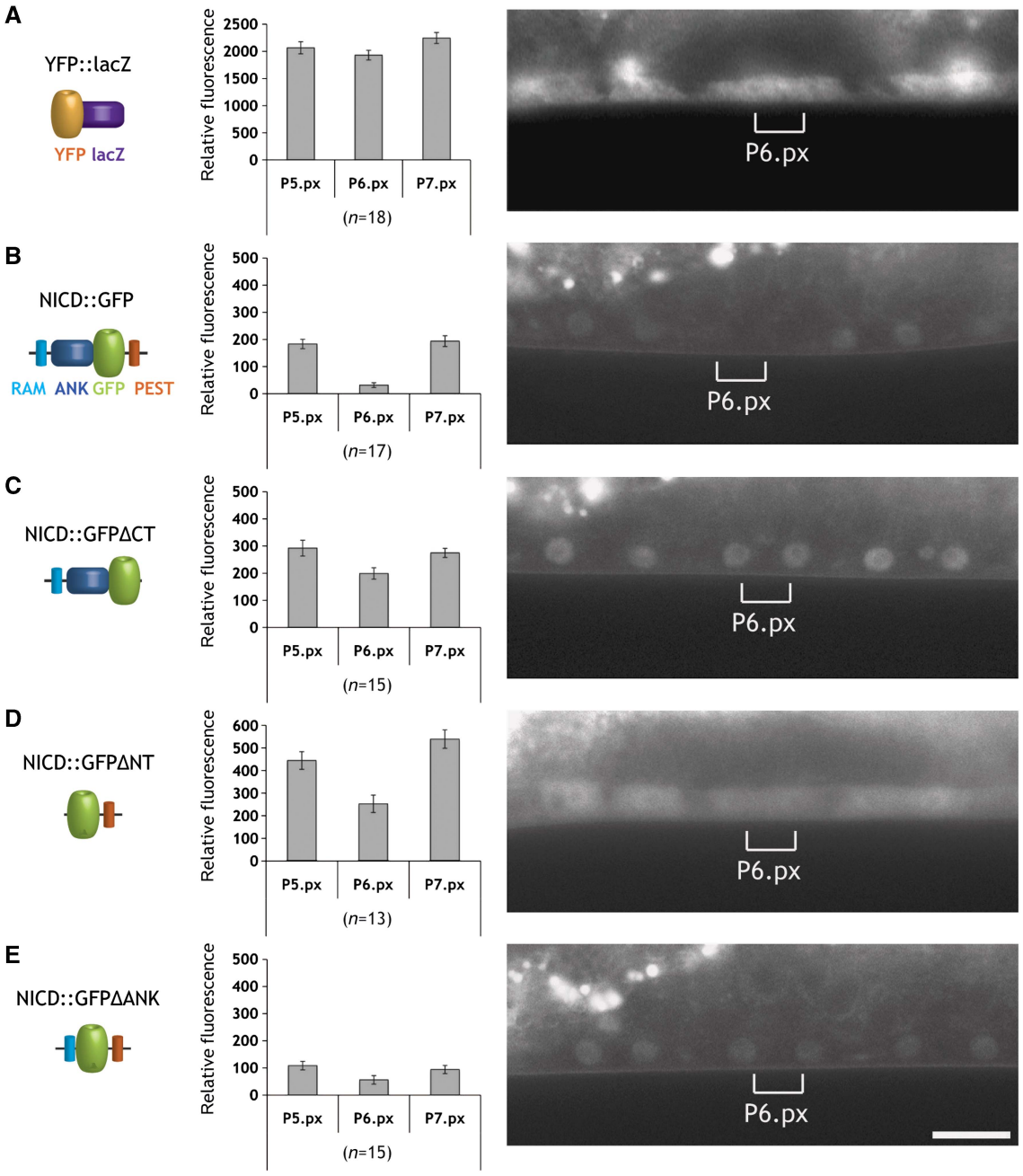

Figure 6 Identification of the domains regulating NICD protein stability. (**A**) Expression pattern of the YFP::LacZ as control, (**B**) the complete LIN-12 intracellular domain (NICD::GFP), (**C**) a C-terminal truncation of 87 amino acids containing the PEST domain (NICD::GFPΔCT), (**D**) an N-terminal deletion of 384 amino acids removing the RAM domain and ANK repeats (NICD::GFPΔNT), and (**E**) an internal deletion of 324 amino acids removing the ANK repeats (NICD::GFPΔANK). All constructs were expressed using the VPC-specific *bar-1* promoter fragment (Natarajan *et al*, 2004) and inserted via MosSCI as single copy transgenes at the same location on LGII. Expression was scored in the descendants of P5.p, P6.p, and P7.p at the Pn.px stage. For each construct, a quantification of the GFP levels is shown in the bar graphs in the center. Error bars indicate the standard error as described in Materials and methods. Representative animals for each construct are shown in the right panels. The brackets indicate the position of the P6.p descendants. The scale bar represents 10 μm. Source data is available for this figure in the Supplementary Information.

Discussion

We have developed a new state-based computational model for cell fate specification during *C. elegans* vulval development and experimentally tested the predictions made by the model. When using interacting state-machine models to describe a biological behavior, we are facing the question of how to compose the components comprising the model. We previously found that the two standard notions of concurrency, in this context, synchrony and asynchrony, are not appropriate to model the VPC interactions (Fisher *et al*, 2008). Synchronous composition is too rigid, making it impossible to break the symmetry between processes without the introduction of additional timing mechanisms. On the other hand,

asynchronous composition introduces a difficulty in deciding how long to wait for a signal that may never arrive, again requiring artificial timing mechanisms. We have therefore implemented *bounded asynchrony* in our previous model of VPC specification (Fisher *et al*, 2007). This allows the components of a system to move independently with a certain degree of randomness, while keeping them coupled within certain boundaries.

The concept of *bounded asynchrony* may apply particularly well to the case of VPC fate specification in *C. elegans*. First, the progression of VPCs through the cell cycle does indeed occur with a certain degree of variability, as the VPCs enter the M phase in a random order. After a long G1-phase arrest during the L2 larval stage, the VPCs enter S phase at the L2-to-L3 transition (Euling and Ambros, 1996) and progress through the remainder of the cell cycle in a more or less synchronized way. Second, cell-cycle progression and signaling events are coupled, as a cell cycle-dependent sequence of 1° and 2° cell fate specification has previously been observed (Ambros, 1999). Our data suggest that the degradation of NICD during the late G2 phase is an additional mechanism used to establish this temporal order in 1° and 2° fate specification.

By arresting the cell cycle of the VPC that normally adopts the 1° cell fate in the G1 phase without affecting the progression of the other VPCs, we could experimentally test the concept of *bounded asynchrony*. Even though 1° fate specification in P6.p occurs already toward the end of the G1 phase (Ambros, 1999), G1-arrested P6.p cells could not adopt a stable 1° cell fate, resulting in the simultaneous expression of 1° and 2° cell fate markers. We traced this instability in fate specification back to a persisting expression of LIN-12 NOTCH in the arrested cells. It has previously been reported that 1° cell fate specification results in the rapid endocytosis of full-length LIN-12 from the apical plasma membrane, a process that depends on Ser/Thr phosphorylation of a cis-acting down-regulation (DTS) element in the cytoplasmic portion of LIN-12 (Shaye and Greenwald, 2005). Endocytosis of LIN-12 is followed by rapid degradation in the lysosomes. Interestingly, the LIN-12::GFP protein in G1-arrested VPCs did not remain on the apical cell membrane, where it is normally concentrated in VPCs adopting the 2° cell lineage. Rather, the intracellular LIN-12 cleavage product (NICD) accumulated in the cytoplasm and nucleus. We conclude that the endocytosis and lysosomal degradation of full-length LIN-12 is already occurring during the G1 phase of the cell cycle (Ambros, 1999), or it is not linked to cell-cycle progression at all. We thus postulate the existence of a second LIN-12 NOTCH degradation pathway that is tightly coupled to cell-cycle progression and dedicated to the destruction of NICD in the nucleus (Figure 7). This nuclear NICD degradation pathway is only effective during the G2 phase of the cell cycle.

On the basis of our findings, we propose a model, in which NICD is stabilized and accumulates in the VPCs during the G1 phase thanks to the activity of the CDK-4/CYD-1 and CDK-2/CYE-1 complexes. In analogy to *Drosophila* dacapo, constitutive expression of CKI-1 blocks entry into S phase most likely by inhibiting CDK-2/CYE-1 activity (de Nooij *et al*, 1996; Boxem and van den Heuvel, 2001; van den Heuvel, 2005). Similarly to its mammalian homologs, CKI-1 and CDK-4/CYD-1 may form a complex, which sequesters and inhibits CKI-1 and

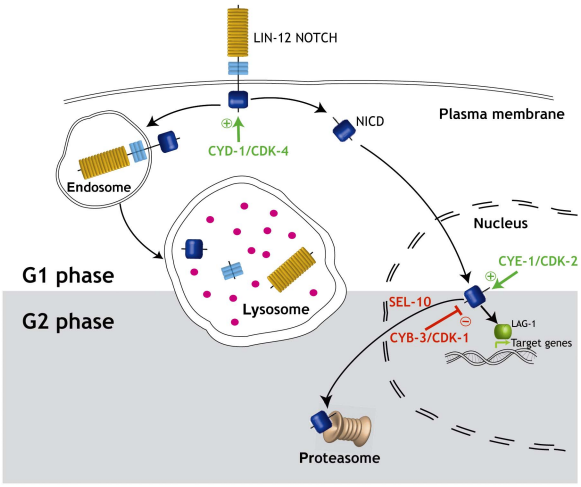

Figure 7 Model for cell-cycle regulation of LIN-12 NOTCH signaling. During the G1 phase of the cell cycle, LIN-12 NOTCH is cleaved upon binding to a DSL ligand, thereby releasing the NICD fragment that activates transcription of target genes. Alternatively, NOTCH can undergo endocytosis followed by lysosomal degradation. The activity of the G1-specific CDK-4/CYD-1 and CDK-2/CYE-1 complexes positively regulate LIN-12 NOTCH signaling in P5.p, P6.p, and P7.p by stabilizing full-length NOTCH at the apical plasma membrane and NICD in the nucleus, respectively. Degradation of NICD in P6.p occurs during the G2 phase, when activation of the G2-specific CDK-1/CYB-3 complex terminates NOTCH signaling by inducing ubiquitin-mediated proteasomal degradation of NICD.

at the same time stabilizes CDK-4/CYD-1 (LaBaer *et al*, 1997; Cheng *et al*, 1999; Boxem and van den Heuvel, 2001). Therefore, arresting a 1° VPC in the G1 phase by CKI-1 overexpression may increase LIN-12 NOTCH activity due to the persisting activity of CDK-4/CYD-1 and the absence of G2 CDK/Cyclin activity. After the VPCs have completed the S phase, activation of the CDK-1/CYB-3 complex during the late G2 phase may directly or indirectly target NICD for degradation, resulting in the termination of the NOTCH signal in the 1° cell lineage before M-phase entry. The nature of the signals targeting NICD for destruction and causing a higher rate of NICD decay in the 1° than in the 2° lineage remains to be identified. In vertebrate cells, the stability of NICD is negatively regulated by phosphorylation of the PEST domain and deacetylation of the ANK repeats (Cornell *et al*, 1999; Gupta-Rossi *et al*, 2001; Oberg *et al*, 2001; Wu *et al*, 2001; Guarani *et al*, 2011). Accordingly, our *in vivo* structure function analysis indicated that both the ANK repeats and the PEST domain are required for efficient degradation of NICD in the VPCs.

Taken together, these findings point at a temporal sequence of signaling events and a mechanism, by which the coordinated progression of VPCs through the cell cycle allows the formation of a stable cell fate pattern. First, activation of the EGFR/RAS/MAPK pathway by the AC signal during the G1 phase induces the 1° cell fate in P6.p. Still during the G1 phase, LIN-12 NOTCH signaling is activated in the 2° cells as a consequence of high EGFR/RAS/MAPK activity in the 1° cell, which leads to the induction of DSL ligand expression by P6.p (Tax *et al*, 1994; Chen and Greenwald, 2004). The 1° versus 2° cell fate decision, however, can only be sealed after the G1 arrest has been relieved and NICD has been degraded in the 1°

cell lineage during the late G2 phase. Thus, by linking the inactivation of the key cell fate determinant NOTCH to cell-cycle progression, a boundary is created that prevents VPCs from becoming de-synchronized. The heterochronic gene pathway that regulates the G1-to-S checkpoint in the VPCs may represent a biological equivalent of the global 'scheduler' in the computational model (Euling and Ambros, 1996; van den Heuvel, 2005). The early heterochronic genes maintain the expression of the CDK inhibitor CKI-1 during the L2 larval stage. Expression of *cki-1* ceases due to a switch in heterochronic gene expression at the L2-to-L3 transition, thus lifting the boundary and allowing VPCs to enter S phase (Hong *et al*, 1998).

In many cases of cell fate specification, the coordination of different intercellular signaling pathways is critically dependent on spatial and temporal control mechanisms linked to the cell cycle, which determines a cell's competence to respond to extrinsic signals (Gomer and Firtel, 1987; McConnell and Kaznowski, 1991; Weigmann and Lehner, 1995). Cell-cycle control of developmental decisions may be particularly important in situations where a cell is sensitive to multiple signals that specify distinct outcomes. Therefore, specific cell fate choices need to be executed with a certain priority or temporal sequence. To link different steps of cell fate determination to specific cell-cycle phases could be a general strategy used to temporally coordinate cell fate choices among equivalent cells. This strategy allows the sequencing and prioritizing of different developmental programs within a single cell lineage. In complex multicellular environments, coupling cell-cycle progression to signal transduction could provide a means to limit the number of cells in a population that can respond to extrinsic signals at a given time point. Thus, the deregulation of the cell cycle observed in many tumor cells may not only affect cell proliferation but also the responsiveness of the cells to growth factors, causing cell fate transformations or de-differentiation. While numerous studies have demonstrated a strong influence of intercellular signaling on cell-cycle progression (Boxem and van den Heuvel, 2002; Clayton *et al*, 2008; Yamaguchi *et al*, 2010), fewer studies focused on the impact of the cell cycle on signaling (Moore *et al*, 2007; Davidson *et al*, 2009; Ali *et al*, 2011). *Bounded asynchrony* achieved through cell-cycle control of signal transduction could be a global principle utilized during the development of multicellular organisms. Finally, by exploring the various mechanisms linking cell-cycle progression to signaling we will better understand how deregulation of the cell cycle promotes tumor development.

Materials and methods

Timed automata

A timed automaton is a mathematical model for describing systems that have discrete states that interact with continuous time. Its behavior consists of discrete changes of states and continuous evolution of time. A given automaton describes the possible sequence of changes in discrete states and their timing. Technically, the automaton has one or more clocks that measure time. These clocks can be reset when the automaton changes its discrete states, and in turn, the automaton uses the clocks to determine how long to stay in states and which discrete state changes are possible. This leads to state sequences (with their timing) to be possible (accepted) in the automaton or impossible (rejected). Events attached to transitions of the automaton can serve as a communication mechanism between multiple timed automata. A system is modeled by creating a timed automaton that produces all the possible behaviors of this system and not more. An example of a timed automaton and an explanation of its possible behaviors are given in Figure 1B–D. We used the tool Uppaal for modeling and analysis of timed automata (Larsen *et al*, 1997).

C. elegans strains and constructs

Standard methods were used for maintaining and manipulating *C. elegans* (Brenner, 1974). The following mutations and transgenes were used: LGI: *cye-1(ku256)* (Fay and Han, 2000), *ayIs4[egl-17::gfp]* (Burdine *et al*, 1998), LGII: *zhIs39[bar-1p::nicd::gfp::unc-54 3′utr, unc-119(+)]*, *zhIs49[bar-1p::yfp::unc-54 3′utr, unc-119(+)]*, *zhIs56 [bar-1p::nicd::gfpΔCT::unc-54 3′utr, unc-119(+)]*, *zhIs50.1[bar-1p::nicd::gfpΔNT::unc-54 3′utr, unc-119(+)]*, *zhIs55[bar-1p::nicd::gfp-ΔANK::unc-54 3-1p::nicd::gfp+)]*, *mfIs41[lip-1::yfp, myo-2::rfp]* (gift of Marie-Anne Felix), *cyd-1(q626)* (Tilmann and Kimble, 2005), *unc-4(e120)*, LGIII: *unc-119(ed3)*, *zhIs4[lip-1::gfp]* (Berset *et al*, 2001), LGIV: *dpy-20(e1282)*, LGV: *arIs92[egl-17::cfp, tax-3::gfp]*, *arIs82[*LIN-12::GFP*; unc-4(+); egl-17p::LacZ]* (Shaye and Greenwald, 2002), Balancer chromosome: *+/hT2[dpy-18(h662)]; +/hT2[bli-4(e937)]* (I;III), extrachromosomal arrays: *zhEx314, zhEx315[egl-17p::cki-1, lin-48::gfp], zhEx334, zhEx367[egl-17p::cki-1, myo-2::mcherry], zhEx500 [bar-1p::nicd::gfp::unc-54 3′utr, unc-119(+); myo-2p::mCherry]*.

Plasmid constructs

GFP reporter constructs had been made by gateway cloning (MultiSite Gateway® Three-Fragment Vector Construction Kit; Invitrogen) using PCFJ150 as final destination vector. The reporter constructs were inserted as single copies into the *C. elegans* genome using MosSCI (Frokjaer-Jensen *et al*, 2008). The entry vectors listed in Supplementary Table 2 were sub-cloned using the listed primers and genomic DNA as template, unless otherwise stated.

Additional plasmids used were pVT363(*egl-17p::cki-1*) (Hong *et al*, 1998), pTJ1157(*lin-48p::gfp*) (Johnson *et al*, 2001), backbone plasmids and plasmids containing co-injection markers for MosSCI (Frokjaer-Jensen *et al*, 2008).

Germline transformation

Worms were transformed by microinjection as described (Mello *et al*, 1991).

Plasmids were injected at a concentration of 50 ng/μg together with the co-injection marker pTJ1157 (50 ng/μg) or pCFJ90 (2.5 ng/μg).

To integrate single copies of transgenes, the MosSCI method was used as described (Frokjaer-Jensen *et al*, 2008).

Time-course experiment

Eggs were obtained by bleaching adult animals for 10 min in 1 ml 400 mM NaOH, 7% sodium hypochlorite followed by three washing steps with M9 or water. The eggs were allowed to hatch on an NGM plates without food. To obtain a highly synchronized population of larvae, all the L1 larvae that hatched during a 30-min interval were collected by mouth pipetting, placed on growth plates with food and cultivated at 20°C. After 24 h about 20 worms were analyzed every 30 min until the VPCs had divided. Due to the limited number of larvae that could be collected over a single 30-min time period, the time-course experiment shown in Figure 3 was done in batches over three different days (first day: 24–27 h; second day: 27.5–28.5 h; third day: 30–36 h).

S-phase arrest

Eggs obtained by bleaching (see above) were allowed to hatch in M9 medium overnight without food. After transferring the L1 larvae to NGM plates with food, they were cultivated at 20°C for 28 h, when

early L3 larvae were placed for 14 h on NGM plates containing 40 mM hydroxyurea with food. Control animals remained on NGM plates without hydroxyurea.

RNAi experiments

For RNA interference, the feeding method described by Kamath *et al* (2001) was used. The worms were synchronized by bleaching (see time-course experiment). L1 larvae were placed on growth media plates containing 3 mM IPTG, 50 μg/ml ampicillin and 50 μg/ml tetracycline and bacteria of specific RNAi strains. Worms were allowed to grow for 36 h at 20°C and analyzed.

C. elegans microscopy and image analysis

Animals of the indicated stages (Pn.p, Pn.px, or Pn.pxx) were placed in 4 μl of 5 mM tetramisole solution in M9 on 4% agarose pads. Fluorescent images were acquired on a Leica DMRA wide-field microscope equipped with a cooled CCD camera (Hamamatsu Orca ER) controlled by the Openlab 5 software package (Improvision). For quantification of GFP intensity, images were acquired with the same microscope, camera and software settings using GFP-specific filter sets. The intensity of GFP expression was measured using the measurement tool in the Openlab software. Each measurement was standardized to the background intensity in the same animal (GFP intensity in arbitrary units). Microsoft Excel (Version 11.5.3) and an R 2.11.1 script were used for data processing and statistical analysis. Data were analyzed by the bootstrap method (10 000 bootstrap samples). The standard errors of the samples were estimated by the bootstrap method (Efron, 1981). The significance levels $***P<0.001$, $**P<0.01$, and $*P<0.05$ were determined by calculating the *P*-value for the differences between two samples and corrected for multiple testing according to Bonferroni.

Supplementary information

Supplementary information is available at the *Molecular Systems Biology* website (www.nature.com/msb).

Acknowledgements

We wish to thank all members of the Hajnal laboratory for support and critical input into this work. We are especially grateful to Itay Nakdimon, Matthias Morf, Michael Walser, and Adrian Streit for comments on the manuscript. We thank Victor Ambros for providing the *egl-17p::cki-1* plasmid; Eric Jorgensen for providing the MosSCI vectors; Judith Kimble for the *cyd-1* allele *q626*; Min Han for the *cye-1* allele *ku256*; and the *C. elegans* genetics center for strains. We thank Matthias Morf for writing the R script that was needed for statistical data analysis. This work was funded by the Kanton of Zurich, the FP7 PANACEA project (grant no. 222936) and a grant from the Swiss National Science Foundation to AH.

Author contributions: JF and AH conceived the project and designed the computational model and laboratory experiments; SN-S, IR, MA, JF, and AH performed the laboratory experiments; AB, NP, and JF constructed the computational model; and NP wrote the timed automaton; SN-S, IR, MA, JF, and AH performed statistical analysis and data interpretation of the laboratory experiments; and AB, NP, and JF performed the analysis of the computational model; SN-S, JF, and AH wrote the manuscript.

References

Aguirre A, Rubio ME, Gallo V (2010) Notch and EGFR pathway interaction regulates neural stem cell number and self-renewal. *Nature* **467:** 323–327

Ali F, Hindley C, McDowell G, Deibler R, Jones A, Kirschner M, Guillemot F, Philpott A (2011) Cell cycle-regulated multi-site phosphorylation of Neurogenin 2 coordinates cell cycling with differentiation during neurogenesis. *Development* **138:** 4267–4277

Alur R, Dill D (1994) A theory of timed automata. *Theor Comput Sci* **126:** 183–235

Ambros V (1999) Cell cycle-dependent sequencing of cell fate decisions in Caenorhabditis elegans vulva precursor cells. *Development* **126:** 1947–1956

Baron M (2003) An overview of the Notch signalling pathway. *Semin Cell Dev Biol* **14:** 113–119

Baron M, Aslam H, Flasza M, Fostier M, Higgs JE, Mazaleyrat SL, Wilkin MB (2002) Multiple levels of Notch signal regulation (review). *Mol Membr Biol* **19:** 27–38

Berset T, Hoier EF, Battu G, Canevascini S, Hajnal A (2001) Notch inhibition of RAS signaling through MAP kinase phosphatase LIP-1 during C. elegans vulval development. *Science* **291:** 1055–1058

Boxem M, Srinivasan DG, van den Heuvel S (1999) The Caenorhabditis elegans gene ncc-1 encodes a cdc2-related kinase required for M phase in meiotic and mitotic cell divisions, but not for S phase. *Development* **126:** 2227–2239

Boxem M, van den Heuvel S (2001) lin-35 Rb and cki-1 Cip/Kip cooperate in developmental regulation of G1 progression in C. elegans. *Development* **128:** 4349–4359

Boxem M, van den Heuvel S (2002) C. elegans class B synthetic multivulva genes act in G(1) regulation. *Curr Biol* **12:** 906–911

Brenner S (1974) The genetics of Caenorhabditis elegans. *Genetics* **77:** 71–94

Burdine RD, Branda CS, Stern MJ (1998) EGL-17(FGF) expression coordinates the attraction of the migrating sex myoblasts with vulval induction in C. elegans. *Development* **125:** 1083–1093

Chen N, Greenwald I (2004) The lateral signal for LIN-12/Notch in C. elegans vulval development comprises redundant secreted and transmembrane DSL proteins. *Dev Cell* **6:** 183–192

Cheng M, Olivier P, Diehl JA, Fero M, Roussel MF, Roberts JM, Sherr CJ (1999) The p21(Cip1) and p27(Kip1) CDK 'inhibitors' are essential activators of cyclin D-dependent kinases in murine fibroblasts. *EMBO J* **18:** 1571–1583

Clayton JE, van den Heuvel SJ, Saito RM (2008) Transcriptional control of cell-cycle quiescence during C. elegans development. *Dev Biol* **313:** 603–613

Cornell M, Evans DA, Mann R, Fostier M, Flasza M, Monthatong M, Artavanis-Tsakonas S, Baron M (1999) The Drosophila melanogaster Suppressor of deltex gene, a regulator of the Notch receptor signaling pathway, is an E3 class ubiquitin ligase. *Genetics* **152:** 567–576

Davidson G, Shen J, Huang YL, Su Y, Karaulanov E, Bartscherer K, Hassler C, Stannek P, Boutros M, Niehrs C (2009) Cell cycle control of wnt receptor activation. *Dev Cell* **17:** 788–799

de Nooij JC, Letendre MA, Hariharan IK (1996) A cyclin-dependent kinase inhibitor, Dacapo, is necessary for timely exit from the cell cycle during Drosophila embryogenesis. *Cell* **87:** 1237–1247

Efron B (1981) Nonparametric estimates of standard error: the jackknife, the bootstrap and other methods. *Biometrika* **68:** 589–599

Efroni S, Harel D, Cohen IR (2003) Toward rigorous comprehension of biological complexity: modeling, execution, and visualization of thymic T-cell maturation. *Genome Res* **13:** 2485–2497

Efroni S, Harel D, Cohen IR (2005) Reactive animation: realistic modeling of complex dynamic systems. *Computer* **38:** 38–47

Euling S, Ambros V (1996) Heterochronic genes control cell cycle progress and developmental competence of C. elegans vulva precursor cells. *Cell* **84:** 667–676

Fanto M, Mlodzik M (1999) Asymmetric Notch activation specifies photoreceptors R3 and R4 and planar polarity in the Drosophila eye. *Nature* **397:** 523–526

Fay DS, Han M (2000) Mutations in cye-1, a Caenorhabditis elegans cyclin E homolog, reveal coordination between cell-cycle control and vulval development. *Development* **127:** 4049–4060

Fisher J, Henzinger TA, Mateescu M, Piterman N (2008) Bounded asynchrony: concurrency for modeling cell-cell interactions.

In *Formal Methods in Systems Biology*, Fisher J (ed) pp 17–32. Springer-Verlag, Cambridge, UK

Fisher J, Henzinger TA (2007) Executable cell biology. *Nat Biotechnol* **25:** 1239–1249

Fisher J, Piterman N, Hajnal A, Henzinger TA (2007) Predictive modeling of signaling crosstalk during C. elegans vulval development. *PLoS Comput Biol* **3:** e92

Fisher J, Piterman N, Hubbard EJ, Stern MJ, Harel D (2005) Computational insights into Caenorhabditis elegans vulval development. *Proc Natl Acad Sci USA* **102:** 1951–1956

Frokjaer-Jensen C, Davis MW, Hopkins CE, Newman BJ, Thummel JM, Olesen SP, Grunnet M, Jorgensen EM (2008) Single-copy insertion of transgenes in Caenorhabditis elegans. *Nat Genet* **40:** 1375–1383

Fryer CJ, White JB, Jones KA (2004) Mastermind recruits CycC:CDK8 to phosphorylate the Notch ICD and coordinate activation with turnover. *Mol Cell* **16:** 509–520

Gomer RH, Firtel RA (1987) Cell-autonomous determination of cell-type choice in Dictyostelium development by cell-cycle phase. *Science* **237:** 758–762

Greenwald I (2005) LIN-12/Notch signaling in *C. elegans*, *WormBook* 1–16, ed. The *C. elegans* Research Community, WormBook, doi/10.1895/wormbook.1.10.1, http://www.wormbook.org

Guarani V, Deflorian G, Franco CA, Kruger M, Phng LK, Bentley K, Toussaint L, Dequiedt F, Mostoslavsky R, Schmidt MH, Zimmermann B, Brandes RP, Mione M, Westphal CH, Braun T, Zeiher AM, Gerhardt H, Dimmeler S, Potente M (2011) Acetylation-dependent regulation of endothelial Notch signalling by the SIRT1 deacetylase. *Nature* **473:** 234–238

Gupta-Rossi N, Le Bail O, Gonen H, Brou C, Logeat F, Six E, Ciechanover A, Israel A (2001) Functional interaction between SEL-10, an F-box protein, and the nuclear form of activated Notch1 receptor. *J Biol Chem* **276:** 34371–34378

Hitoshi S, Alexson T, Tropepe V, Donoviel D, Elia AJ, Nye JS, Conlon RA, Mak TW, Bernstein A, van der Kooy D (2002) Notch pathway molecules are essential for the maintenance, but not the generation, of mammalian neural stem cells. *Genes Dev* **16:** 846–858

Hong Y, Roy R, Ambros V (1998) Developmental regulation of a cyclin-dependent kinase inhibitor controls postembryonic cell cycle progression in Caenorhabditis elegans. *Development* **125:** 3585–3597

Hubbard EJ, Wu G, Kitajewski J, Greenwald I (1997) sel-10, a negative regulator of lin-12 activity in Caenorhabditis elegans, encodes a member of the CDC4 family of proteins. *Genes Dev* **11:** 3182–3193

Johnson AD, Fitzsimmons D, Hagman J, Chamberlin HM (2001) EGL-38 Pax regulates the ovo-related gene lin-48 during Caenorhabditis elegans organ development. *Development* **128:** 2857–2865

Kam N, Cohen IR, Harel D (2001) The immune system as a reactive system: modeling T cell activation with statecharts. *Human-Centric Computing Languages and Environments.* Proceedings IEEE Symposia, 2001, pp 15–22, http://ieeexplore.ieee.org/xpl/articleDetails.jsp?arnumber=995228

Kamath RS, Martinez-Campos M, Zipperlen P, Fraser AG, Ahringer J (2001) Effectiveness of specific RNA-mediated interference through ingested double-stranded RNA in Caenorhabditis elegans. *Genome Biol* **2:** RESEARCH0002

Kitano H (2002) Systems biology: a brief overview. *Science* **295:** 1662–1664

Kopan R, Ilagan MX (2009) The canonical Notch signaling pathway: unfolding the activation mechanism. *Cell* **137:** 216–233

LaBaer J, Garrett MD, Stevenson LF, Slingerland JM, Sandhu C, Chou HS, Fattaey A, Harlow E (1997) New functional activities for the p21 family of CDK inhibitors. *Genes Dev* **11:** 847–862

Larsen KG, Pettersson P, Yi W (1997) Uppaal in a Nutshell. *J Softw Tools Technol Transfer* **1:** 134–152

Levitan D, Greenwald I (1998) LIN-12 protein expression and localization during vulval development in C. elegans. *Development* **125:** 3101–3109

Liu ZJ, Shirakawa T, Li Y, Soma A, Oka M, Dotto GP, Fairman RM, Velazquez OC, Herlyn M (2003) Regulation of Notch1 and Dll4 by vascular endothelial growth factor in arterial endothelial cells: implications for modulating arteriogenesis and angiogenesis. *Mol Cell Biol* **23:** 14–25

McConnell SK, Kaznowski CE (1991) Cell cycle dependence of laminar determination in developing neocortex. *Science* **254:** 282–285

Mello CC, Kramer JM, Stinchcomb D, Ambros V (1991) Efficient gene transfer in C.elegans: extrachromosomal maintenance and integration of transforming sequences. *EMBO J* **10:** 3959–3970

Moore NL, Narayanan R, Weigel NL (2007) Cyclin dependent kinase 2 and the regulation of human progesterone receptor activity. *Steroids* **72:** 202–209

Mori H, Palmer RE, Sternberg PW (1994) The identification of a Caenorhabditis elegans homolog of p34cdc2 kinase. *Mol Gen Genet* **245:** 781–786

Natarajan L, Jackson BM, Szyleyko E, Eisenmann DM (2004) Identification of evolutionarily conserved promoter elements and amino acids required for function of the C. elegans beta-catenin homolog BAR-1. *Dev Biol* **272:** 536–557

Oberg C, Li J, Pauley A, Wolf E, Gurney M, Lendahl U (2001) The Notch intracellular domain is ubiquitinated and negatively regulated by the mammalian Sel-10 homolog. *J Biol Chem* **276:** 35847–35853

Setty Y, Cohen IR, Dor Y, Harel D (2008) Four-dimensional realistic modeling of pancreatic organogenesis. *Proc Natl Acad Sci USA* **105:** 20374–20379

Sharma VM, Draheim KM, Kelliher MA (2007) The Notch1/c-Myc pathway in T cell leukemia. *Cell Cycle* **6:** 927–930

Shaye DD, Greenwald I (2002) Endocytosis-mediated downregulation of LIN-12/Notch upon Ras activation in Caenorhabditis elegans. *Nature* **420:** 686–690

Shaye DD, Greenwald I (2005) LIN-12/Notch trafficking and regulation of DSL ligand activity during vulval induction in Caenorhabditis elegans. *Development* **132:** 5081–5092

Sternberg PW (2005) Vulval development. *WormBook* 1–28, ed. The *C. elegans* Research Community, WormBook, doi/10.1895/wormbook.1.6.1, http://www.wormbook.org

Stylianou S, Clarke RB, Brennan K (2006) Aberrant activation of notch signaling in human breast cancer. *Cancer Res* **66:** 1517–1525

Sundaram MV (2005) The love-hate relationship between Ras and Notch. *Genes Dev* **19:** 1825–1839

Tax FE, Yeargers JJ, Thomas JH (1994) Sequence of C. elegans lag-2 reveals a cell-signalling domain shared with Delta and Serrate of Drosophila. *Nature* **368:** 150–154

Tilmann C, Kimble J (2005) Cyclin D regulation of a sexually dimorphic asymmetric cell division. *Dev Cell* **9:** 489–499

van den Heuvel S (2005) Cell-cycle regulation. *WormBook* 1–16, ed. The *C. elegans* Research Community, WormBook, doi:10.1895/wormbook.1.28.1, http://www.wormbook.org

Weigmann K, Lehner CF (1995) Cell fate specification by even-skipped expression in the Drosophila nervous system is coupled to cell cycle progression. *Development* **121:** 3713–3721

Wu G, Lyapina S, Das I, Li J, Gurney M, Pauley A, Chui I, Deshaies RJ, Kitajewski J (2001) SEL-10 is an inhibitor of notch signaling that targets notch for ubiquitin-mediated protein degradation. *Mol Cell Biol* **21:** 7403–7415

Yamaguchi T, Cubizolles F, Zhang Y, Reichert N, Kohler H, Seiser C, Matthias P (2010) Histone deacetylases 1 and 2 act in concert to promote the G1-to-S progression. *Genes Dev* **24:** 455–469

6.2 Degradation of NICD is connected to cell cycle progression - further results not included in the manuscript

Mutating putative phosphorylation sites

NICD has been shown to be degraded in a proteasome dependent manner as consequence of hyperphosphorylation and ubiquitylation (Gupta-Rossi *et al*, 2001; Oberg *et al*, 2001; Wu *et al*, 2001). It is known that in *C. elegans* vulval development, the E3 ubiquitin ligase SEL-10 is responsible for ubiquitylation (Wu *et al*, 2001). However, the kinase that phosphorylates NICD to target it for degradation has not been identified yet. Cyclin dependent kinases phosphorylate their substrates at a serine or a threonine residue followed by a proline (Morgan, 2007). Therefore, the NICD protein sequence was scanned for consecutive amino acids SP or TP. Two potential phosphorylation sites could be found upstream of the *gfp* insertion site and five downstream (Figure 1). As shown in Figure 1, these phosphorylation sites had been mutated in three clusters to alanine to prevent phosphorylation. All three constructs had been controlled by the promoter of *bar-1* like the previously examined NICD::GFP construct and integrated via MosSCI into the genome as a single copy to be able to compare the amount of protein and its degradation rate. All three constructs resulted in diminished NICD::GFP signal in the VPCs (Figure 2). Mutations to alanine of the two first putative phosphorylation sites caused the weakest signal. This result could also be confirmed by counting inductions (Table 1).

If hyperphosphorylation leads to degradation, then a higher signal level of a mutated protein that cannot be phosphorylated would have been expected. However, since we rather observed weaker signals, we mutated the same putative phosphorylation sites in clusters to aspartic acid to mimic phosphorylation and expected to detect more stable protein. Examining

extrachromosomal arrays of the phosphorylation mimicking constructs due to lesser expenditure of time, did not support the assumption that dephosphorylation is responsible for degradation, because these constructs neither resulted in more stable protein (Figure 2; data not shown).

Rather than going more into detail and examining single mutations instead of clusters, we decided to clone deletion constructs and do a structure function analysis of NICD::GFP (see manuscript, chapter 6.1). This approach identified the PEST domain and ankyrin repeats as critical domains for NICD degradation.

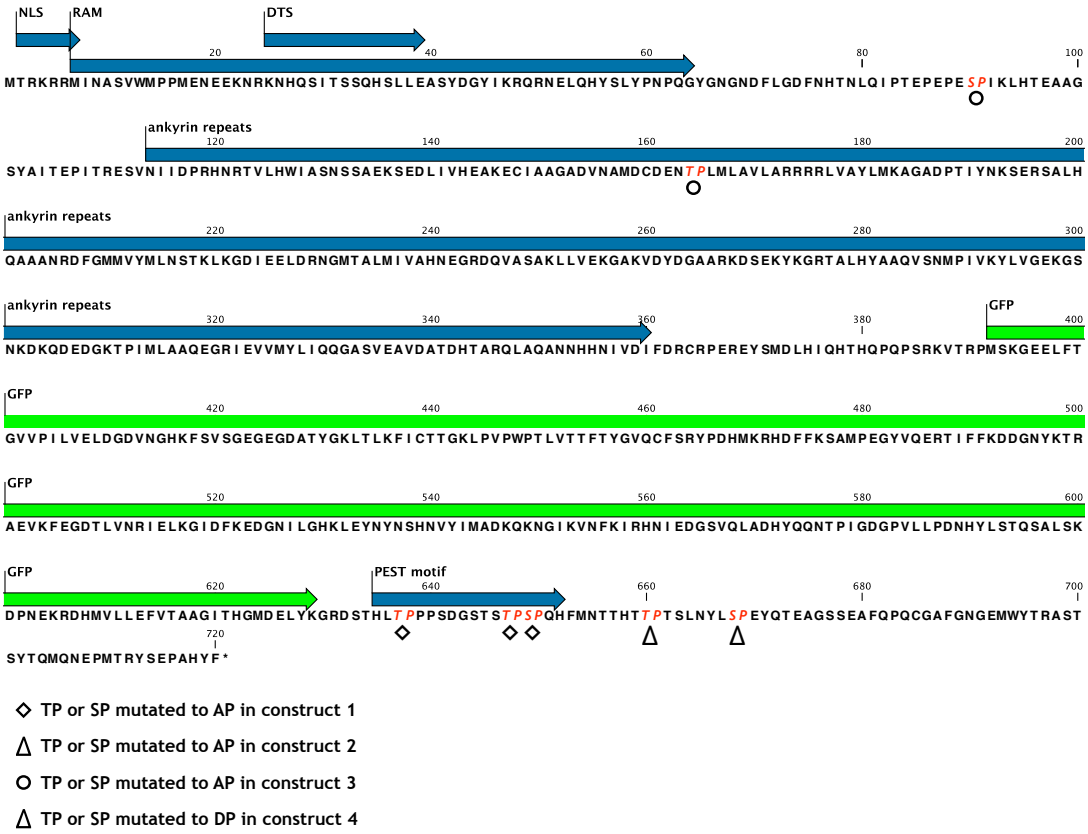

Figure 1: The NOTCH intracellular domain NICD with GFP.
The protein sequence of the NICD::GFP construct contains following domains: NLS (nuclear localisation signal, predicted by the Rost lab, www.predictprotein.org), RAM (RBP-Jkappa-associated) module (Shaye and Greenwald, 2002) containing the DTS (downregulation targeting signal) that is important for endocytosis of the full-length receptor (Shaye and Greenwald, 2005), the ankyrin repeats (predicted by CLC Main Workbench 5) that are responsible for protein interaction with CSL and other transcription factors, the PEST (proline/glutamic acid/serine/threonine rich) motif that is important for proteasome-dependent degradation (Gupta-Rossi *et al*, 2001). The green labelled sequence marks the integrated green fluorescent protein (GFP). In red the putative serine/threonine phosphorylation sites are labelled. They were mutated either to alanine (A) to prevent phosphorylation or to aspartic acid (D) to mimic phosphorylation. The four different mutations sites are indicated by the circle (construct 3), the diamond (construct 1) and the triangle (construct 2 and 4).

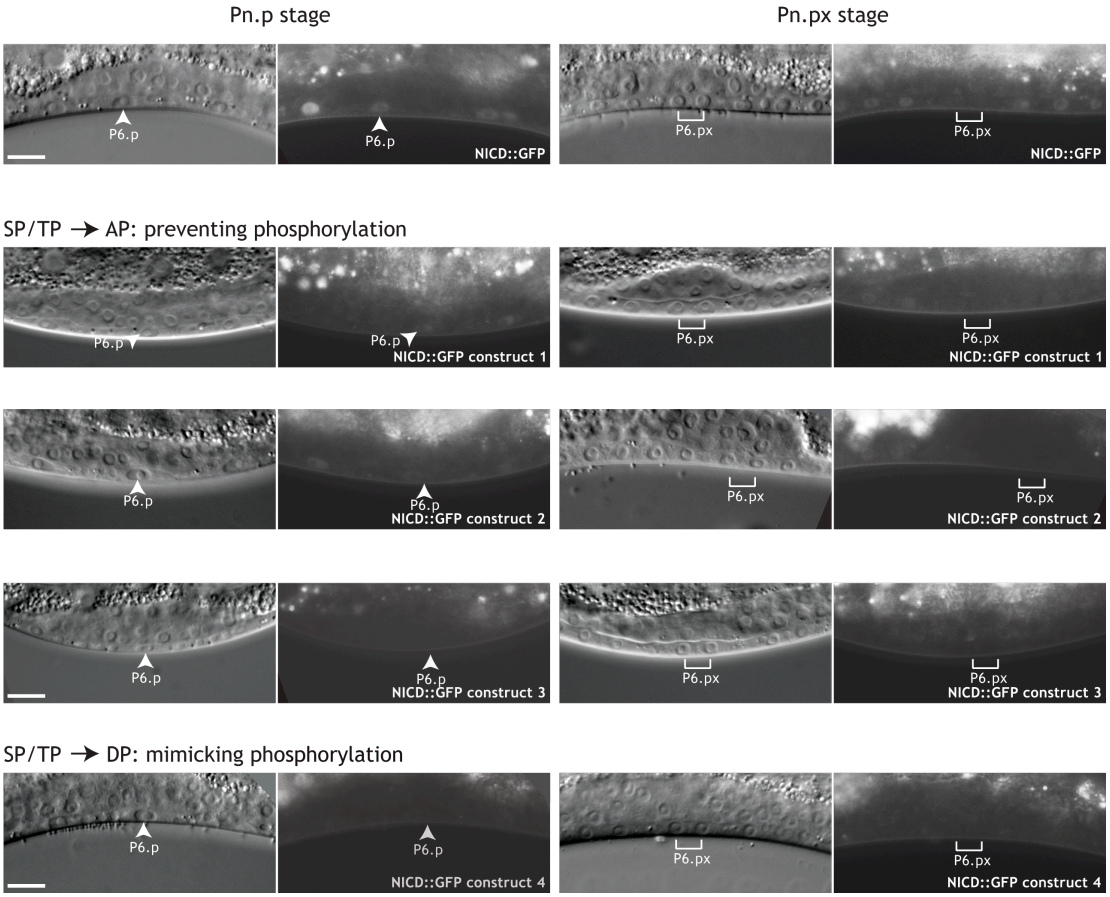

Figure 2: NICD::GFP constructs with mutated phosphorylation sites exhibit less signal than the wild-type NICD::GFP reporter.
In animals carrying the wild-type NICD::GFP reporter construct a clear expression in the secondary VPCs and VPC descendants and a weaker expression in the primary VPCs can be detected (upper panels). Different phosphorylation sites had been mutated in clusters (like indicated in Figure 1) from serine proline or threonine proline (SP/TP) to alanine proline (AP) to prevent phosphorylation (construct 1,2,3). The two constructs 1 and 2 with mutations in the PEST domain or after the PEST domain still showed some detectable expression during Pn.p stage and Pn.px stage; however, this expression was definitively weaker than the expression of the wild-type construct. Construct 3 with mutations at the N-terminus did not exhibit any detectable expression. When the phosphorylation sites at the C-terminus had been mutated to aspartic acid (D) to mimic phosphorylation no expression could be seen (lower panel, construct 4). Corresponding Nomarski pictures are to the left of the fluorescent pictures. The scale bar represents 10 µm.

Row	Genotype	construct	Inductionindex ± SE (n) [#]	% Muv [†]
1	*zhIs39 [nicd::gfp]*	wild-type	5.85 ± 0.04 (38)	100
2	*zhIs40 [nicd::gfp ($T_{637}A$; $T_{647}A$; $T_{649}A$)]*	construct 1	5.57 ± 0.10 (22) ***(1)	100
3	*zhIs41 [nicd::gfp ($T_{660}A$; $S_{668}A$)]*	construct 2	5.43 ± 0.09 (45) ***(1)	100
4	*zhIs42 [nicd::gfp ($S_{90}A$; $T_{164}A$)]*	construct 3	3.41 ± 0.12 (22) ***(1)	41

Table 1
Asterisks indicate the significance as described in material and methods. In brackets the row that was used for comparison is indicated.
[#] The inductionindex presents how many VPCs per worm adopt a 1° or 2° fate. SE indicates the standard error.
[†] Muv is defined as ≥ 3 induced VPCs.

Testing candidates for NICD stabilising potency

CDK-8 hyperphosphorylates NICD in mammalian cells

Fryer *et al.* showed in 2004 that expression of CycC and CDK8 in mammalian cells leads to hyperphosphorylation of NICD and following PEST-dependent degradation via the ubiquitin ligase Fbw7/Sel10 (Fryer *et al*, 2004). CDK-8 plays a role in transcriptional repression, but the downstream targets of CDK-8 kinase activity in *C. elegans* are till today unknown (Clayton *et al*, 2008). Therefore, the influence of the *cdk-8* deletion allele *tm1238* and the *cic-1* deletion allele *tm3740* on full-length LIN-12::GFP was tested. (The full-length reporter of LIN-12 was used for this experiment since the *nicd::gfp* construct was not available at this time.) If CDK-8 plays the same role in NICD degradation in *C. elegans* as in mammalian cells, then a diffuse signal as in G1 arrested primary VPCs would have been expected. However, compared to control animals, neither mutants for *cdk-8* nor mutants for *cic-1* did show any alteration in LIN-12::GFP expression in P6.p, neither of the membrane bound protein nor of the released activated form (Figure 3). Thus, a small RNAi screen against all known CDKs in *C. elegans* was performed later in the NICD::GFP transgenic background. Positive results are reported in the manuscript (chapter 6.1).

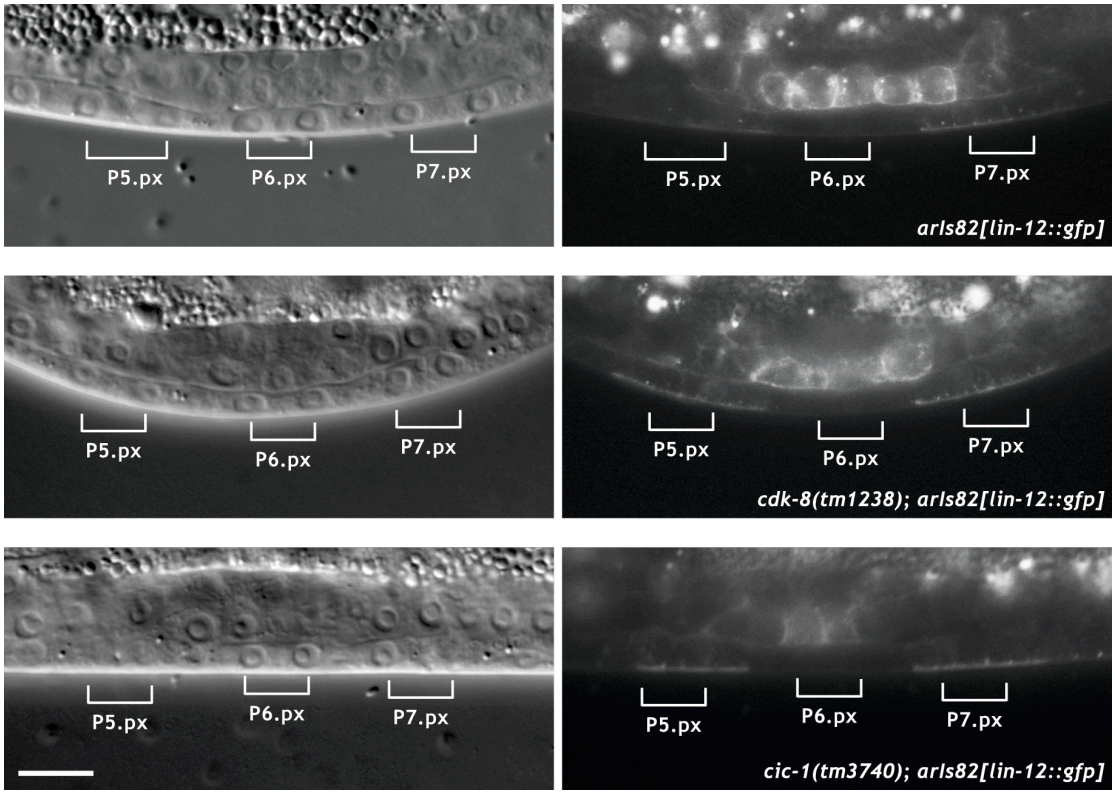

Figure 3: Neither CDK-8 nor its cyclin CIC-1 has an effect on the LIN-12 NOTCH reporter.
The LIN-12::GFP full-length reporter is expressed during Pn.px stage in secondary descendants. It can be found at the apical membrane, in intracellular spots and weakly in the nucleus (upper panels). Neither the deletion allele of *cdk-8* nor *cic-1* has an impact on this expression pattern (lower panels). The corresponding Nomarski pictures are to the left of the fluorescent pictures. The scale bar represents 10 µm.

SIR-2.1 deacetylates NICD in human endothelial cells

Recently, Guarani *et al*. showed that the NAD^+-dependent deacetylase SIRT1 in human endothelial cells functions as NICD deacetylase and thereby works against the acetylation-dependent stabilisation of NICD (Guarani *et al*, 2011). We hytothesised that the cell cycle could influence NICD turnover indirectly via *sir-2.1*, the closest homologous gene of SIRT1. Therefore, the deletion allele *ok434* was crossed into the strain carrying the NICD::GFP transgene. If SIR-2.1 deacetylates and destabilises NICD, the *sir-2.1* (*ok434*) allele should cause an increase of the NICD::GFP signal. However, we detect rather a decrease in *C. elegans sir-2.1* (*ok434*) mutants compared to wild-type animals (Figure 4). Interestingly, this significant decrease seems to be coupled to cell cycle progression of the VPCs since it only appears in Pn.px stages and not in Pn.p stages.

Since this experiment showed the opposite outcome than expected it raises more questions than it answers. Therefore, further examination has to be done and it was not included into the manuscript.

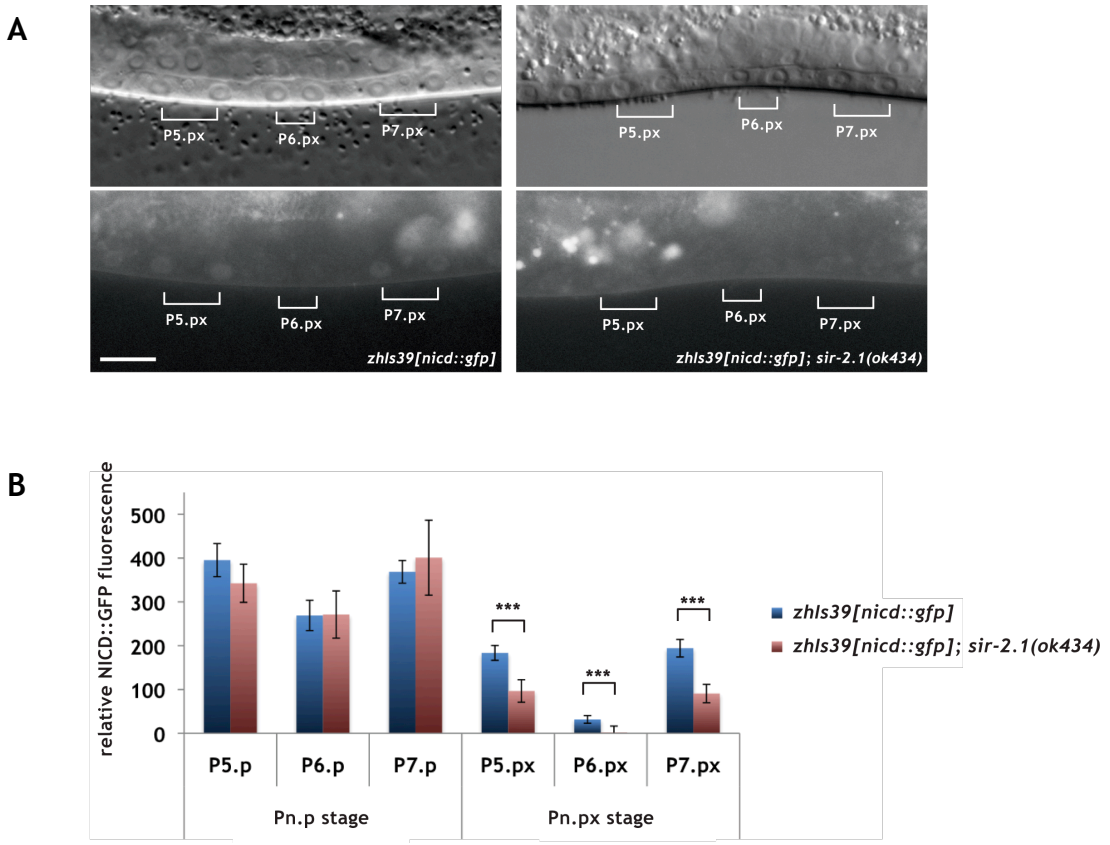

Figure 4: The deacetylase SIR-2.1 stabilises NICD::GFP during Pn.px stage.
(A) Fluorescence pictures and corresponding Nomarski pictures on top of clearly visible NICD::GFP signal in wild-type background (left) and diminished NICD::GFP signal in a *sir-2.1(ok434)* mutant background (right). The scale bar represents 10 µm. (B) Quantitative analysis revealed that a difference in NICD::GFP signal only could be detected after cell cycle division from Pn.p stage to Pn.px stage. Error bars indicate the standard error and asterisks indicate the significance as described in materials and methods. (Pn.p stage: *zhIs39[nicd::gfp]* n=27; *zhIs39[nicd::gfp]; sir-2.1(ok434)* n=13; Pn.px stage: *zhIs39[nicd::gfp]* n=17; *zhIs39[nicd::gfp]; sir-2.1(ok434)* n=12)

RNAi against *cyb-1* and *cyb-2* diminishes NICD stability

In the manuscript it is mentioned that RNAi against *cyb-3* interferes with the degradation of NICD::GFP. Therefore, NICD::GFP is stabilised in P6.p descendants in *cyb-3* RNAi treated animals. Together with *cyb-3* RNAi also RNAi against the other G2-specific B-type cyclins *cyb-1*, *cyb-2.1* and *cyb-2.2* had been tested, whereupon *cyb-2.1* and *cyb-2.2* were

simultaneously affected by the same RNAi clone. Instead of also causing an increase in NICD::GFP expression, RNAi against these other cyclins resulted in overall diminished NICD::GFP signal (Figure 5). These findings suggest different functions of CDK-1/cycline B complexes. Whereas CYB-3 seems to have a role in destabilising NICD, CYB-1 and CYB-2 might act together with CDK-1 to stabilise NICD providing a sharp switch to turn off LIN-12 NOTCH signalling.

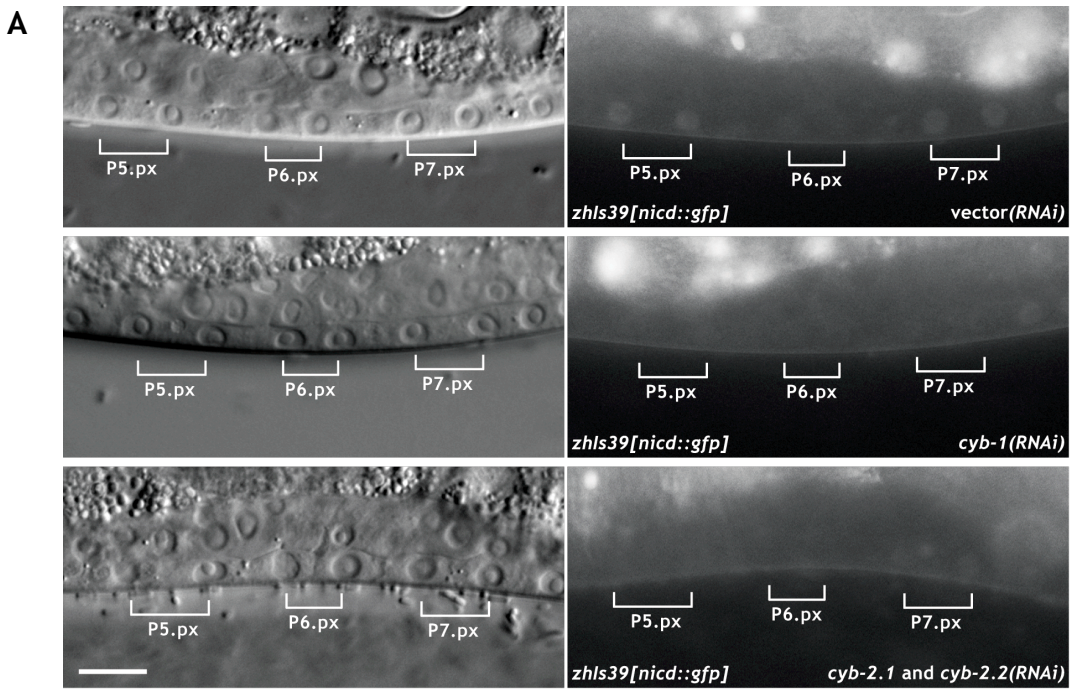

Figure 5: RNAi against *cyb-1*, *cyb-2.1* and *cyb-2.2* reduces the stability of NICD::GFP. (A) Representative fluorescent pictures and corresponding Nomarski pictures (to the left). The scale bar represents 10 µm. (B) Quantitative analysis of the RNAi treatment against *cyb-1*, *cyb-2.1* and *cyb-2.2*. Error bars indicate the standard error and asterisks indicate the significance as described in materials and methods.

Cyclins *cyd-1* and *cye-1* may be LIN-12 NOTCH targets

In parallel to the examinations on how cell cycle progression influences NICD stability and LIN-12 NOTCH signalling in the VPCs, chromatin immunoprecipitation (ChIP) was performed by Erika Fröhli using the *zhIs39[nicd::gfp]* reporter to screen for LIN-12 NOTCH downstream targets.

Interestingly, binding sites in promoter regions of two cell cycle components, *cyd-1* and *cye-1*, could be detected (Figure 6). Some of the binding regions are closely located to putative CSL sites. Therefore, the question came up, if LIN-12 NOTCH signalling not only is influenced by the cell cycle progression but also might influence cell cycle progression in a feedback loop. To address this question, two transcriptional reporters for *cyd-1* were built by cloning enhancer fragment 1, which is located 4101 bp upstream of the translational start codon, or fragment 2, which comprises the third intron, upstream of the minimal promoter of *pes-10*, which only gives rise to expression in combination with an enhancer fragment (Figure 6). These two regions had been selected due to the overlap of ChIP peaks and CSL binding sites. Additionally, expression patterns of an available transcriptional reporter of *cyd-1* and of an available translational reporter of *cye-1* were analysed (Fujita *et al*, 2007; Park *et al*, 1999).

As expected, *pes-10p::gfp* alone did not result in any expression (data not shown). However, in combination with the third intron (fragment 2) of *cyd-1*, a clear GFP signal in gonadal tissue, in seam cells and occasionally a weak signal in some induced VPCs could be detected (Figure 7 A; data not shown). The promoter fragment 1 of *cyd-1*, cloned upstream of the minimal promoter, resulted in gonadal expression and showed a weak signal in 3° VPC descendants (Figure 7 B). The transcriptional reporter of Park *et al*. showed additionally expression in neuronal descendants of the P cells (Park *et al*, 1999). However, a specific LIN-12 NOTCH dependent expression pattern would be expected to look like following: higher signal in 2° compared to 1° VPCs and expression in the π cells that are induced by

LIN-12 NOTCH signalling by the AC (Newman *et al*, 1995). None of the constructs gave rise to such an expression pattern.

The promoter used by Park *et al*. does not include any of the ChIP peaks. To address the question, if the reporter of Park *et al*. just misses some important intronic sites for a LIN-12 NOTCH dependent regulation, the reporter was co-injected with fragment 2. Several lines were scored, but again no LIN-12 NOTCH specific expression pattern could be detected (Figure 7 C).

Transcription of *cye-1* is known to be ubiquitous during embryonic stages and only becomes restricted and dynamic during postembryonic development. Bodigan *et al*. could detect nuclear CYE-1 protein in all proliferating tissues, but CYE-1 becomes absent when the lineage is completed (Brodigan *et al*, 2003). The translational reporter of *cye-1*, which I received from Hitoshi Sawa (Fujita *et al*, 2007), showed equal GFP signal in all VPCs. No bias for secondary VPCs or their descendants could be seen (Figure 7 D).

Thus, although the data of the ChIP experiment point to a transcriptional feedback loop between NOTCH signalling and cell cycle regulation, we could not prove it at least for vulval tissue.

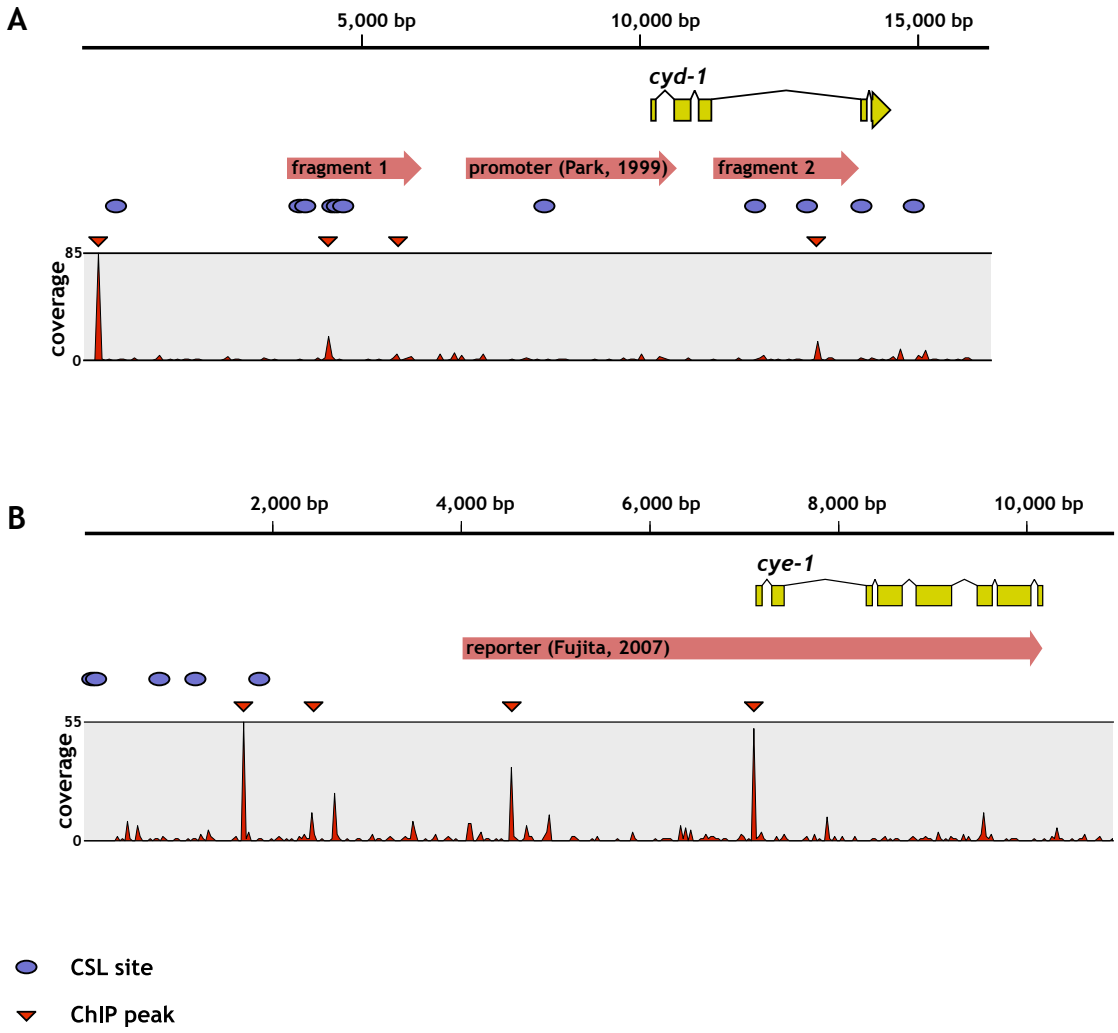

Figure 6: Chromatin immunoprecipitation revealed binding sites of NICD in promoter regions of two cyclins.
ChIP peaks could be detected for the promoter and intron region of *cyd-1* (A) and for the promoter region of *cye-1* (B). The open reading frames of the genes are indicated in yellow. Cloned or received reporter sequences are indicated as red arrows (Fujita *et al*, 2007; Park *et al*, 1999). Putative CSL sites with the consensus sequence RTGGGAA are labelled as blue circles (Berset *et al*, 2001). Red triangles represent ChIP peaks. The lower graphs show the coverage rate of the ChIP experiment. The alignment was made using CLC Workbench.

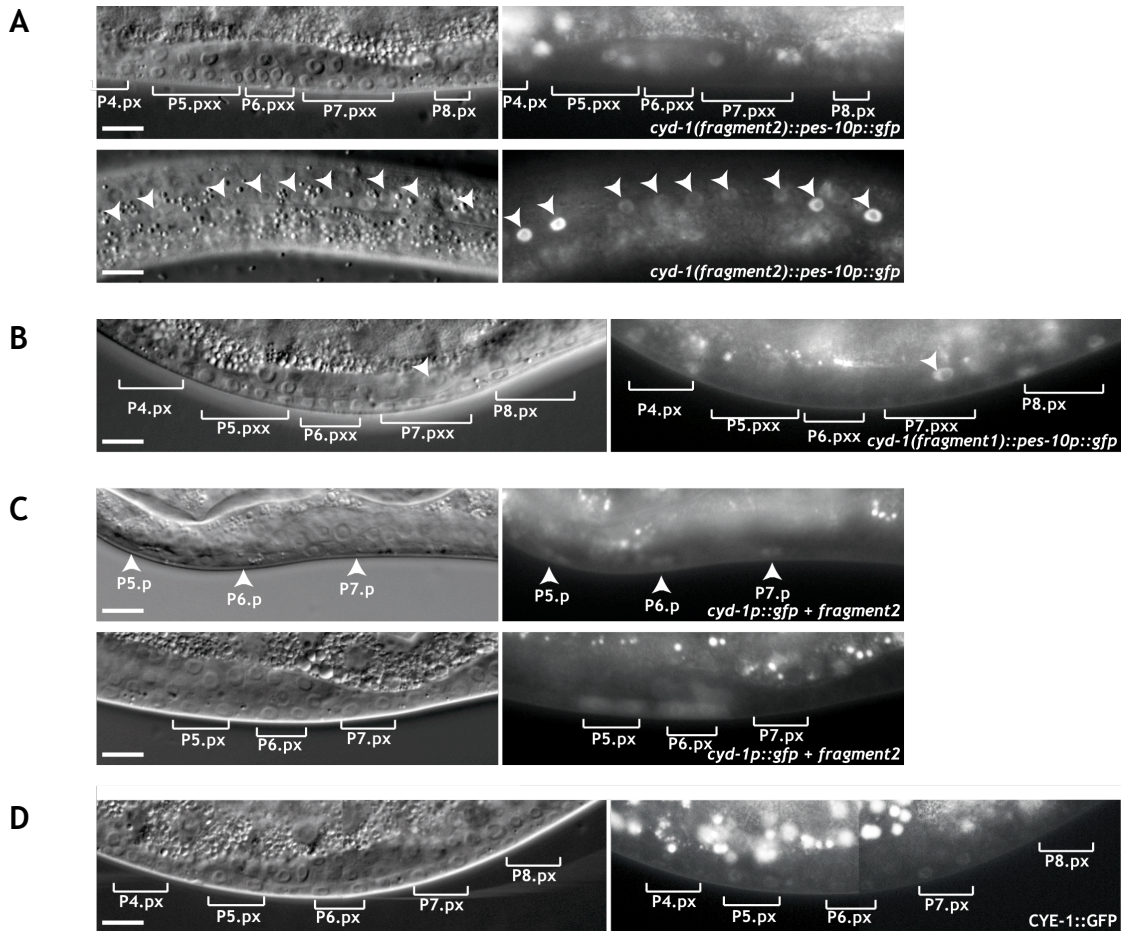

Figure 7: Expression of *cyd-1* and *cye-1*.
(A) The third intron of *cyd-1* (fragment 2) cloned upstream of the minimal promoter of *pes-10 zhEx414[cyd-1(fragment2)::pes-10::gfp]* drives expression in gonadal tissue, in 3° VPCs (upper panels) and in the seam cells (lower panels). (B) A 2450 bp long promoter fragment (fragment 1) that is cloned upstream of the minimal promoter of *pes-10 zhEx415[cyd-1(fragment1)::pes-10::gfp]* leads to expression in single gonadal cells, 3° VPCs and to a weak signal in descendants of induced VPCs. (C) When a transcriptional reporter for *cyd-1* that comprises 3338 bp upstream of the ATG (Park *et al*, 1999) is co-injected with the third intron (fragment 2) *zhEx464[pKM1109(cyd-1p::gfp);pSN36(fragment2)]* expression in gonadal tissue and all VPCs and descendants could be detected. (D) A translational reporter for *cye-1* (Fujita *et al*, 2007) resulted in expression in all VPCs and their descendants as long they proliferate. Corresponding Nomarski pictures are located to the left of the fluorescent pictures. The scale bars represent 10 µm.

6.3 Characterisation of the LIN-12 NOTCH target gene *ttr-11*

The expression pattern of *ttr-11*

The *ttr-11* gene had been identified in a reverse genetic screen for LIN-12 NOTCH targets during vulval development (Rimann, 2008). RNAi against *ttr-11*, using the clone JA:F46B3.3 from Julie Ahringer's library, resulted in diminished expression of the 2° cell fate marker *egl-17p::yfp* (Kamath *et al*, 2003; Rimann, 2008). An extrachromosomal transcriptional reporter of *ttr-11* (*zhEx200*) gave rise to occasional vulval expression in 2° descendants during Pn.px and Pn.pxx stages (Figure 1). Additionally, it showed expression in the ventral uterine cells (Figure 1) (Rimann, 2008). Both expression patterns support the theory that *ttr-11* might be a LIN-12 NOTCH target, since 2° cell fates are specified via LIN-12 NOTCH and also the induction of the π cell fate in the ventral uterus is induced via LIN-12 NOTCH signalling by the AC.

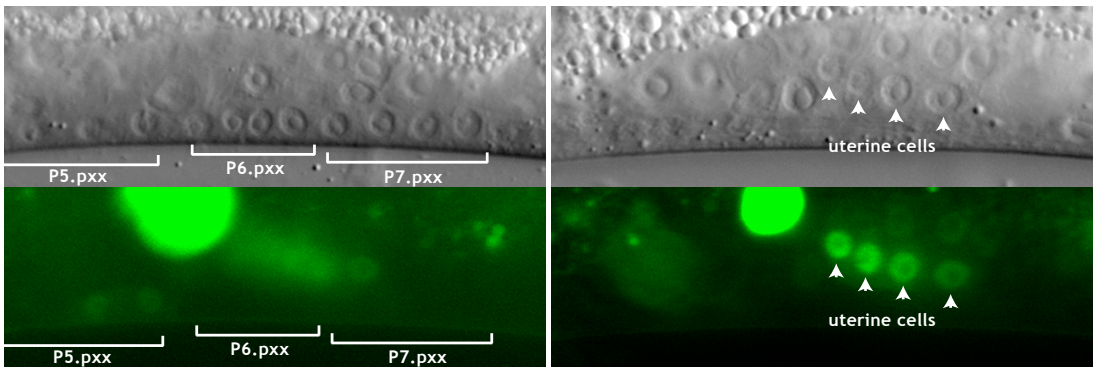

Figure 1: Expression of *ttr-11* in wild-type *C. elegans*.
An extrachromosomal array of a transcriptional reporter for *ttr-11* gave rise to GFP expression in 2° VPC descendants (left) and vulval uterine cells (right). (Adopted from (Rimann, 2008))

To prove that *ttr-11* expression is LIN-12 NOTCH dependent, the transcriptional reporter was injected into the mutant strain MT2343 carrying

the gain-of-function allele *lin-12*(*n137*) over the loss-of-function allele *lin-12*(*n137n720*) (Sternberg *et al*, 1989). Segregation in the F1 progeny allowed examining the expression of the reporter in homozygous *gf* and *lf* mutants. Mutants for *lin-12*(*n137gf*) showed expression of *ttr-11* in descendants of all VPCs and enhanced expression in the uterus (Figure 2). In *lin-12*(*n137n720lf*) mutants *ttr-11* expression could not be detected at all during Pn.px and Pn.pxx stage (data not shown) and during late L3/L4 only two cells in the uterus exhibited weak GFP signal (Figure 2). Since in *lin-12*(*n137gf*) mutants all VPCs adopt a 2° fate but in *lin-12*(*n137n720lf*) mutants only 1° and 3° cell fates are established and no induction of π cell fates happens, the expression pattern of the transcriptional *ttr-11* reporter proves that *ttr-11* is regulated directly or indirectly via LIN-12 NOTCH signalling during the early L3 stage. Later during the L4 stage, *ttr-11* might be regulated independently of LIN-12 NOTCH.

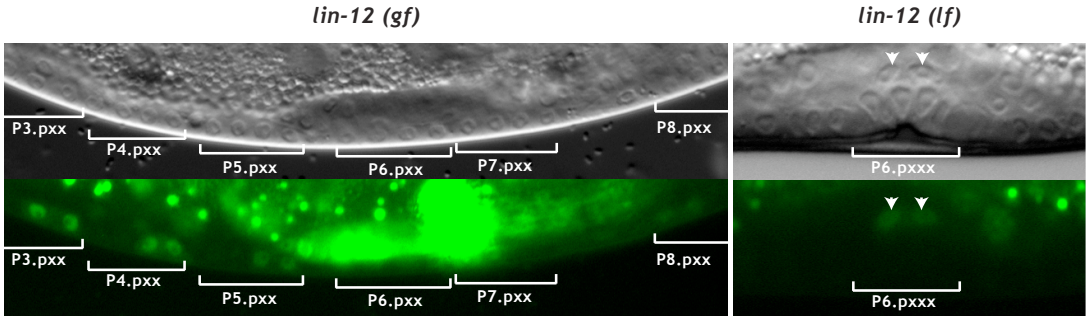

Figure 2: Expression of *ttr-11* in *lin-12*(*gf*) and *lin-12*(*lf*).
In animals with a *lin-12*(*n137gf*) background, an extrachromosomal array containing the reporter for *ttr-11* (*zhEx307.4*) was expressed in descendants of ectopic 2° VPCs (left). In *lin-12*(*n137n720lf*) only 2 cells in the uterus during late L3/L4 stage showed expression of the *ttr-11* reporter construct (*zhEx307.6*) (right).

The annotation of *ttr-11* changed over time

Since 2008, when the screen that identified *ttr-11* as potential LIN-12 NOTCH target was performed, the annotation of the *ttr-11* locus in wormbase (www.wormbase.org/) changed. Originally the RNAi clone only affected the gene *ttr-11*. However, in 2009, two genes had been annotated instead of one, *ttr-11* and *ttr-57* (Figure 3). Yet, no analysis of expressed sequence tags (ESTs) existed that would confirm the transcripts. Therefore, reverse transcription of total mRNA extract of wild-type *C. elegans* was used

to obtain a pool of cDNA transcripts that served as templates for PCR performed with different preselected primers (see material and methods) to amplify and sequence the transcripts of the potential genes *ttr-11* and *ttr-57*. Analysis of wild-type cDNA transcripts revealed again a difference in the transcripts compared to the wormbase annotation in 2009. The transcripts comprised both genes, though stop codons separated always the two open reading frames. Variations of exon compositions and individual exon lengths could be detected (Figure 3). The difference in the transcripts to the wormbase annotation existed in the fact that the sequenced transcripts always resulted in shorter proteins than the transcripts annotated in wormbase due to different exon lengths and following frame shifts. However, in 2010, wormbase annotation changed anew and covers now at least one of the transcript variants found for each gene (Figure 3). The fact that other research efforts resulted in the same conclusions proves the trueness of the cDNA transcript analysis in this experiment.

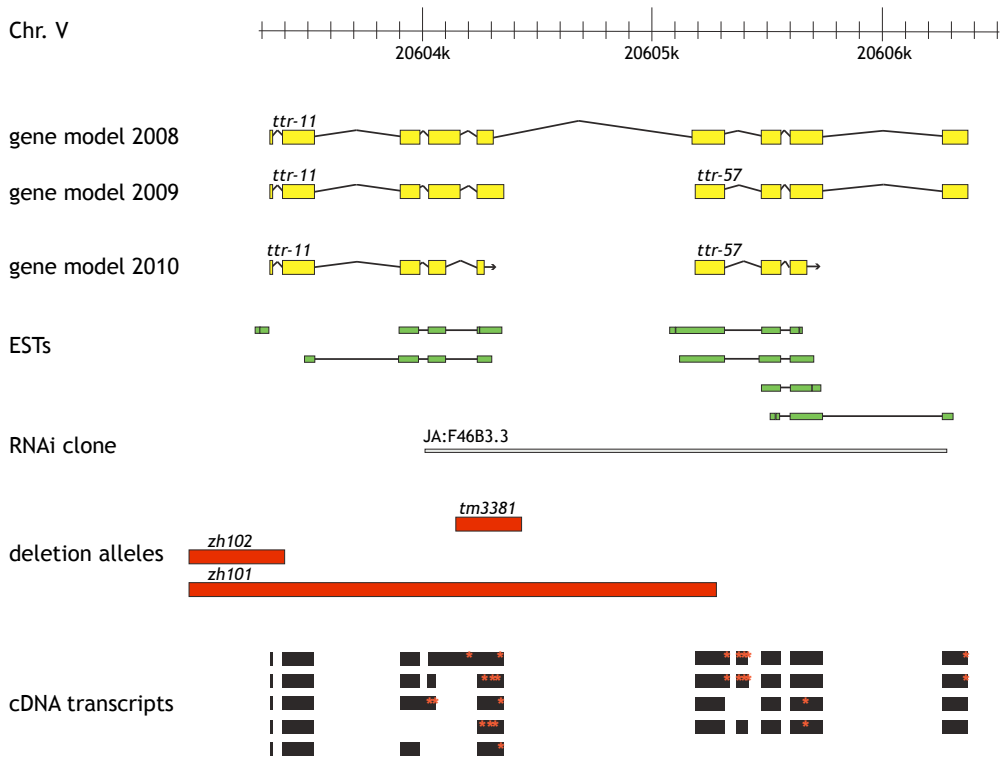

Figure 3: Gene models of *ttr-11* and cDNA transcripts.
The annotation on wormbase of the gene *ttr-11* changed over time. There had been three different historical gene models annotated (yellow). Expressed sequence tags are recently annotated (green).The RNAi clone (grey) affects the two genes *ttr-11* and *ttr-57*. Red bars present deletion alleles. Sequencing of cDNA transcripts (black) indicated that the annotation of 2009 could not be true. Red stars present stop codons. (partly adapted from wormbase.org)

Similarity of TTR-11 to other TTRs

Besides *ttr-11* and *ttr-57*, another 57 *ttr* genes exist in the *C. elegans* genome. For some of them, like *ttr-12* or *ttr-59*, two transcript variants exist (www.wormbase.org). Thus, also the additional, not annotated mRNA variations for *ttr-11* and *ttr-57* that had been found in the transcript analysis might be transcribed. Highest homology exists between *ttr-11* and *ttr-57* (Figure 4 A and B). All TTR proteins contain a transthyretin-like (TTL) domain, whose function still is unknown. Most members of the TTL protein family, also TTR-11 and TTR-57, contain a hydrophobic signal peptide (SP) sequence, which leads to the assumption that these proteins are secreted. Therefore, TTR-11 might be anchored in the plasma membrane or has to be processed to be secreted. For TTR-57 an aspartic peptidase active site is also predicted (www.wormbase.org). However, experimental data about its functionality are missing. The next closest related *ttr* gene to *ttr-11* is *ttr-9* with 34% maximal identity (NCBI/BLAST; Figure 4 A and B).

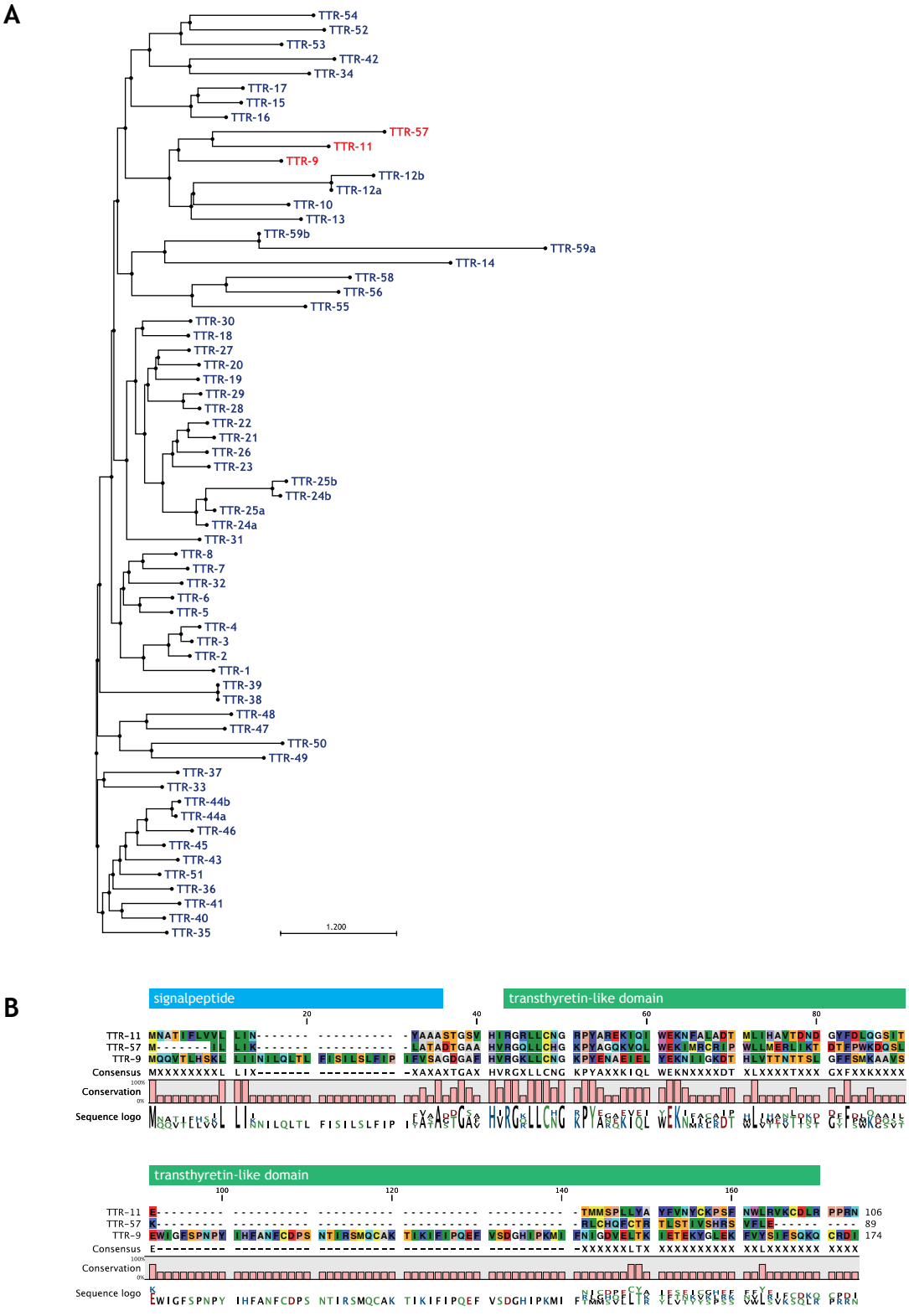

Figure 4: Relationship of TTR-11.
(A) Phylogenetic tree of all known *ttr* genes of *C. elegans*. Alignment was done by clustalX 2.1, tree was generated using CLC Main Workbench 5 (algorithm: neighbour joining, 10000 bootstraps). (B) Alignment of TTR-11 and its two closest related genes TTR-57 and TTR-9 (done by using CLC Main Workbench 5). Protein domains of TTR-11 predicted by CLC Main workbench 5 are indicated by the colour bars above the alignment. The transthyretin-like domain is supposed to be located extracellular.

To test if either knockdown of *ttr-11* or *ttr-57* was responsible for the effect that led to the detection of the *ttr* gene during the RNAi screen, two smaller RNAi constructs had been cloned complementary to either *ttr-11* or *ttr-57*. However, neither the clone for *ttr-11* nor for *ttr-57* showed any effect when fed to a strain containing the reporter *ayIs4[egl-17p::gfp]* (NH2246) or even to the RNAi sensitive strain AH760 containing the same reporter *ayIs4* (Figure 5 B, data not shown). Moreover, the RNAi clone JA:F46B3.3 from Julie Ahringer's library did not result in diminishment of *egl-17p::gfp* in L4 nematodes, as it did in the screen for NOTCH targets (Figure 5 A, C). Nevertheless, since the outcome of RNAi experiments can be quite variable depending on the circumstances (location of experiment, person who is performing the experiment, gene that is affected, et cetera) and the strong evidence that *ttr-11* is regulated via LIN-12 NOTCH signalling, we decided to further examine the function of *ttr-11* and its possible redundant neighbour gene *ttr-57*.

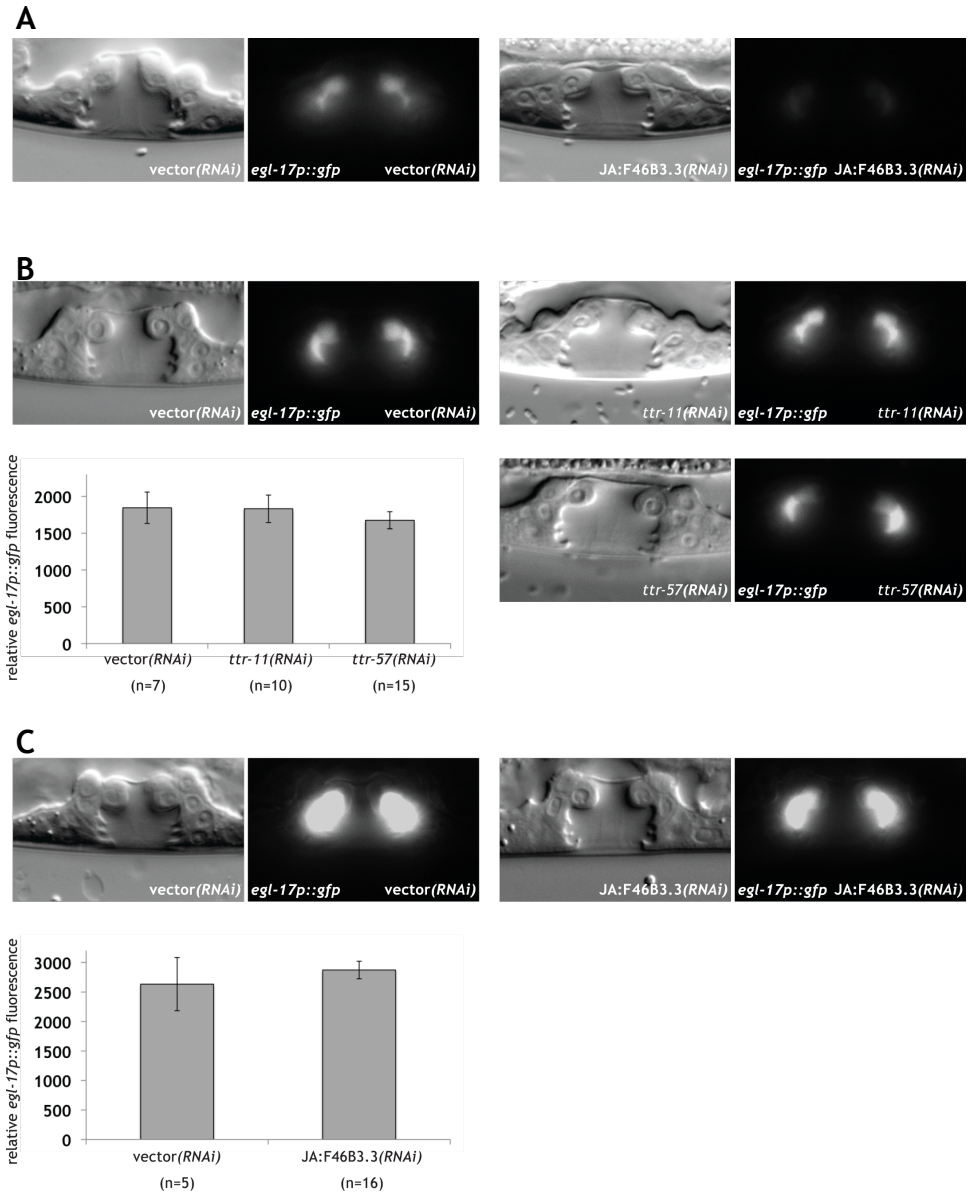

Figure 5: Knockdown of *ttr-11* and *ttr-57* via RNAi in the background of the 2° cell fate marker *egl-17p::gfp*.
(A) Repetition of the results observed during the screen. 30 % of the animals showed a 2° cell fate marker defect in the RNAi sensitive background *rrf-3(pk1426)*. (Ivo Rimann performed this experiment.) (B) Individual knockdown of *ttr-11* or *ttr-57* did not show an effect on *egl-17p::gfp* expression in wild-type background. (C) Repetition of the RNAi against *ttr-11* and *ttr-57* together in the RNAi sensitive background *rrf-3(pk1426)* to reproduce the results observed during the screen failed. In all panels the corresponding Nomarski pictures are shown to the left. Error bars indicate the standard error as described in materials and methods.

Generation and analysis of mutants for *ttr-11*

The deletion allele *tm3381* was available from the Caenorhabditis Genomic Centre (CGC) (Figure 3). However, no obvious phenotype in single mutants and no change in GFP expression in a strain containing *egl-17p::gfp* in the background could be detected (Figure 6). The deletion of *tm3381*

affects only the last exon of *ttr-11* that does not code for the transthyretin-like domain (Figure 3, wormbase.org). Therefore, efforts to create complete knockout mutants of *ttr-11* alone or *ttr-11* and *ttr-57* were made. A strain containing an insertion of the transposon *Mos1* 400 bp upstream of the *ttr-11* start codon was used to insert (1) a deletion (*zh102*) affecting the transcriptional start and the first two exons of *ttr-11* and (2) a deletion (*zh101*) affecting the whole ORF of *ttr-11* and the transcriptional start of *ttr-57* including part of its first exon (Figure 3). This was achieved by *Mos1* excision induced **t**ransgene **i**nstructed gene **c**onversion, shortly called *Mos*TIC (Robert and Bessereau, 2007). However, both knockout mutants, like the *tm3381* allele, did not show any morphological defect as single mutants in neither 2° nor 1° lineage during vulval development (data not shown).

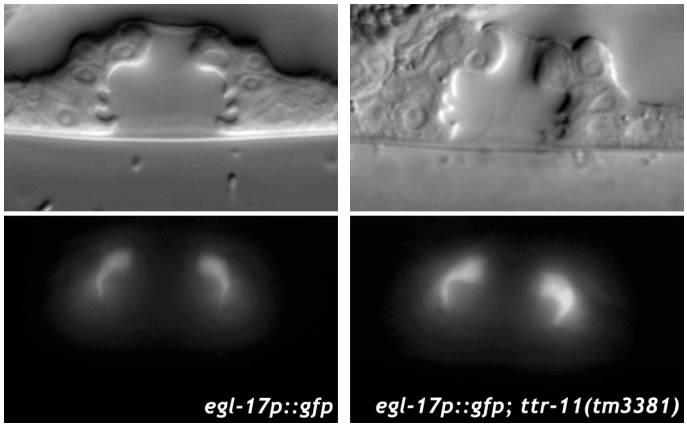

Figure 6: *ttr-11(tm3381)* mutants did not show a 2° cell fate marker defect.
The 2° cell fate marker *egl-17::gfp* was not diminished in a *ttr-11*(*tm3381*) background (right) compared to wild-type background (left). Corresponding Nomarski pictures are shown on top.

Mutants for *ttr-11* enhance the number of pseudovulvae in a *lin-12(n302)* background

Single mutants of *ttr-11* or mutants for *ttr-11* and *ttr-57* do not show phenotypic defects. Therefore, the different alleles of *ttr-11* were crossed into a *lin-12*(*gf*) background to test if they have a positive or negative effect on LIN-12 NOTCH signalling. The ligand-dependent *lin-12*(*gf*) allele *n302* was used for this purpose (de Souza *et al*, 2007; Greenwald *et al*, 1983). Animals carrying the *n302* allele have no AC. Since the two potential AC precursor cells Z1.ppp and Z4.aaa inhibit each other mutually via LIN-12 NOTCH

signalling from adopting an AC fate, both cells adopt the alternative uterine cell fate. Therefore, no induction of vulval development via LIN-3 EGF occurs in these mutants and no lateral inhibition between the VPCs takes place because no 1° cell fate is established. Animals carrying the allele *n302* show a vulvaless (Vul) phenotype (Figure 7 A). Only few worms show occasional pseudovulvae. Overall the induction index in *lin-12* (*n302*) animals is 0.16 (Table 1). However, already the *tm3381* allele of *ttr-11* elevated the number of pseudovulvae per worm, thus the percentage of the Muv phenotype was increased. The *zh101* allele that affects *ttr-11* and *ttr-57* enhanced the effect of the *tm3381* allele only insignificantly (Table 1). Strikingly, the *zh102* allele that affects only *ttr-11* showed significantly more pseudovulvae than the *ttr-11 ttr-57* double mutant or the mutant carrying the *tm3381* allele. We can only speculate that this phenotype is highly variable and easily influenced by environmental conditions at different days when pseudovulvae were counted. Thus, we can conclude that *ttr-11*(*lf*) mutants show a higher number of pseudovulvae. However, we cannot make any statement about *ttr-57* being redundant to *ttr-11* or being not redundant.

Row	Genotype	Inductionindex ± SE (n) [#]	% Muv [†] (n)	Pseudovulvae [◊]
1	*lin-12(n302)*	0.16 ± 0.05 (70)	12 (41)	0.34
2	*lin-12(n302); ttr-11(tm3381)*	0.50 ± 0.07 (119) ***(1)	31 (35)	0.83 ***(1)
3	*lin-12(n302); ttr-11(zh102)*	na	52 (31)	1.68 ***(1,2,4)
4	*lin-12(n302); ttr-11/57(zh101)*	na	35 (48)	1.00 ***(1)

Table 1
Asterisks indicate the significance as described in material and methods. In brackets the row that was used for comparison is indicated.
[#] The inductionindex presents how many VPCs per worm adopt a 1° or 2° fate. SE indicates the standard error.
[†] Muv is defined as ≥ 2 pseudovulvae.
[◊] Average number of pseudovulvae.

To be able to interpret the fact that *ttr-11*(*lf*) alleles lead to a higher number of pseudovulvae, it was important to identify the fates of these pseudovulvae. Therefore, we crossed the cell fate marker *egl-17p::gfp* into the strain. Examination did not achieve clear results, since only cells of some pseudovulvae showed 2° cell fate marker expression during the L4 stage (Figure 7 B). During the Pn.pxx stage no GFP signal could be detected

(data not shown). Therefore, we can conclude that at least some pseudovulvae derive from 2° cell fates, but we cannot exclude that also 1° fates are established.

Pseudovulvae caused by specification of 1° cell fate would indicate that an inductive signal was re-established in the double mutants which implies the formation of an AC. To identify possible ACs, the AC fate marker *lin-3p::gfp* (pAH67) was injected into the double mutant strain. However, transgenic animals could develop a wild-type vulva (data not shown). Thus, the reporter – even if only transcriptional – has by its own an effect on the phenotype. Therefore, this reporter could not be used for AC identification in *lin-12*(*n302*); *ttr-11*(*tm3381*) mutants. Another transcriptional AC marker (*cdh-3p::gfp*) was crossed into the double mutant. This marker showed weak expression in all invaginations due to its expression in 2° vulC and vulD cells and 1° vulE and vulF cells (Figure 7 C) (Inoue *et al*, 2002; Pettitt *et al*, 1996), but no AC in the uterus could be detected during earlier stages.

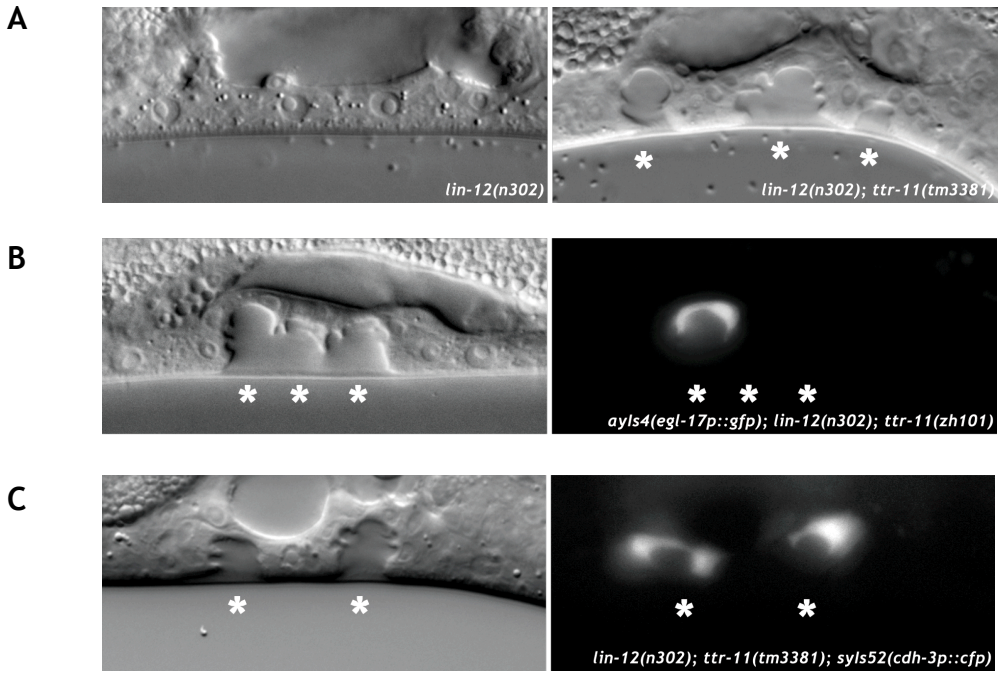

Figure 7: *ttr-11* mutants elevate the Muv phenotype of *lin-12(n302)*.
(A) Nomarski pictures of a vulvaless *lin-12(n302)* mutant and a multivulva *lin-12(n302); ttr-11(tm3381)* double mutant. (B) The 2° cell fate marker *egl-17p::gfp* can be detected in some but not in all pseudovulvae of a *lin-12(n302); ttr-11(zh101)* double mutant. (C) *cdh-3p::cfp* marks induced VPC descendants. Corresponding Nomarski pictures are shown to the left for B and C.

Taken together, *ttr-11* mutants have a higher induction index. However, it is not clear weather these inductions are of 1° or 2° nature. Interpreting the morphological phenotype, the branches of the invaginations might advert to 2° fate deviation. Then, *ttr-11*(*tm3381*) and *ttr-11*(*zh101*) would elevate LIN-12 NOTCH signalling activity independently of ligand binding in *lin-12*(*n302*) mutants. Thus, under wild-type conditions, *ttr-11* would have a negative effect on LIN-12 NOTCH signalling. However, the underlying facts of these observations might be more complex, since *ttr-11* seems to have the ability to alter the nature of a ligand-dependent allele of LIN-12 NOTCH and turn it into a weak ligand-independent allele.

The gene *ttr-11* has a positive effect on lateral signalling in a *lin-15(n309)* background

No obvious morphological defect was apparent in mutants carrying the *zh102* or *zh101* alleles. This is not so surprising since also RNAi experiments in the screen showed only 2° marker defects and no morphological phenotype. To further investigate if *ttr-11*(*lf*) has an impact on lateral inhibition of the 1° fate in the 2° lineage, the *ttr-11* allele *tm3301* was crossed into a strain containing the cell fate reporter *egl-17p::gfp* and the *lin-15*(*n309*) mutation. The promoter for the fibroblast growth factor (FGF)-like gene *egl-17* drives expression not only in specific 2° descendants during L4 stage but also in the 1° lineage during vulval Pn.px and Pn.pxx stages (Burdine *et al*, 1998). Whereas during the screen the reporter *ayIs4[egl-17p::gfp]* was used as a 2° cell fate marker, in this experiment it served for 1° lineage detection. Worms mutated in *lin-15*(*n309*) show a Muv phenotype since all six VPCs are induced due to derepression of the inductive LIN-3 EGF signal (Ferguson and Horvitz, 1985; Sternberg *et al*, 1995). Consequently, the VPCs in *lin-15*(*n309*) mutants adopt vulval fates in an alternating fashion: 2°-1°-2°-1°-2°-1°. If additionally lateral signalling is impaired, adjacent primary fates (APFs) occur and can easily be visualized during early vulval development by using a primary cell fate marker like *egl-17p::gfp*. In fact, already the *tm3381* allele resulted in a higher number of APFs (Table 2). This experiment was

repeated with the *ttr-11* knockout allele *zh102* and again gave rise to a higher number of APFs than the control animals (Figure 8, Table 2). The allele *zh101* was not examined in this context, since in parallel analysis of both *ttr-11* knockout alleles in the background of another mutant allele (*lin-12*(*n302*)) *zh101* did not elevate the effect of *zh102*.

Taken together, *ttr-11* seems to have a positive impact on lateral signalling during vulval development. This has to be discussed further, since experiments with the *lin-12*(*n302*) allele came to the opposite conclusions.

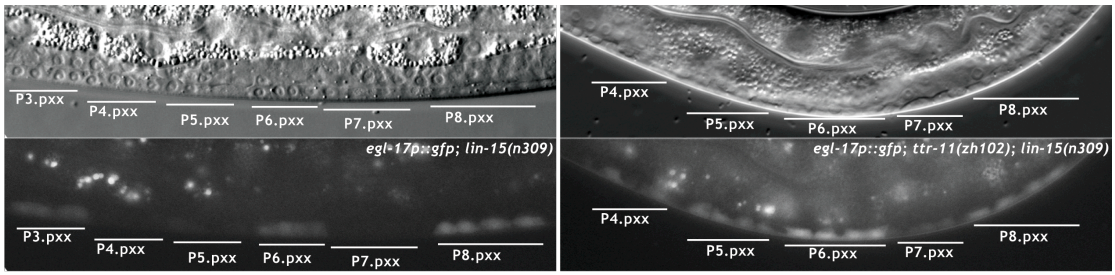

Figure 8: Adjacent primary fates (APFs) in *lin-15*(*n309*); *ttr-11*(*zh102*) double mutants. In *lin-15*(*n309*) mutants alternating 2° and 1° cell fates can be detected (left panels). In *lin-15*(*309*); *ttr-11*(*zh102*) double mutants 1° fates adjacent to each other indicate an impaired lateral signalling (right panels). For 1° cell fate detection during Pn.pxx stage the cell fate marker *aysls4[egl-17p::gfp]* was used. The upper panels are the corresponding Nomarski pictures to the lower GFP pictures.

Row	Genotype	APFs ± SE (n) [#]
1	*aysls4[egl-17p::gfp]; lin-15(n309)* [◊]	0.17 ± 0.08 (23)
2	*aysls4[egl-17p::gfp]; ttr-11(tm3381); lin-15(n309)* [◊]	0.64 ± 0.12 (68) [***(1)]
3	*aysls4[egl-17p::gfp]; lin-15(n309)* [‡]	0.58 ± 0.12 (24)
4	*aysls4[egl-17p::gfp]; ttr-11(zh102); lin-15(n309)* [‡]	0.93 ± 0.16 (44) [**(3)]

Table 2
Asterisks indicate the significance as described in material and methods. In brackets the row that was used for comparison is indicated.
[‡] / [◊] Experiments with the same symbol had been done on the same day.
[#] Average number of APFs per animal. SE indicates the standard error.

The gene *ttr-11* has no effect on lateral signalling in a *let-60(n1046)* background

So far, the role of *ttr-11* in LIN-12 NOTCH signalling is still obscure and different experiments lead to conflicting interpretations. To get a more secure idea of the role of *ttr-11* in lateral inhibition, we took again advantage of counting APFs in an additional mutant strain developing adjacent primary VPCs. For this purpose, a gain-of-function allele of *let-60*(*n1046*) was crossed into *ttr-11*(*zh101*). The gene *let-60* belongs to the family of GTP-binding RAS proto-oncogenes. During vulval development it functions as a component of the EGFR/RAS/MAPK pathway downstream of LET-23 EGFR to specify 1° cell fate (Sundaram, 2005). The allele *n1046* is supposed to convert LET-60 into a constitutive active form leading to the hyperactivation of the EGFR/RAS/MAPK pathway (Beitel *et al*, 1990; Ferguson *et al*, 1985). Therefore, APFs can be detected in *let-60*(*n1046*) mutants. However, *ttr-11*(*zh101*) did not cause a different number of APFs in this genetic background (Table3). Taken together, we could not confirm the positive influence of *ttr-11* on lateral signalling that we assumed to have discovered within the *lin-15*(*n309*) background.

Row	Genotype	APFs ± SE (n) [#]
1	*aylS4[egl-17p::gfp]; let-60(n1046)*	0.18 ± 0.12 (11)
2	*aylS4[egl-17p::gfp; let-60(n1046); ttr-11(zh101)*	0.08 ± 0.08 (12)

Table 3
[#] Average number of APFs per animal. SE indicates the standard error.

The protein TTR-11 is located nuclear, in the cytoplasm and in intracellular spots

To investigate TTR-11 at the protein level, a translational TTR-11::GFP construct under the control of the *ttr-11* promoter was built and integrated as single copy into the *C. elegans* genome via MosSCI (Frokjaer-Jensen *et al*, 2008). However, transgenic lines did not show any expression. Therefore, the construct was fused via fusion PCR to the promoter of *bar-1* instead of *ttr-11* and was injected to generate

extrachromosomal arrays carrying multiple copies of the transgene. This should result in stronger expression in all VPCs. Interestingly, only strong expression in 2° descendants could be detected suggesting a degradation or an impaired translation in 1° descendants (Figure 9). Since the TTR-11 sequence contains a signal peptide, it is predicted to be transported to the membrane or to be secreted (www.wormbase.org). However, the translational reporter gave rise to a diffuse signal in the cytoplasm and nucleus and only occasionally at some spots that could be intercellular (Figure 9). It cannot be ruled out that small amounts of TTR-11 are integrated into the membrane or secreted and the intracellular strong signal might be due to overexpression of the reporter. However, it is also possible that the GFP tag interferes with function and localisation of TTR-11. The functionality of the translational reporter could not be proven due to the lack of a clear phenotype that could be examined in rescue experiments.

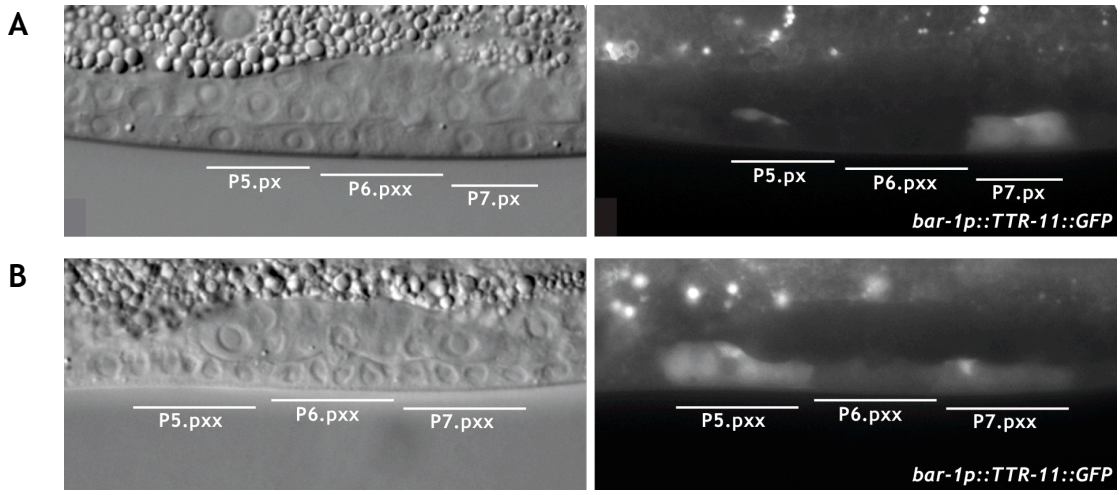

Figure 9: TTR-11 is localised mainly intracellular.
(A) Expression of the translational reporter *zhEx357[bar-1p::TTR-11::GFP]* is detected intracellular in descendants of P7.p and a in a weak spot basal of P5.pa in an animal in vulval 2 cell stage. (B) The same translational reporter as in (A) also gave rise to expression in descendants of 2° VPCs and weaker signal in descendants of the 1° VPC P6.p during vulval 4 cell stage. Nomarski pictures on the left correspond to the fluorescence pictures on the right side.

Overexpression of TTR-11 does not have an impact on LIN-12 NOTCH signalling

Reduced or loss-of-function of *ttr-11* did not reveal a clear phenotype. This might be caused by redundancy to other *ttr* genes. To test if overexpression of the gene *ttr-11* displays a better visible effect in the animal the open reading frame of *ttr-11* was cloned downstream of the promoter of the heat shock protein *hsp-16.1* and injected into a strain carrying the *ayIs82[LIN-12::GFP]* reporter to examine the effect of overexpression of TTR-11 on NOTCH (Levitan and Greenwald, 1998; Shaye *et al*, 2002). However, heat shocked animals containing the transgenic construct did not show any difference in marker expression compared to heat shocked animals that did not carry the transgene. When examining vulval morphology during the Christmas tree stage, as well no alterations could be seen (data not shown).

7 DISCUSSION

7.1 Discussing further results of the project "Degradation of NICD is connected to cell cycle progression"

Computational modelling revealed that changing the cell cycle progression interferes with the correct establishment of cell fate specification pattern during *C. elegans* vulval development (see manuscript, chapter 6.1). We could show experimentally that in P6.p, when it is arrested before M phase, NICD could not be properly degraded. Further, we could show that the N-terminal ankyrin and the C-terminal PEST domain are important for NICD degradation.

Previous research has shown that hyperphosphorylation at the NICD PEST domain is responsible for its degradation (Fryer *et al*, 2002; Fryer *et al*, 2004). Besides conserved putative phosphorylation sites in the PEST domain putative phosphorylation sites in the ankyrin repeats and at the N-terminus of NICD could be found. However, mutating these sites resulting in a change from a serine or threonine into an alanine residue, thereby preventing phosphorylation, resulted in reduced NICD stability, whereas in mammals mutations of this kind resulted in elevated NICD stability (Fryer *et al*, 2004). Mimicking phosphorylation at the C-terminus also resulted in diminished NICD stability. Therefore, mutating these sites, either to prevent or to mimic phosphorylation had the same effect, indicating that one effect is artificial. Reasons for this observation could be that on the one hand, alanine has an unpolar character and serine and threonine are polar amino acids. Using alanine instead of threonine or serine at specific positions might result in wrong protein folding and reduced protein stability as

consequence. On the other hand, aspartatic acid does not have the same structure as phosphorylated threonine or serine residues. Glutamic acid has one chemical bond more and thus resembles fairly the structure of phosphorylated threonine or serine residues. Therefore it might be a better candidate for phosphomimicking mutations of these amino acids.

Examination of a mutant in the CDK8 homologue or in its cyclin (CycC) that leads to hyperphosphorylation of NICD in mammalian cells did not reveal any change in the full-length reporter of LIN-12 NOTCH. However, the knockout allele *cdk-8*(*tm1238)* is reported to show only in 2 % of the mutant animals a Muv phenotype, as commented by Dr. H. Sawa (wormbase.org). If this Muv phenotype were a consequence of NICD stabilisation, it would be difficult to detect the higher GFP signal due to the low penetrance. Nevertheless, Clayton *et al*. found that RNAi against *cdk-8* in *C. elegans* enhances the Muv phenotype of a *lin-12*(*gf*) mutant (Clayton *et al*, 2008). The authors interpreted this effect as a proof that CDK-8 has a role in cell cycle quiescence since *cdk-8*(RNAi) resulted in further divisions that lead to additional VPCs. However, we observed in animals carrying *zhIs39[nicd::gfp]* occasionally additional inductions in P9.p to P11.p (data not shown), assuming that NOTCH overexpression might result in additional competent VPCs. Since we have been interested in how NICD stabilisation is regulated and to a lesser extend in how VPC competence is specified, we did not focus on the additional competence. Nevertheless, in this context the results of Clayton *et al*. with *cdk-8*(RNAi) would be another hint that CDK-8 might influence LIN-12 NOTCH signalling in a negative way. However, if there is an impact of CDK-8 on *zhIs39[nicd::gfp]* and if it is cell cycle dependent, remains to be examined.

Other modifications such as acetylation and deacetylation might also influence NICD stability. In human endothelial cells, the deacetylase SIRT1 functions to destabilise NICD (Guarani *et al*, 2011). SIRT1 removes acetyl residues at histones or proteins and thus regulates gene silencing as well as protein interactions or posttranslational protein modifications. A second negative effect on NOTCH signalling mediated by SIRT1 has been detected by Mulligan *et al*. who elucidated a SIRT1 dependent transcriptional

repression of NOTCH targets in *D. melanogaster* (Mulligan *et al*). Examining a mutant for the SIRT1 homologue *sir-2.1*, we found the opposite effect: NICD is destabilised compared to wild-type levels. These findings provide the first evidence for a positive role of *sir-2.1* on NICD. However, it is not the first role for a SIRT1 homologue in enhancement of NOTCH signalling. Donmez *et al*. showed in 2010 that SIRT1 promotes NOTCH signalling in murine brain cells via activating transcription of ADAM10, the α-secretase, which is known to cleave the NOTCH receptor to release NICD (Donmez *et al*). Thus, the role of SIRT1 and its homologues seems to be strongly dependent on the cellular context and the organism. Interestingly, in *C. elegans* the NICD stabilising effect of SIR-2.1 is only detected after the first VPC division. It remains to be elucidated if the activity of SIR-2.1 is influenced by cell cycle progression. Moreover, the question of SIR-2.1 specificity is not answered: Does it act in all induced VPCs or does it specifically affect the 2° VPCs? In the latter case, it could provide the counterpart to CDK-1/CYB-3: While cell cycle progression triggers destabilisation of NICD in P6.p via CDK-1/CYB-3 and in concert with an unknown 1° target, cell cycle progression might act in a 2° cell fate dependent manner and via SIR-2.1 to stabilise NICD in 2° descendants. This would help to create a clear spatial border between NOTCH signal-sending and NOTCH signal-receiving cells.

A cell cycle dependent sharp temporal border could be provided by the other B-type cyclins. Before CDK-1 acts in concert with CYB-3 to degrade NICD, CDK-1 is known to function also together with the CYB-1, CYB2.1 and CYB-2.2 during cell cycle progression (van der Voet *et al*, 2009). Even though a temporal difference in expression could not be detected between *cyb-1* and *cyb-3*, they take on consecutive functions during cell cycle progression: CYB-1 together with CDK-1 functions to align chromosomes at the spindle while CDK-1/CYB-3 initiates sister chromatid separation. The roles of CYB-2.1 and CYB-2.2 remain uncertain during mitosis, however these cyclins affect redundantly with CYB-1 and CYB-3 chromosome segregation during meiosis (van der Voet *et al*, 2009). We found that RNAi against *cyb-1* and *cyb-2.1*/*cyb-2.2* has a destabilising effect

on NICD. However, it cannot be excluded that RNAi against *cyb-2.1*/cyb-2.2 also affects CYB-1 levels (van der Voet *et al*, 2009). We hypothesise that CDK-1 acts together with CYB-1 to stabilise NICD in all VPCs and later on CDK-1 acts together with CYB-3 and a so far unknown 1° specific target to ensure proper degradation of NICD, and thus provides a clear temporal switch to turn NOTCH signalling off.

Taken together my observations hint at several regulatory connections between cell cycle progression and NOTCH signalling. Obviously, cell signalling requires spatial but also temporal restriction for proper communication between cells and for cell fate execution. Spatial regulation is ensured by cell position and separation by basal laminae and by distances. For the temporal control, thresholds in concentrations of signalling mediators might be responsible. However, time is needed to reach specific protein concentrations via *de novo* synthesis or via transport to specific cell components. Protein modification and/or degradation are the faster ways to change concentration levels. Yet, for a fast and exact "turning-off" mechanism, a precise regulator is needed. The cell cycle provides an excellent tool to regulate these fast and precise mechanisms, since its specific CDKs act only over a relatively short time period (S phase lasts about 20 minutes, for example) together with different cyclins that even cycle in smaller time windows within one cell cycle phase. Thus, connecting the cell cycle clock to signalling events might be a universally used strategy of multicellular organisms to tightly regulate cell communication and differentiation.

The contrary effect that signalling pathways cause cell cycle progression or cell cycle arrest has been described in several cases during development (Byrd and Kimble, 2009; Chang *et al*, 2003; Niehrs and Acebron). However, in the context of LIN-12 NOTCH signalling and VPC division in *C. elegans*, this opposite influence remains to be elucidated.

7.2 Discussing results of the project "Characterisation of the LIN-12 NOTCH target gene *ttr-11*"

The gene *ttr-11* was detected in a reverse genetic screen for 2° cell fate defects (Rimann, 2008). Though RNAi against *ttr-11* did not show any morphological defects but only abnormal 2° fate marker expression, it seemed to be a promising candidate for a LIN-12 NOTCH modulator due to its predicted protease function. Therefore, we attempted to characterise *ttr-11* and to deduce its function during vulval development.

We could show that *ttr-11* is expressed in a LIN-12 NOTCH dependent manner. Additionally, expression during late L3 stage in the two ACs that are specified in a *lin-12*(*lf*) background could be detected. This expression seems to be regulated independently of LIN-12 NOTCH signalling. The gene *egl-43* that was identified in the same reverse genetic screen shows also a NOTCH dependent and a NOTCH independent expression pattern (Rimann *et al*, 2007). The gene *egl-43* is the homologue of the *Evi-1* oncogene and promotes AC invasion as a target gene of *fos-1* (Rimann *et al*, 2007). Additionally, it is expressed in a NOTCH dependent manner in the VU cells to regulate cell fate specification. Thus, *ttr-11* might also have several functions in different tissues, NOTCH dependent and NOTCH independent ones.

The fact that a translational reporter of *ttr-11* that was expressed equally in all VPCs resulted in stronger signal in 2° than in 1° VPC descendants additionally promotes the assumption that *ttr-11* is specifically needed for 2° fate specification during vulval development. Thus, not only transcriptional regulation but also regulation at the posttranscriptional level is used by *C. elegans* to ensure that *ttr-11* is present in 2° but diminished in 1° descendants. The posttranscriptional regulation happens independently of the 3'UTR, since in the experiment the 3'UTR of *ttr-11* has been replaced by the commonly used one of *unc-54*. Therefore, the observed

posttranscriptional regulation might depend on protein degradation as consequence of 1° cell fate establishment or protein stabilisation in 2° VPC descendants.

To elucidate the function of *ttr-11*, RNAi was performed against *ttr-11* and its closest related gene *ttr-57*. After revision of the gene annotation in wormbase, the protease function was assigned to TTR-57. Since the RNAi clone used in the screen affects the transcripts of both genes, also *ttr-57* came into the focus of interest. However, neither RNAi against *ttr-11* nor *ttr-57* nor against both together could reproduce the 2° marker defect scored in the screen. Therefore, *ttr-11* single and *ttr-11 ttr-57* double knockout mutants had been generated and examined. These mutants neither showed any morphological phenotype nor defect of the 2° cell fate marker *egl-17p::gfp*, suggesting that the lack of reproducing the results of the screen is rather due to a redundancy with other *ttr* genes than to the inefficiency of gene knockdown of *ttr* genes by RNAi like proposed by Jacob *et al*. (Jacob *et al*, 2007).

In search of an apparent phenotype, overexpression of *ttr-11* was examined. In the wild-type background, this did not result in any effect, suggesting that in the pathway wherever *ttr-11* might function, it is not rate limiting.

Finally, quantifiable phenotypes in different mutant backgrounds could be detected. In mutants of *lin-12*(*n302*), a ligand-dependent gain-of-function allele of the LIN-12 NOTCH receptor, *ttr-11*(*lf*) elevated the number of pseudovulvae. The simplest explanation would be that wild-type *ttr-11* functions to reduce NOTCH signalling. However, it is not proven that the additional pseudovulvae have a 2° cell fate nature. Even if the morphology of the invaginations suggested a 2° fate origin, the 2° cell fate marker *egl-17p::gfp* was not expressed in all pseudovulvae in a worm. Thus, it cannot be ruled out that some pseudovulvae originate from a 1° fate specification due to reestablishment of an AC in this mutant. However, since first an AC never could be detected in double mutants, second the *egl-17p::gfp* is not expressed in all 2° descendants and third the *lin-12*(*n302)*

allele alone already results in some pseudovulvae without reestablishment of an AC, it is more likely that *ttr-11* diminishes NOTCH signalling for example in reducing the ability for NOTCH to be cleaved. This hypothesis also leaves the possibility that loss of *ttr-11* might change the nature of the *n302* allele and might turn it into a ligand-independent gain-of-function allele.

Contradictory to this hypothesis are the effects of *ttr-11*(*lf*) detected in another genetic background. The observation that in *lin-15*(*n309*) mutants *ttr-11*(*lf*) gives rise to more adjacent primary fates (APFs) suggests a supporting role for *ttr-11* in lateral NOTCH signalling in wild-type animals. Yet, this positive role could not be confirmed using the gain-of-function allele *let-60*(*n1046*): No diminishment of lateral signalling in this mutant background could be scored. Therefore, the effect of *ttr-11* on LIN-12 NOTCH signalling remains still to be elucidated.

The *ttr* genes in *C. elegans* form a large, nematode-specific family comprising 59 members based on the conservation of their transthyretin-like protein domain. They can be sub-divided into five classes I – V. The functions of these different gene classes are unclear. RNAi against different *ttr* genes performed by Saverwyns *et al*. neither resulted in any effect, supporting the assumption that high redundancy between *ttr* genes or inefficiency of gene knockdown by RNAi of this gene group complicates examining their functions in general (Saverwyns *et al*, 2008). Indeed only six of all 59 *ttr* genes reported aberrant phenotypes when knocked down by RNAi (wormbase.org). These phenotypes included extended lifespan, hyperactivity, increased fat content, reduced brood size and extraneous germline material. However, these phenotypes could not be assigned a specific ttr gene class. Furthermore, the gene class III, to which *ttr-11* belongs, does not contain any of the members whose knockdown resulted in a described phenotype. Yet, the genes *ttr-11* and *ttr-57* in their old combined annotated version had been assigned to class III, which is also the most numerous *ttr* gene class in *C. elegans* giving reason to believe that high redundancy in this gene class exists (Saverwyns *et al*, 2008). Interestingly, this class is less represented in EST datasets of parasitic

species compared to the free-living nematode *C. elegans*, suggesting a role of the *ttr* gene class III in dealing with problems of free-living animals, for example temperature fluctuations or defence against vermin.

Only the function of one member of the 59 *ttr* genes is described in more detail: The gene *ttr-52* has a role during apoptotic corpse engulfment. It binds to phosphatidylserine of dying cells that serves as an "eat-me signal" and to the extracellular domain of the phagocyte receptor CED-1, building a bridge between apoptotic and engulfing cell (Wang *et al*). Wang *et al*. claim that extracellular bridging is a conserved mechanism for recognition of apoptotic cells that have to be engulfed although the responsible bridging components vary in different organisms. In mammals, for example, amongst others thrombospondin seems to take over that role (Anderson *et al*, 2003; Savill *et al*, 1992). Further, Wang *et al*. suggest a general role for members of the transthyretin-like protein family in mediating cell-cell interactions since many TTLs are predicted to be secreted (Wang *et al*). TTR-11 contains also a signal peptide and is supposed to be secreted to extracellular space. The fact that we detected a TTR-11::GFP protein in the cytoplasm might seem to be contradictory. However, since the proof for the functionality of this reporter still has to be produced, we cannot rule out that the reporter shows a wrong localisation due to the relative large size of the GFP tag. Furthermore, overexpression of the TTR-11 reporter might lead to a saturation of secretion and therefore an accumulation of the reporter in the cytoplasm. Even if TTR-11 functions in the extracellular space, its concentrations might be so low that it is not detectable. Thus, TTR-11 still might function in the extracellular space during cell-cell communication, as Wang *et al*. have proposed it for several members of the transthyretin-like protein family (Wang *et al*, 2010). We have some hints that TTR-11 might be involved in lateral LIN-12 NOTCH signalling during vulval development. Speculating that also TTR-11 could possess a bridging role, it might mediate the recognition between the NOTCH receptor and the DELTA ligand presenting cells. Weak effects of mutants could then be explained: Bridging might be - in the case of NOTCH signalling - not mandatory but supporting for signalling.

Interestingly, the human transthyretin (TTR) has been shown to bind the amyloid beta (Abeta) proteins Abeta1-42 and Abeta1-40, the products of cleavage of the amyloid precursor protein APP (Schwarzman *et al*, 1994; Tsuzuki *et al*, 2000). Especially Abeta1-42 seems to be responsible for the pathogenesis during the neurodegenerative disorder Alzheimer's Disease (De Strooper, 2010). TTR is reported to be protective against this disease via Abeta proteolysis (Costa *et al*, 2008). For example, transgenic mice that overexpress mutant APP showed a slower pathogenic progression and revealed less neurodegenerative effects if expression of TTR was increased (Stein and Johnson, 2002). Even in *C. elegans* expressing both, human TTR and Abeta peptide, the protective role of TTR could be proven (Link, 1995).

The bridge between APP biology and NOTCH signalling can be made via the processing of these proteins: The sequence of proteolytic events in NOTCH signalling is reminiscent of APP proteolysis (Kopan *et al*, 2000). The NOTCH receptor after binding to its ligand is first cleaved by a α-sectretase, a member of the group of ADAM family-metalloproteases. APP also can be processed by a α-sectretase, but also by the β-secretase BACE1. Stimulation of these APP processing events is unclear. Although APP was originally predicted to be a transmembrane receptor, no ligand could be identified to date. Then both, APP and NOTCH processing events, are followed by a cleavage mediated by a pesenilin dependent γ-secretase complex to release the intracellular domains NICD during NOTCH signalling or AICD (APP ICD) during APP processing to activate gene transcription (Pardossi-Piquard and Checler, 2012; Schroeter *et al*, 1998). Thus, there are quite some parallels in APP and NOTCH signalling. If human TTR has a role in APP processing or Abeta proteolysis, related proteins, like TTR-11, might influence NOTCH signalling in other organisms. Various functions are imaginable, like bridging the ligand receptor interaction, binding to and processing of the released transmembrane peptide, whose physiology still remains elusive, or regulating the cleavage events of NOTCH signalling.

Although further studies will be needed to elucidate the specific function of *ttr-11* and its related genes of the transthyretin-like protein family, we could collect some hints during my PhD suggesting that even if

nematode-specific, studying this gene family can be interesting, since some members might be involved in important signalling pathways like NOTCH signalling. Additionally, even connections to human biology might be possible one day.

8 MATERIAL AND METHODS NOT DESCRIBED IN THE MANUSCRIPT

8.1 *C. elegans* strains and constructs

The following mutations and transgenes were used:

LGI: *ayIs4[egl-17p::gfp]* (Burdine *et al*, 1998), *cdk-8(tm1238)* (gift of Shohei Mitani).

LGII: *rrf-3(pk1426)* (Simmer *et al*, 2002), *cyd-1(q626)* (Tilmann and Kimble, 2005), *zhIs39[bar-1p::nicd::gfp, unc-119(+)]*, *zhIs40[bar-1p::nicd::gfp (T637A; T647A; T649A)]*, *zhIs41[bar-1p::nicd::gfp (T660A; S668A)]*, *zhIs42[bar-1p::nicd::gfp (S90A; T164A)]*, *ttTi5605* (transposon insertion) (Duverger *et al*, 2007).

LGIII: *unc-119(e2498)* (Maduro and Pilgrim, 1995), *unc-119(ed3)* (Maduro *et al*, 1995), *zhIs4[pTB10(lip-1p::gfp)]* (Berset *et al*, 2001), *dpy-19(e1259) lin-12(n137) / unc-32(e189) lin-12(n137n720)* (Greenwald, 1985), *lin-12(n302)* (Greenwald *et al*, 1983), *cic-1(tm3740)* (gift of Shohei Mitani).

LGIV: *let-60(n1046)* (Ferguson *et al*, 1985), *sir-2.1(ok434)* (Robert Barstead).

LGV: *ttr-11(tm3381)* (gift of Shohei Mitani), *arIs82[LIN-12::GFP, unc-4(+), egl-17p::LacZ]* (gift of Victor Ambros), *ttTi53215* (transposon insertion) (Duverger *et al*, 2007), *ttr-11(zh101)*, *ttr-11(zh102)*.

LGX: *lin-15(n309)* (Ferguson *et al*, 1985), *syIs52[cdh-3p::cfp, unc-119(+)]* (Inoue *et al*, 2002), *osIs2[CYE-1::GFP]* (Fujita *et al*, 2007).

Extrachromosomal arrays: *zhEx200[ttr-11p::gfp, unc-119(+)]* (injected in unc-119(-) background) (Rimann, 2008), *zhEx307[ttr-11p::gfp,*

lin-48p::gfp] (Rimann, 2008) (injected in lin-12(*gf/lf*) background, *zhEx315[egl-17p::cki-1, lin-48p::gfp], zhEx318[lin-3p::gfp, lin-48p::gfp], zhEx367[egl-17p::cki-1, myo-2p::mCherry], zhEx357[bar-1p::ttr-11::gfp::unc-54 3'utr, unc-119(+), myo-2p::mCherry], zhEx414[cyd-1(intron/fragment2)::pes-10p::gfp, myo-2p::mCherry], zhEx415[cyd-1(promoter/fragment1)::pes-10p::gfp, myo-2p::mCherry], zhEx416[pes-10p::gfp, myo-2p::mCherry], zhEx434[cyd-1p::gfp, intron/fragment2, myo-2p::mCherry], zhEx435[cyd-1p::gfp, intron/fragment2, myo-2p::mCherry].*

8.2 Maintaining and Manipulating *C. elegans*

Standard methods were used for maintaining and manipulating *C. elegans* (Brenner, 1974).

Reporter constructs were inserted as single copies into the *C. elegans* genome using MosSCI (Frokjaer-Jensen *et al*, 2008) or transgenic lines carrying extrachromosomal arrays had been generated by microinjection of plasmids and PCR fusion constructs (Mello *et al*, 1991).

To generate knockout mutations of *ttr-11* and *ttr-57* the method of MosTIC (Robert *et al*, 2007) was used.

RNAi was performed by the feeding method (Kamath *et al*, 2001). The L1 or L4 worms were used for treatment. If L1 stages had been used, the worms were synchronized by bleaching (see time course experiment in the manuscript). L1 or L4 larvae were placed on growth media plates containing 3mM IPTG, 50µg/ml ampicillin and 50µg/ml tetracycline and bacteria of specific RNAi strains. Worms were allowed to grow at 20 C° before they were analysed. If L4 larvae had been used, the F1 generation had been analysed. The following RNAi clones were used: JA:ZC168.4 to knock down *cyb-1*, JA:43E12A.1 to knock down *cyb-2.1* and *cyb-2.2*, JA:T06E6.2 or MV_SV:mv_AAA84395 to knock down *cyb-3*, JA:T05G5.3 or MV_SV:mv_T05G5.3 to knock down *cdk-1* and the empty vector L4440 as control.

8.3 Plasmids and constructs

Constructs were made by molecular cloning, PCR fusion (Hobert, 2002) or gateway cloning (MultiSite Gateway® Three-Fragment Vector Construction Kit, Invitrogen) using PCFJ150 as final destination vector. The reporter constructs were inserted as single copies into the *C. elegans* genome using MosSCI (Frokjaer-Jensen *et al*, 2008) or transgenic lines carrying extrachromosomal arrays had been generated by microinjection of plasmids and PCR fusion constructs (Mello *et al*, 1991). To generate knockout mutations of *ttr-11* and *ttr-57* the method of MosTIC (Robert *et al*, 2007) was used.

Constructs made by molecular cloning:

To amplify sequences used for RNAi against *ttr-11* OSN21(GAATTCTTACGCTGCGGCTTCCACG) and OSN20(GAATTCGTGACTGCATGAATAAGCATAG) and for RNAi against ttr-57 OSN22(GAATTCATTGTGTCACCAATTCTGTAC) and OSN23(GAATTCGTGTTGAGGAAGATGTCCC) were used. The PCR was performed using cDNA as template. The obtained fragments were subcloned into pGEM T (pGEM®-T and pGEM®-T Easy Vector Systems, Promega) to facilitate digestion with *Eco*RI. After digestion with *Eco*RI of the obtained pGEM T plasmids and the destination vector L4440, fragments and destination vector were ligated. Final transformation was performed into the RNAseIII (-) *E. coli* strain HT115.

The constructs to obtain pSN1 to create *zh101* and pSN3 to create *zh102* were cloned as follows: The left flanking site had been amplified using genomic DNA as template and OEF11(tttgggcccCTGGTCTGGCTTCAGGGC) and OEF12(tttggcgcgccAGTACTGGTATAGATTGTCCTT) as primers. The right flanking sites was amplified using genomic DNA as template and

OEF15(tttggcgcgccGGTGAGAGAGTTACAGAGTG) and OEF16(tttttaattaaACTCCACGTGAGCCCCTATT) for pSN1 and OEF19(tttggcgcgccCCAGAAAGTGCAACTTTGGGA) and OEF20(tttttaattaaCTACATTTTTAAGCTTTTTCCCTT) for pSN3. The rescuing sequence of unc-119(+) was amplified using pCFJ150 as template and OEF13(tttggcgcgccGACATTCTCTAATGAAAAAATCTT) and OEF14(tttggcgcgccCTTATCTCGAATGAGACCCTTG) as primers. The right flanking sites were subcloned into pGEM T (pGEM®-T and pGEM®-T Easy Vector Systems, Promega). The obtained plasmids as well as the left flanking site had been digested with *Apa*I and *Asc*I. Ligation resulted in a plasmid containing left and right flanking sites. Further these plasmids and the rescuing sequence of unc-119(+) were digested with *Asc*I. Ligation resulted in unc-119(+) placed between the two flanking sites in reverse direction.

Reporter constructs for *cyd-1* were built by molecular cloning. For amplification of the promoter/fragment 1 and the intron/fragment 2 following primers were used: OSN259(ttttttttctagaCTCGAGTAAAGCCAGTTTCGAGAAAT), OSN258(ttttttttctagaTAATCCCTATTAACTTTCAACTAAC), OSN261(ttttttttctagaGAGTTTTCATTTCTTTCATTCCACC) and OSN260(ttttttttctagaGAAAAACCAATATTCATATTATTG). The amplified constructs and the vector pTB11 were digested with *Xba*I and ligated. Thus, transcriptional reporters containing the 2460 bp promoter/fragment1 (pSN33) and the 2250 bp intron/fragment2 (pSN30) were generated. Screening for forward integrated constructs was done by PCR and sequencing.

Additionally the undigested 2652 bp intron/fragment 2 was also cloned into pGEM-T Easy (pSN36) (pGEM®-T and pGEM®-T Easy Vector Systems, Promega) to co-inject it with the reporter received from the lab of Michael W. Krause (Brodigan *et al*, 2003).

Constructs made by PCR fusion:

The translational reporter for *ttr-11* driven by the promoter of *bar-1* was made by fusion PCR. For the single fragments following primers had been used: OIN88(atagaaaagttgCTTAGCAAAGCCGTGTCAAAACCC), OSN167(CATCCCAGTTTTCTGAAAAAAAAAGCC), OSN168(GGCTTTTTTTTTCAGAAAACTGGGATGaacgcggtatgtgacttttcag), OSN169(CCAGTGAAAAGTTCTTCTCCTTTACTCATGTTTCGTGGAGGTCGAAGGTC TGAAATTC), Left CFP noATG (ATGAGTAAAGGAGAAGAACTTTTCACTGG) and D(AAGGGCCCGTACGGCCGACTAGTAGG). To fuse the three constructs following primers had been used: CW27(CTTAGCAAAGCCGTGTCAAAACCC) and D*(GGAAACAGTTATGTTTGGTATATTGGG).

To overexpress *ttr-11*, its open reading frame was fused to the promoter of hsp-16.48, coding for a 16 kD heat shock protein. For amplification of the promoter the plasmid pWD79 was used as template and OSN141(GCTGGACGGAAATAGTGGTAAAG) and OSN142(TTTTACGCGTTCTTGAAGTTTAGAG) were used as primers. To amplify the genomic sequence of *ttr-11* worm lysate was used as template and the primers OSN143(CTCTAAACTTCAAGAACGCGTAAAAatgaacgcggtatgtgacttttcag) and OSN169(CCAGTGAAAAGTTCTTCTCCTTTACTCATGTTTCGTGGAGGTCGAAGGTC TGAAATTC). To amplify the sequence of *gfp* and the *unc-54* 3'UTR pPD95_75 was used as template and the primers Left CFP noATG (ATGAGTAAAGGAGAAGAACTTTTCACTGG) and D(AAGGGCCCGTACGGCCGACTAGTAGG). To fuse the three constructs the primers OSN141(GCTGGACGGAAATAGTGGTAAAG) and D*(GGAAACAGTTATGTTTGGTATATTGGG) had been used.

Constructs made by gateway cloning:

zhEx39 (see manuscript)

Site directed mutagenesis:

Putative phosphorylation sites of the *bar-1p::nicd::gfp* construct were mutated specifically following the instructions of the Kit manual (QuikChange Multi Site-Directed Mutagenesis Kit, Stratagene). To mutate phosphorylation sites in construct 1 to generate pSN22 following primers were used: OSN157(TGAACCTGAAgcCCCCATCAAACTACACACAGAAG) and OSN158(TGCGACGAGAACgCCCCATTGATGCTGG). To mutate phosphorylation sites in construct 2 to generate pSN19 following primers were used: OSN159(TCAACTCATCTGgCACCTCCACCATCGG) and OSN160(ATGGATCAACGTCAgCACCGgCACCACAGCATTTTATGAATACC). To mutate phosphorylation sites in construct 3 to generate pSN21 following primer was used: OSN161(CACTCATACTgcACCGACGAGTTTGAACTATTTGgcCCCAGAATATC). To mimic constitutive phosphorylation sites in construct 4 to generate pSN25 following primer was used: OSN166(CACTCATACTgacCCGACGAGTTTGAACTATTTGgaCCCAGAATATC). To mimic constitutive phosphorylation sites to generate pSN24 following primer was used: OSN162(TGAACCTGAAgaCCCCATCAAACTACACACAG) and OSN163(TTGCGACGAGAACgaCCCATTGATGCTGGCTG).

Additional plasmids:

pVT363(*egl-17p::cki-1*) (Hong *et al*, 1998), pTJ1157(*lin-48p::gfp*) (Johnson *et al*, 2001), pCJF90(*myo-2p::mCherry*) (Frokjaer-Jensen *et al*, 2008), backbone plasmids and plasmids containing co-injection markers and the transposase needed for MosSCI (Frokjaer-Jensen *et al*, 2008), pAH67(*lin-3p::gfp*), pTB11(*pes-10p::gfp*), pKMW1109(cyd-1p::gfp) (Brodigan *et al*, 2003).

8.4 cDNA sequence analysis

Total RNA was extracted using the phenol-chloroform extraction method. Worms of 10-12 dishes were collected and pelletised, 1.8 ml of solution D (guanidiniumthiocyanat [4 M], sodiumcitrate [25 mM], sarcosyl [0.5 %], β-mercaptoethanol [0.27%]), 180 µl of sodium acetate ([2 M], pH4.0), 1.8 ml of phenol and 360 µl of chloroform/isoamylalcohol (49/1 ratio). After vortexing and centrifugation the supernatant was collected and substituted by 1 volume of isopropanol. An other centrifugation step resulted in a pellet that was resuspended in 400 µl of solution D and 400 µl of isopropanol for reprecipitation. After solubilisation at 55°C in 400 µl of water a washing step with 40 µl sodium acetate [3 M] and 880µl ethanol [100 %] followed. The final pellet after centrifugation was dissolved in a volume of 50 µl of water.

Approximately 2 µg total RNA extract was used for cDNA transcription. 1 µl of oligo$(dT)_{18}$ primer [0.5 µg/µl] and water were added to a volume of 12 µl. The mixture was heated for 5 minutes at 70°C. After cooling on ice following components were added: 4 µl reaction buffer (5x, RevertAid™ H Minus First Strand cDNA Synthesis Kit), 1 µl RiboLock™ Ribonuclease inhibitor [20 u/µl] and 2 µl dNTP [10 mM]. An incubation phase at 37°C for further 5 minutes followed. Then, 1 µl of RevertAid™ H Minus M-MuLV Reverse Transcriptase was added and the mixture was incubated for one hour at 42°C. The reaction was stopped by heating it for 10 minutes to 70°C.

Following primers were used in different combinations to amplify and sequence cDNA transcripts of *ttr-11* and *ttr-57*:

Forward primers: OSN1(ATTCAAATTTGGGAGAAAAACTTTG), OSN2(GCCGACACTATGCTTATTCATG), OSN4(CTCGCCACCGCTGACACG), OSN9(ATGAACGCGACAATTTTTCTCG), OSN10(ATGATTCTTCTCATCAAGCTCG).

Reverse primers: OSN3(AAGTTAACGACTTGTTCAAGGCC), OSN5(CCAAAAATACTGAACGATGGCTC), OSN6(GAGTAGAAGACTTGCTCGAGGC), OSN14(CTAGCGGCATTCTTTATGATTG), OSN15(TTACCCAGAAGGACGACATTC).

8.5 Statistical analysis

See Manuscript, chapter 6.1, *C. elegans* microscopy and image analysis.

9 ACKNOWLEDGMENT

There are several reasons to thank Alex Hajnal as my supervisor: First, for giving me the opportunity to study developmental biology in his lab, secondly, for being a patient and sympathetic supervisor, thirdly, for his ability to motivate me when I obtained results that did not bring the projects forward, fourthly, for giving me the freedom to choose the direction of the projects and in the same time always having an open ear for arising problems, and finally, for giving me the opportunity to meet several distinguished researchers and visit conferences all over the world.

I also want to thank the members of my Thesis Committee, Adrian Streit, Konrad Basler and Yves Barral, for their support during my PhD studies and for good discussions and helpful suggestions during the several meetings we had.

Special thanks go to Ivo Rimann, who supervised me during the first year of my PhD. Especially, the calmness and willingness to answer all my questions during his own post-doctoral studies, writing of grants and searching for new positions, impressed me a lot.

Without Jasmin Fisher, Antje Beyer and Nir Piterman, we wouldn't have been able to do this great collaboration between computational and molecular biology research groups. Thanks to Jasmin and Nir, who computationally modelled *C. elegans* vulval development, the project about cell cycle arrest and its influence on signalling was born. And thanks to Antje, the modelling was deepened and new molecular observations could be incorporated. Thus, a very nice and fruitful exchange of knowledge could be established.

Additionally to our collaborators, I want to thank my former master student Magdalene Adamczyk, who also focused on cell cycle regulation and its influence on signalling and contributed to our study.

I got the pleasure to get known to and teach several highly motivated students during my PhD: Here I want to mention Magda again, but also the summer student Daniel Roiz Lafuente, who made several reporters for *ttr* genes, and students that had smaller projects during courses: Anina and Fabienne; Martin, Erik and Christine; Gabriele, Donna and Andrea. Furthermore, I should not forget my summer student Ye Fan. Although we did not find the right way to communicate, he contributed to a specific extent to the molecular part of the project about cell cycle regulation of NOTCH signalling and he taught me to deal with people who think in a different way for different cultural or personal reasons.

For aid and support, nice coffee breaks, birthday cakes and barbecues, I thank a lot all present and former Hajnal lab members: Erika Fröhli, Juan Miguel Escobar, Itay Nakdimon, Sarfarazhussain Farooqui, Matthias Morf, Louisa Mueller, Daniel Roiz Lafuente, Tobias Schmid, Michael Walser, Yang Qiutan, Andrea Haag, Philipp Leu, Sabrina Merkle, Alessandra Bühler, Peter Gutierrez, Christina Herrmann, Debora Kehrli, David Kradolfer, Anne Pacquelet, Mark Pellegrino, Sara Vasalli and Claudia Walser.

Thanks also to Irene Hofmann, for her support for all organisational issues and once in a while sweetening our days with “Zuger Kirschtorte”.

I am also very much obliged to Juan, who helped me with organising the bureaucracy around the registration of the Thesis Defence.

For funding of my projects and travel grants I would like to acknowledge the Swiss National Foundation, the PANACEA project and the Molecular Life Sciences PhD programme.

Finally, I want to close with a very warm “Thank You” to my husband Soki, who was the driving force to apply for a PhD position in Zurich, for his patience and support, and to my parents Inge and Ulrich and my sister Anja, who excited my interest in biology already during childhood and supported me through all my academic education and studies.

10 REFERENCES

Ambros V (1989) A hierarchy of regulatory genes controls a larva-to-adult developmental switch in C. elegans. *Cell* **57:** 49-57.

Anderson HA, Maylock CA, Williams JA, Paweletz CP, Shu H, Shacter E (2003) Serum-derived protein S binds to phosphatidylserine and stimulates the phagocytosis of apoptotic cells. *Nat Immunol* **4:** 87-91.

Barker KR, Hussey RS, Krusberg LR, Bird GW, Dunn RA, Ferris H, Ferris VR, Freckman DW, Gabriel CJ, Grewal PS, Macguidwin AE, Riddle DL, Roberts PA, Schmitt DP (1994) Plant and soil nematodes: societal impact and focus for the future. *J Nematol* **26:** 127-137.

Beitel GJ, Clark SG, Horvitz HR (1990) Caenorhabditis elegans ras gene let-60 acts as a switch in the pathway of vulval induction. *Nature* **348:** 503-509.

Berset T, Hoier EF, Battu G, Canevascini S, Hajnal A (2001) Notch inhibition of RAS signaling through MAP kinase phosphatase LIP-1 during C. elegans vulval development. *Science* **291:** 1055-1058.

Berset TA, Hoier EF, Hajnal A (2005) The C. elegans homolog of the mammalian tumor suppressor Dep-1/Scc1 inhibits EGFR signaling to regulate binary cell fate decisions. *Genes Dev* **19:** 1328-1340.

Boxem M, Srinivasan DG, van den Heuvel S (1999) The Caenorhabditis elegans gene ncc-1 encodes a cdc2-related kinase required for M phase in meiotic and mitotic cell divisions, but not for S phase. *Development* **126:** 2227-2239.

Boxem M, van den Heuvel S (2001) lin-35 Rb and cki-1 Cip/Kip cooperate in developmental regulation of G1 progression in C. elegans. *Development* **128:** 4349-4359.

Brenner S (1974) The genetics of Caenorhabditis elegans. *Genetics* **77:** 71-94.

Brodigan TM, Liu J, Park M, Kipreos ET, Krause M (2003) Cyclin E expression during development in Caenorhabditis elegans. *Dev Biol* **254:** 102-115.

Burdine RD, Branda CS, Stern MJ (1998) EGL-17(FGF) expression coordinates the attraction of the migrating sex myoblasts with vulval induction in C. elegans. *Development* **125:** 1083-1093.

Byrd DT, Kimble J (2009) Scratching the niche that controls Caenorhabditis elegans germline stem cells. *Semin Cell Dev Biol* **20:** 1107-1113.

Chalfie M, Horvitz HR, Sulston JE (1981) Mutations that lead to reiterations in the cell lineages of C. elegans. *Cell* **24:** 59-69.

Chan MS (1997) The global burden of intestinal nematode infections--fifty years on. *Parasitol Today* **13:** 438-443.

Chang F, Steelman LS, Shelton JG, Lee JT, Navolanic PM, Blalock WL, Franklin R, McCubrey JA (2003) Regulation of cell cycle progression and apoptosis by the Ras/Raf/MEK/ERK pathway (Review). *Int J Oncol* **22:** 469-480.

Chen N, Greenwald I (2004) The lateral signal for LIN-12/Notch in C. elegans vulval development comprises redundant secreted and transmembrane DSL proteins. *Developmental cell* **6:** 183-192.

Cheng M, Olivier P, Diehl JA, Fero M, Roussel MF, Roberts JM, Sherr CJ (1999) The p21(Cip1) and p27(Kip1) CDK 'inhibitors' are essential activators of cyclin D-dependent kinases in murine fibroblasts. *The EMBO journal* **18:** 1571-1583.

Cinar HN, Sweet KL, Hosemann KE, Earley K, Newman AP (2001) The SEL-12 presenilin mediates induction of the Caenorhabditis elegans uterine pi cell fate. *Dev Biol* **237:** 173-182.

Clark SG, Chisholm AD, Horvitz HR (1993) Control of cell fates in the central body region of C. elegans by the homeobox gene lin-39. *Cell* **74:** 43-55.

Clarke EM, Grumberg O, Peled D (1999) *Model Checking*: MIT press.

Clayton JE, van den Heuvel SJ, Saito RM (2008) Transcriptional control of cell-cycle quiescence during C. elegans development. *Dev Biol* **313:** 603-613.

Connors LH, Lim A, Prokaeva T, Roskens VA, Costello CE (2003) Tabulation of human transthyretin (TTR) variants, 2003. *Amyloid* **10:** 160-184.

Costa R, Ferreira-da-Silva F, Saraiva MJ, Cardoso I (2008) Transthyretin protects against A-beta peptide toxicity by proteolytic cleavage of the peptide: a mechanism sensitive to the Kunitz protease inhibitor. *PLoS One* **3:** e2899.

de Souza N, Vallier LG, Fares H, Greenwald I (2007) SEL-2, the C. elegans neurobeachin/LRBA homolog, is a negative regulator of lin-12/Notch activity and affects endosomal traffic in polarized epithelial cells. *Development* **134:** 691-702.

De Strooper B (2010) Proteases and proteolysis in Alzheimer disease: a multifactorial view on the disease process. *Physiol Rev* **90:** 465-494.

Donmez G, Wang D, Cohen DE, Guarente L (2010) SIRT1 suppresses beta-amyloid production by activating the alpha-secretase gene ADAM10. *Cell* **142:** 320-332.

Duverger Y, Belougne J, Scaglione S, Brandli D, Beclin C, Ewbank JJ (2007) A semi-automated high-throughput approach to the generation of transposon insertion mutants in the nematode Caenorhabditis elegans. *Nucleic acids research* **35:** e11.

Edgar LG, McGhee JD (1988) DNA synthesis and the control of embryonic gene expression in C. elegans. *Cell* **53:** 589-599.

Eisenmann DM, Maloof JN, Simske JS, Kenyon C, Kim SK (1998) The beta-catenin homolog BAR-1 and LET-60 Ras coordinately regulate the Hox gene lin-39 during Caenorhabditis elegans vulval development. *Development* **125:** 3667-3680.

Euling S, Ambros V (1996) Heterochronic genes control cell cycle progress and developmental competence of C. elegans vulva precursor cells. *Cell* **84:** 667-676.

Farooqui S (2012) Regulation of C. elegans Vulval Morphogenesis by LIN-12 Notch Signaling. *PhD Thesis*.

Fay DS, Han M (2000) Mutations in cye-1, a Caenorhabditis elegans cyclin E homolog, reveal coordination between cell-cycle control and vulval development. *Development* **127:** 4049-4060.

Ferguson EL, Horvitz HR (1985) Identification and characterization of 22 genes that affect the vulval cell lineages of the nematode Caenorhabditis elegans. *Genetics* **110:** 17-72.

Fisher J, Henzinger TA (2007a) Executable cell biology. *Nat Biotechnol* **25:** 1239-1249.

Fisher J, Piterman N (2010) The executable pathway to biological networks. *Brief Funct Genomics* **9:** 79-92.

Fisher J, Piterman N, Hajnal A, Henzinger TA (2007b) Predictive modeling of signaling crosstalk during C. elegans vulval development. *PLoS Comput Biol* **3:** e92.

Fisher J, Piterman N, Hubbard EJ, Stern MJ, Harel D (2005) Computational insights into Caenorhabditis elegans vulval development. *Proc Natl Acad Sci U S A* **102:** 1951-1956.

Fleming RJ (1998) Structural conservation of Notch receptors and ligands. *Semin Cell Dev Biol* **9:** 599-607.

Foss TR, Wiseman RL, Kelly JW (2005) The pathway by which the tetrameric protein transthyretin dissociates. *Biochemistry* **44:** 15525-15533.

Frokjaer-Jensen C, Davis MW, Hopkins CE, Newman BJ, Thummel JM, Olesen SP, Grunnet M, Jorgensen EM (2008) Single-copy insertion of transgenes in Caenorhabditis elegans. *Nature genetics* **40:** 1375-1383.

Fryer CJ, Lamar E, Turbachova I, Kintner C, Jones KA (2002) Mastermind mediates chromatin-specific transcription and turnover of the Notch enhancer complex. *Genes Dev* **16:** 1397-1411.

Fryer CJ, White JB, Jones KA (2004) Mastermind recruits CycC:CDK8 to phosphorylate the Notch ICD and coordinate activation with turnover. *Mol Cell* **16:** 509-520.

Fujita M, Takeshita H, Sawa H (2007) Cyclin E and CDK2 repress the terminal differentiation of quiescent cells after asymmetric division in C. elegans. *PLoS One* **2:** e407.

Gaiano N, Fishell G (2002) The role of notch in promoting glial and neural stem cell fates. *Annu Rev Neurosci* **25:** 471-490.

Greenwald I (1985) lin-12, a nematode homeotic gene, is homologous to a set of mammalian proteins that includes epidermal growth factor. *Cell* **43:** 583-590.

Greenwald I (2005) LIN-12/Notch signaling in C. elegans. *WormBook, ed The C elegans Research Community* **doi/10.1895/wormbook.1.10.1:** 1-16.

Greenwald IS, Sternberg PW, Horvitz HR (1983) The lin-12 locus specifies cell fates in Caenorhabditis elegans. *Cell* **34:** 435-444.

Guarani V, Deflorian G, Franco CA, Kruger M, Phng LK, Bentley K, Toussaint L, Dequiedt F, Mostoslavsky R, Schmidt MH, Zimmermann B, Brandes RP, Mione M, Westphal CH, Braun T, Zeiher AM, Gerhardt H, Dimmeler S, Potente M (2011) Acetylation-dependent regulation of endothelial Notch signalling by the SIRT1 deacetylase. *Nature* **473:** 234-238.

Gupta-Rossi N, Le Bail O, Gonen H, Brou C, Logeat F, Six E, Ciechanover A, Israel A (2001) Functional interaction between SEL-10, an F-box protein, and the nuclear form of activated Notch1 receptor. *J Biol Chem* **276:** 34371-34378.

Hambleton S, Valeyev NV, Muranyi A, Knott V, Werner JM, McMichael AJ, Handford PA, Downing AK (2004) Structural and functional properties of the human notch-1 ligand binding region. *Structure* **12:** 2173-2183.

Hedgecock EM, White JG (1985) Polyploid tissues in the nematode Caenorhabditis elegans. *Dev Biol* **107:** 128-133.

Heitzler P, Simpson P (1991) The choice of cell fate in the epidermis of Drosophila. *Cell* **64:** 1083-1092.

Hennebry SC, Wright HM, Likic VA, Richardson SJ (2006) Structural and functional evolution of transthyretin and transthyretin-like proteins. *Proteins* **64:** 1024-1045.

Hobert O (2002) PCR fusion-based approach to create reporter gene constructs for expression analysis in transgenic C. elegans. *Biotechniques* **32:** 728-730.

Hong Y, Roy R, Ambros V (1998) Developmental regulation of a cyclin-dependent kinase inhibitor controls postembryonic cell cycle progression in Caenorhabditis elegans. *Development* **125:** 3585-3597.

Hutter H, Schnabel R (1995) Establishment of left-right asymmetry in the Caenorhabditis elegans embryo: a multistep process involving a series of inductive events. *Development* **121:** 3417-3424.

Inoue T, Sherwood DR, Aspock G, Butler JA, Gupta BP, Kirouac M, Wang M, Lee PY, Kramer JM, Hope I, Burglin TR, Sternberg PW (2002) Gene expression markers for Caenorhabditis elegans vulval cells. *Mechanisms of development* **119 Suppl 1:** S203-209.

Jacob J, Vanholme B, Haegeman A, Gheysen G (2007) Four transthyretin-like genes of the migratory plant-parasitic nematode Radopholus similis: members of an extensive nematode-specific family. *Gene* **402:** 9-19.

Johnson AD, Fitzsimmons D, Hagman J, Chamberlin HM (2001) EGL-38 Pax regulates the ovo-related gene lin-48 during Caenorhabditis elegans organ development. *Development* **128:** 2857-2865.

Kamath RS, Fraser AG, Dong Y, Poulin G, Durbin R, Gotta M, Kanapin A, Le Bot N, Moreno S, Sohrmann M, Welchman DP, Zipperlen P, Ahringer J (2003) Systematic functional analysis of the Caenorhabditis elegans genome using RNAi. *Nature* **421:** 231-237.

Kamath RS, Martinez-Campos M, Zipperlen P, Fraser AG, Ahringer J (2001) Effectiveness of specific RNA-mediated interference through ingested double-stranded RNA in Caenorhabditis elegans. *Genome Biol* **2:** RESEARCH0002.

Kidd S, Lieber T (2002) Furin cleavage is not a requirement for Drosophila Notch function. *Mechanisms of development* **115:** 41-51.

Kitano H (2002) Systems biology: a brief overview. *Science* **295:** 1662-1664.

Kopan R, Goate A (2000) A common enzyme connects notch signaling and Alzheimer's disease. *Genes Dev* **14:** 2799-2806.

Kurooka H, Honjo T (2000) Functional interaction between the mouse notch1 intracellular region and histone acetyltransferases PCAF and GCN5. *J Biol Chem* **275:** 17211-17220.

LaBaer J, Garrett MD, Stevenson LF, Slingerland JM, Sandhu C, Chou HS, Fattaey A, Harlow E (1997) New functional activities for the p21 family of CDK inhibitors. *Genes Dev* **11:** 847-862.

Lai EC (2002) Protein degradation: four E3s for the notch pathway. *Curr Biol* **12:** R74-78.

Lambie EJ, Kimble J (1991) Two homologous regulatory genes, lin-12 and glp-1, have overlapping functions. *Development* **112:** 231-240.

Leclerc V, Leopold P (1996) The cyclin C/Cdk8 kinase. *Prog Cell Cycle Res* **2:** 197-204.

Lee RC, Feinbaum RL, Ambros V (1993) The C. elegans heterochronic gene lin-4 encodes small RNAs with antisense complementarity to lin-14. *Cell* **75:** 843-854.

Lee Y, Lee DH, Kho CW, Lee AY, Jang M, Cho S, Lee CH, Lee JS, Myung PK, Park BC, Park SG (2005) Transthyretin-related proteins function to facilitate the hydrolysis of 5-hydroxyisourate, the end product of the uricase reaction. *FEBS Lett* **579:** 4769-4774.

Levitan D, Greenwald I (1998) LIN-12 protein expression and localization during vulval development in C. elegans. *Development* **125:** 3101-3109.

Li J (2005) Brassinosteroid signaling: from receptor kinases to transcription factors. *Curr Opin Plant Biol* **8:** 526-531.

Link CD (1995) Expression of human beta-amyloid peptide in transgenic Caenorhabditis elegans. *Proc Natl Acad Sci U S A* **92:** 9368-9372.

Liu J, Kipreos ET (2000) Evolution of cyclin-dependent kinases (CDKs) and CDK-activating kinases (CAKs): differential conservation of CAKs in yeast and metazoa. *Mol Biol Evol* **17:** 1061-1074.

Liu ZJ, Shirakawa T, Li Y, Soma A, Oka M, Dotto GP, Fairman RM, Velazquez OC, Herlyn M (2003) Regulation of Notch1 and Dll4 by vascular endothelial growth factor in arterial endothelial cells: implications for modulating arteriogenesis and angiogenesis. *Mol Cell Biol* **23:** 14-25.

Logeat F, Bessia C, Brou C, LeBail O, Jarriault S, Seidah NG, Israel A (1998) The Notch1 receptor is cleaved constitutively by a furin-like convertase. *Proc Natl Acad Sci U S A* **95:** 8108-8112.

Maduro M, Pilgrim D (1995) Identification and cloning of unc-119, a gene expressed in the Caenorhabditis elegans nervous system. *Genetics* **141:** 977-988.

Mello CC, Kramer JM, Stinchcomb D, Ambros V (1991) Efficient gene transfer in C.elegans: extrachromosomal maintenance and integration of transforming sequences. *The EMBO journal* **10:** 3959-3970.

Morgan DO (2007) The Cell Cycle: Principles of Control. *London: New Science Press* **1st edition**.

Morgan TH (1917) The theory of the gene. *American naturalist* **51:** 513-544.

Moskowitz IP, Rothman JH (1996) lin-12 and glp-1 are required zygotically for early embryonic cellular interactions and are regulated by maternal GLP-1 signaling in Caenorhabditis elegans. *Development* **122:** 4105-4117.

Moss EG (2007) Heterochronic genes and the nature of developmental time. *Curr Biol* **17:** R425-434.

Mulligan P, Yang F, Di Stefano L, Ji JY, Ouyang J, Nishikawa JL, Toiber D, Kulkarni M, Wang Q, Najafi-Shoushtari SH, Mostoslavsky R, Gygi SP, Gill G, Dyson NJ, Naar AM (2011) A SIRT1-LSD1 corepressor complex regulates Notch target gene expression and development. *Mol Cell* **42:** 689-699.

Mumm JS, Schroeter EH, Saxena MT, Griesemer A, Tian X, Pan DJ, Ray WJ, Kopan R (2000) A ligand-induced extracellular cleavage regulates gamma-secretase-like proteolytic activation of Notch1. *Mol Cell* **5:** 197-206.

Newman AP, White JG, Sternberg PW (1995) The Caenorhabditis elegans lin-12 gene mediates induction of ventral uterine specialization by the anchor cell. *Development* **121:** 263-271.

Niehrs C, Acebron SP (2012) Mitotic and mitogenic Wnt signalling. *The EMBO journal* **31:** 2705-2713.

Oberg C, Li J, Pauley A, Wolf E, Gurney M, Lendahl U (2001) The Notch intracellular domain is ubiquitinated and negatively regulated by the mammalian Sel-10 homolog. *J Biol Chem* **276:** 35847-35853.

Pardossi-Piquard R, Checler F (2012) The physiology of the beta-amyloid precursor protein intracellular domain AICD. *J Neurochem* **120 Suppl 1:** 109-124.

Park M, Krause MW (1999) Regulation of postembryonic G(1) cell cycle progression in Caenorhabditis elegans by a cyclin D/CDK-like complex. *Development* **126:** 4849-4860.

Parkinson J, Mitreva M, Whitton C, Thomson M, Daub J, Martin J, Schmid R, Hall N, Barrell B, Waterston RH, McCarter JP, Blaxter ML (2004) A transcriptomic analysis of the phylum Nematoda. *Nature genetics* **36:** 1259-1267.

Pettitt J, Wood WB, Plasterk RH (1996) cdh-3, a gene encoding a member of the cadherin superfamily, functions in epithelial cell morphogenesis in Caenorhabditis elegans. *Development* **122:** 4149-4157.

Platt HM (1994) Foreword in The Phylogenetic Systematics of Free-living Nematodes (Lorenzen, S.). *The Ray Society, London*.

Priess JR (2005) Notch signaling in the C. elegans embryo. *WormBook*: 1-16.

Rimann I (2008) Screens for Components of the lin-12 Notch Pathway during Vulval Development and Regulation of Anchor Cell Invasion and Uterine Cell Fates by the egl-43 Evi1 Proto-Oncogene in C. elegans. *PhD Thesis*.

Rimann I, Hajnal A (2007) Regulation of anchor cell invasion and uterine cell fates by the egl-43 Evi-1 proto-oncogene in Caenorhabditis elegans. *Dev Biol* **308:** 187-195.

Robert V, Bessereau JL (2007) Targeted engineering of the Caenorhabditis elegans genome following Mos1-triggered chromosomal breaks. *The EMBO journal* **26:** 170-183.

Saverwyns H, Visser A, Van Durme J, Power D, Morgado I, Kennedy MW, Knox DP, Schymkowitz J, Rousseau F, Gevaert K, Vercruysse J, Claerebout E, Geldhof P (2008) Analysis of the transthyretin-like (TTL) gene family in Ostertagia ostertagi--comparison with other strongylid nematodes and Caenorhabditis elegans. *Int J Parasitol* **38:** 1545-1556.

Savill J, Hogg N, Ren Y, Haslett C (1992) Thrombospondin cooperates with CD36 and the vitronectin receptor in macrophage recognition of neutrophils undergoing apoptosis. *J Clin Invest* **90:** 1513-1522.

Schroeter EH, Kisslinger JA, Kopan R (1998) Notch-1 signalling requires ligand-induced proteolytic release of intracellular domain. *Nature* **393:** 382-386.

Schwarzman AL, Gregori L, Vitek MP, Lyubski S, Strittmatter WJ, Enghilde JJ, Bhasin R, Silverman J, Weisgraber KH, Coyle PK, et al. (1994) Transthyretin sequesters amyloid beta protein and prevents amyloid formation. *Proc Natl Acad Sci U S A* **91:** 8368-8372.

Schweisguth F (1999) Dominant-negative mutation in the beta2 and beta6 proteasome subunit genes affect alternative cell fate decisions in the Drosophila sense organ lineage. *Proc Natl Acad Sci U S A* **96:** 11382-11386.

Seydoux G, Greenwald I (1989) Cell autonomy of lin-12 function in a cell fate decision in C. elegans. *Cell* **57:** 1237-1245.

Seydoux G, Schedl T (2001) The germline in C. elegans: origins, proliferation, and silencing. *International review of cytology* **203:** 139-185.

Shaye DD, Greenwald I (2002) Endocytosis-mediated downregulation of LIN-12/Notch upon Ras activation in Caenorhabditis elegans. *Nature* **420:** 686-690.

Shaye DD, Greenwald I (2005) LIN-12/Notch trafficking and regulation of DSL ligand activity during vulval induction in Caenorhabditis elegans. *Development* **132:** 5081-5092.

Shaye DD, Greenwald I (2011) OrthoList: a compendium of C. elegans genes with human orthologs. *PLoS One* **6:** e20085.

Shim EY, Walker AK, Shi Y, Blackwell TK (2002) CDK-9/cyclin T (P-TEFb) is required in two postinitiation pathways for transcription in the C. elegans embryo. *Genes Dev* **16:** 2135-2146.

Simmer F, Tijsterman M, Parrish S, Koushika SP, Nonet ML, Fire A, Ahringer J, Plasterk RH (2002) Loss of the putative RNA-directed RNA polymerase RRF-3 makes C. elegans hypersensitive to RNAi. *Curr Biol* **12:** 1317-1319.

Stein TD, Johnson JA (2002) Lack of neurodegeneration in transgenic mice overexpressing mutant amyloid precursor protein is associated with increased levels of transthyretin and the activation of cell survival pathways. *J Neurosci* **22:** 7380-7388.

Sternberg PW (2005) Vulval development. *WormBook, ed The C elegans Research Community* **doi/10.1895/wormbook.1.6.1:** 1-28.

Sternberg PW, Horvitz HR (1989) The combined action of two intercellular signaling pathways specifies three cell fates during vulval induction in C. elegans. *Cell* **58:** 679-693.

Sternberg PW, Lesa G, Lee J, Katz WS, Yoon C, Clandinin TR, Huang LS, Chamberlin HM, Jongeward G (1995) LET-23-mediated signal transduction during Caenorhabditis elegans development. *Mol Reprod Dev* **42:** 523-528.

Sulston JE, Horvitz HR (1981) Abnormal cell lineages in mutants of the nematode Caenorhabditis elegans. *Dev Biol* **82:** 41-55.

Sundaram MV (2005) The love-hate relationship between Ras and Notch. *Genes Dev* **19:** 1825-1839.

Tan PB, Lackner MR, Kim SK (1998) MAP kinase signaling specificity mediated by the LIN-1 Ets/LIN-31 WH transcription factor complex during C. elegans vulval induction. *Cell* **93:** 569-580.

Tilmann C, Kimble J (2005) Cyclin D regulation of a sexually dimorphic asymmetric cell division. *Developmental cell* **9:** 489-499.

Tsuzuki K, Fukatsu R, Yamaguchi H, Tateno M, Imai K, Fujii N, Yamauchi T (2000) Transthyretin binds amyloid beta peptides, Abeta1-42 and Abeta1-40 to form complex in the autopsied human kidney - possible role of transthyretin for abeta sequestration. *Neurosci Lett* **281:** 171-174.

van den Heuvel S (2005a) Cell-cycle regulation. *WormBook, ed The C elegans Research Community* **doi/10.1895/wormbook.1.28.1:** 1-16.

van den Heuvel S (2005b) The C. elegans cell cycle: overview of molecules and mechanisms. *Methods Mol Biol* **296:** 51-67.

van der Voet M, Lorson MA, Srinivasan DG, Bennett KL, van den Heuvel S (2009) C. elegans mitotic cyclins have distinct as well as overlapping functions in chromosome segregation. *Cell Cycle* **8:** 4091-4102.

Wallenfang MR, Seydoux G (2002) cdk-7 Is required for mRNA transcription and cell cycle progression in Caenorhabditis elegans embryos. *Proc Natl Acad Sci U S A* **99:** 5527-5532.

Wang X, Li W, Zhao D, Liu B, Shi Y, Chen B, Yang H, Guo P, Geng X, Shang Z, Peden E, Kage-Nakadai E, Mitani S, Xue D (2010) Caenorhabditis elegans transthyretin-like protein TTR-52 mediates recognition of apoptotic cells by the CED-1 phagocyte receptor. *Nature cell biology* **12:** 655-664.

Weijzen S, Rizzo P, Braid M, Vaishnav R, Jonkheer SM, Zlobin A, Osborne BA, Gottipati S, Aster JC, Hahn WC, Rudolf M, Siziopikou K, Kast WM, Miele L (2002) Activation of Notch-1 signaling maintains the neoplastic phenotype in human Ras-transformed cells. *Nat Med* **8:** 979-986.

Weng AP, Ferrando AA, Lee W, Morris JPt, Silverman LB, Sanchez-Irizarry C, Blacklow SC, Look AT, Aster JC (2004) Activating mutations of NOTCH1 in human T cell acute lymphoblastic leukemia. *Science* **306:** 269-271.

Wightman B, Ha I, Ruvkun G (1993) Posttranscriptional regulation of the heterochronic gene lin-14 by lin-4 mediates temporal pattern formation in C. elegans. *Cell* **75:** 855-862.

Wilkinson HA, Fitzgerald K, Greenwald I (1994) Reciprocal changes in expression of the receptor lin-12 and its ligand lag-2 prior to commitment in a C. elegans cell fate decision. *Cell* **79:** 1187-1198.

Wu G, Lyapina S, Das I, Li J, Gurney M, Pauley A, Chui I, Deshaies RJ, Kitajewski J (2001) SEL-10 is an inhibitor of notch signaling that targets notch for ubiquitin-mediated protein degradation. *Mol Cell Biol* **21:** 7403-7415.

Yanowitz J, Fire A (2005) Cyclin D involvement demarcates a late transition in C. elegans embryogenesis. *Dev Biol* **279:** 244-251.

Zagouras P, Stifani S, Blaumueller CM, Carcangiu ML, Artavanis-Tsakonas S (1995) Alterations in Notch signaling in neoplastic lesions of the human cervix. *Proc Natl Acad Sci U S A* **92:** 6414-6418.

Zhou S, Fujimuro M, Hsieh JJ, Chen L, Miyamoto A, Weinmaster G, Hayward SD (2000) SKIP, a CBF1-associated protein, interacts with the ankyrin repeat domain of NotchIC To facilitate NotchIC function. *Mol Cell Biol* **20:** 2400-2410.

Zhu J, Li W, Mao Z (2011) Cdk5: mediator of neuronal development, death and the response to DNA damage. *Mech Ageing Dev* **132:** 389-394.

11 CURRICULUM VITAE

PERSONAL INFORMATION

Surname: Nusser-Stein

Given name: Stefanie

Date of birth: 20th October, 1982

Citizenship: German

PUBLICATION

Nusser-Stein S, Beyer A, Rimann I, Adamczyk M, Piterman N, Hajnal A and Fisher J (2012) Cell-Cycle Regulation of NOTCH Signaling during *C. elegans* Vulval Development. *Molecular Systems Biology* (in press)

EDUCATION

1989 - 1993	Grundschule, in Raidwangen, Germany
1993 - 2002	Hölderlin-Gymnasium, in Nürtingen, Germany
June 2002	Certificate: Abitur
October 2002 – December 2007	Biology, Eberhard Karls Universität Tübingen, Germany
February 2007 – December 2007	Diploma thesis at the Max Planck Institute for Developmental Biology, Department of Integrative Evolutionary Biology, in Tübingen, Germany
	Thesis title: Vergleichende Analyse der Promotorevolution in Hox-Genen von Nematoden
	Supervisors: Christoph Dieterich and Ralf Sommer
January 2008	Certified biologist (A-level)
April 2008 – date	PhD study in Developmental Biology, Institute of Molecular Life Sciences, University of Zurich, Switzerland
	Thesis title: Modification of LIN-12 NOTCH signalling during vulval development in *C. elegans*
	Supervisor: Alex Hajnal

INTERNATIONAL EXPERIENCE AND MEETINGS

August 2004	Symbiose 2004: Symposium of European biology students, in Zagreb and Zadar, Croatia
June 2008	*C. elegans* Development and Evolution Topic Meeting, University of Wisconsin, in Madison, Wisconsin, USA
June 2009	17th International *C. elegans* Meeting, University of California, in Los Angeles, California, USA
June 2010	*C. elegans*: Development and Gene Expression Topic Meeting, EMBL ATC conference centre, in Heidelberg, Germany
July 2011	SDB 70th Annual Meeting, Hyatt Regency, in Chicago, Illinois, USA

TEACHING EXPERIENCE

July – August 2008	Supervision of a BUSS (biology Undergraduate Summer School) project
	Student: Ye Fan
January 2010 – January 2011	Supervision of an M.Sc. project
	Thesis title: Cell Cycle Regulation of Secondary Cell Fate Specification in *C. elegans* Vulval Precursor Cells
	Student: Magdalene Adamczyk
	University of Zurich, Switzerland
July – August 2010	Supervision of a BUSS (biology Undergraduate Summer School) project
	Student: Daniel Roiz Lafuente
2008 -2012	Assistant in various courses for M.Sc. biology and medical students
	University of Zurich, Switzerland